NPS ARCHIVE
1968
WILLIAMS, D.

DETERMINATION OF PERFORMANCE PARAMETERS OF A DUAL DISCHARGE RADIAL TURBINE

by

David Daniel Williams

DUDLEY KNOX LIBRARY
NAVAL POSTGRADUATE SCHOOL
TEREY CA 93943-5101

UNITED STATES
NAVAL POSTGRADUATE SCHOOL

THESIS

DETERMINATION OF PERFORMANCE PARAMETERS
OF A
DUAL DISCHARGE RADIAL TURBINE

by

David Daniel Williams

December 1968

This document has been approved for public release and sale; its distribution is unlimited.

LIBRARY
NAVAL POSTGRADUATE SCHOOL
MONTEREY, CALIF. 93940

DETERMINATION OF PERFORMANCE PARAMETERS
OF A
DUAL DISCHARGE RADIAL TURBINE

by

David Daniel Williams
Lieutenant, United States Navy
B. S., Naval Academy, 1962

Submitted in partial fulfillment of the
requirements for the degree of

MASTER OF SCIENCE IN AERONAUTICAL ENGINEERING

from the

NAVAL POSTGRADUATE SCHOOL
December 1968

NPS ARCHIVE
1968
WILLIAMS, D.

~~Thesis~~ W59737 c.1

ABSTRACT

This study was conducted to establish the performance parameters of a radial inflow, dual discharge turbine and to determine the effect of variations in axial clearance on these parameters. The representative stream surface is taken at the outer discharge radius instead of at a computed mass-average discharge radius, as was done previously. This technique results in considerably simplified computations and in better correlation of the rotor loss parameters.

Tests were conducted at axial clearances from 0.015 to 0.081 inches and at total-to-static pressure ratios from 1.2 to 1.7 for each clearance. The test installation is located at the Turbo-Propulsion Laboratory of the Naval Postgraduate School, Monterey, California.

LIBRARY
NAVAL POSTGRADUATE SCHOOL
MONTEREY, CALIF. 93940

DUDLEY KNOX LIBRARY
NAVAL POSTGRADUATE SCHOOL
MONTEREY CA 93943-5101

TABLE OF CONTENTS

SECTION PAGE

1. INTRODUCTION 17
2. THE ICP RADIAL TURBINE 19
  2.1 Description of Turbine Assembly 19
  2.2 Modifications to Turbine Assembly 21
3. ANALYSIS OF SCROLL AND GUIDE VANE PERFORMANCE 23
  3.1 Instrumentation and Test Procedures 24
  3.2 Theoretical Analysis 28
  3.3 Data Reduction: Program SCROLL 31
  3.4 Discussion of Results 31
4. ANALYSIS OF OVERALL TURBINE PERFORMANCE 36
  4.1 Instrumentation 36
  4.2 Test Procedures 39
  4.3 Theoretical Analysis 43
  4.4 Data Reduction: Programs RADIAL and NOSPD 52
  4.5 Discussion of Results 52
5. CONCLUSIONS 61
ILLUSTRATIONS 63
REFERENCES 101
APPENDIX A: Program SCROLL 102
  A1. Main Program 102
  A2. Subroutine TEMP 103
  A3. Subroutine FLOW 103
  A4. Subroutine PRESS 105
  A5. Method of Assembly of Input Data 105

APPENDIX B: Program RADIAL 119

B1. Subroutines TEMP and FLOW 120

B2. Subroutine PRESS 120

B3. Subroutine EDC 121

B4. Subroutines TORQ and DYNA 122

B5. Subroutine TURB 123

B6. Subroutine PHIAL 123

B7. Subroutine REFER 124

B8. Method of Assembly of Input Data 124

APPENDIX C: Program NOSPD 148

LIST OF TABLES

TABLE PAGE

A1 Listing of Program SCROLL 107

A2 Results from Program SCROLL Clearance 0.081 In. 111

A3 Results from Program SCROLL Clearance 0.072 In. 112

A4 Results from Program SCROLL Clearance 0.061 In. 113

A5 Results from Program SCROLL Clearance 0.050 In. 114

A6 Results from Program SCROLL Clearance 0.041 In. 115

A7 Results from Program SCROLL Clearance 0.030 In. 116

A8 Results from Program SCROLL Clearance 0.024 In. 117

A9 Results from Program SCROLL Clearance 0.015 In. 118

B1 Listing of Program RADIAL 126

B2 Additional Control Cards Required for Program RADIAL 136

B3 Torque Calibration Data 137

B4 Program RADIAL Input Data Clearance 0.081 In. 138

B5 Results from Program RADIAL Clearance 0.081 In. 139

B6 Program RADIAL Input Data Clearance 0.061 In. 140

B7 Results from Program RADIAL Clearance 0.061 In. 141

B8 Program RADIAL Input Data Clearance 0.041 In. 142

B9 Results from Program RADIAL Clearance 0.041 In. 143

TABLE PAGE

B10 Program RADIAL Input Data Clearance 0.024 In. 144

B11 Results from Program RADIAL Clearance 0.024 In. 145

B12 Program RADIAL Input Data Clearance 0.015 In. .146

B13 Results from Program RADIAL Clearance 0.015 In. .147

C1 Listing of Program NOSPD 149

C2 Results from Program NOSPD 154

LIST OF ILLUSTRATIONS

FIGURE PAGE

1. Active Rotor Test Installation 63

2. Dummy Rotor Test Installation 64

3. Wooden Scroll Insert 65

4. Turbine Scroll and Guide Vane Assembly 66

5. Cross-Section of Turbine 67

6. Dummy Rotor and Flow Straighteners 68

7. Active Rotor 69

8. Left Turbine Discharge 70

9. Turbine Inlet Piping, Flow Control Valves, and Flow Measuring Orifice 71

10. Remote Control for Flow Regulation, Vortec Remote Throttle Control, and Daytronic Strain Gage Digital Indicator 72

11. Schematic of Radial Turbine Instrumentation 73

12. Meriam Mercury Micromanometers 74

13. Brown Potentiometer 75

14. Temperature-Entropy Diagram for Radial Turbine 76

15. Velocity Diagrams for Radial Turbine 77

16. Velocity Coefficient vs. Mach Number 78

17. Absolute Rotor Inlet Flow Angle vs. Mach Number 79

18. Velocity Coefficient vs. Mach Number from Derived Equation 80

19. Absolute Rotor Inlet Flow Angle vs. Mach Number from Derived Equation 81

20. Dummy Alignment Shaft 82

21. Flux Cutter, Quill Shaft, and Dynamometer Torque Capsule 83

FIGURE PAGE

22. Electronic Speed Counter and Vibration Analyzer 84

23. Five Inch Inlet Pipe and Bearing Lubrication Unit 85

24. Schematic of Turbine Lubrication System 86

25. Automatic Data Acquisition System 87

26. Torque Capsule Calibration Apparatus 88

27. Degree of Reaction vs. Head Coefficient 89

28. Overall Efficiency (No Bearing Losses) vs. Referred Speed 90

29. Overall Efficiency (No Bearing Losses) vs. Head Coefficient 91

30. Overall Efficiency (with Bearing Losses) vs. Referred Speed 92

31. Overall Efficiency (with Bearing Losses) vs. Head Coefficient 93

32. Rotor Velocity Coefficient (No Bearing Losses) vs. Head Coefficient 94

33. Rotor Velocity Coefficient (with Bearing Losses) vs. Head Coefficient, Clearance 0.081 In. 95

34. Rotor Velocity Coefficient (with Bearing Losses) vs. Head Coefficient, Clearance 0.061 In. 96

35. Rotor Velocity Coefficient (with Bearing Losses) vs. Head Coefficient, Clearance 0.041 In. 97

36. Rotor Velocity Coefficient (with Bearing Losses) vs. Head Coefficient, Clearance 0.024 In. 98

37. Rotor Velocity Coefficient (with Bearing Losses) vs. Head Coefficient, Clearance 0.015 In. 99

38. Referred Moment (with Bearing Losses) vs. Referred Speed 100

TABLE OF SYMBOLS

Symbol	FORTRAN	Definition	Units
A_1	- - - -	Meridional cross-sectional area of rotor inlet	ft^2
A_5	- - - -	Cross-sectional area of five inch inlet pipe	ft^2
B_1	B1	Perpendicular distance between shroud inner extremities	in
C	- - - -	Flow measurement factor dependent on units, orifice diameter, and type of pressure taps	- - -
C_{f1}	CF1	Pressure conversion factor	$lb/ft^2/in$ Hg
Clnc	CLNC	Rotor axial tip clearance, on one side of blade only	in
C_0	CO	Velocity corresponding to the isentropic enthalpy drop through the turbine	ft/sec
C_p	CP5	Constant pressure specific heat, based on total inlet temperature	BTU/lb_m-°F
C_p(avg)	CP	Constant pressure specific heat, based on average temperature t	BTU/lb_m-°F
D_1	D1	Rotor diameter at inlet, 9.40 in.	in
D_{20}	- - - -	Rotor outer discharge diameter, 5.88 in.	in
F	SR	Scale reading	lb
Fr	- - - -	Reynolds number correction factor	- - - -
G_{Hg}	GHG	Specific gravity of mercury at t_{rm}	- - - -
G_{H20}	GWR	Specific gravity of water at t_{rm}	- - - -
g	32.174	Unit Conversion Factor	$ft\text{-}lb_m/lb\text{-}sec^2$
H_E	- - - -	Total enthalpy at equivalent state point E	BTU/lb_m

Symbol	FORTRAN	Definition	Units
HP_f	HPF	Power required to overcome bearing friction	hp
H_R	- - - -	Relative total enthalpy at rotor inlet	BTU/lb_m
H_{ref1}	HREF1	Measured reference pressure applied to water manometer board	in Hg gage
h_1	- - - -	Static enthalpy at rotor inlet	BTU/lb_m
h_2	- - - -	Static enthalpy at rotor discharge	BTU/lb_m
h_1(avg)	H1	Average static pressure ahead of rotor	in H_2O gage
ΔH_{is}	DHIS	Isentropic total enthalpy drop across turbine	BTU/lb_m
ΔH_w	- - - -	Enthalpy drop representing work output of turbine	BTU/lb_m
Δh_{1vc}	DPVC	Measured pressure differential across flow orifice, from vena contracta taps	in Hg
J	778.16	Joule's constant	ft-lb/BTU
k_{is}	HEAD	Isentropic head coefficient	- - - -
M	TNET	Net torque output of turbine	ft-lb
M_f	BFM	Bearing friction moment	ft-lb
M_{ref}	TNETR	Referred net torque output of turbine	ft-lb
M_1	ACH1	Mach number at rotor inlet	- - - -
N	RPM	Measured turbine speed	rpm
N_{ref}	RPMR	Referred turbine speed	rpm
P_{atm}	PATM	Barometric pressure	in Hg
P_{t0}	PTO	Absolute total pressure ahead of turbine	in Hg abs

Symbol	FORTRAN	Definition	Units
p_{t0}/p_1	PR1	Pressure ratio across scroll and guide vanes	- - - -
p_{t0}/p_2	PR2	Pressure ratio across turbine	- - - -
p_E	- - - -	Equivalent rotor inlet static pressure	in Hg abs
p_0	PS5	Absolute static pressure at turbine inlet	in Hg abs
p_1	P1	Average absolute static pressure at rotor inlet	in Hg abs
p_{1VC}'	PUVC	Measured pressure upstream of flow orifice, from vena contracta tap	in Hg gage
p_{1VC}	PVC	Absolute pressure upstream of flow orifice from vena contracta taps	in Hg abs
p_2	P2	Static discharge pressure	in Hg abs
p_5'	P5P	Measured static pressure at turbine inlet	in Hg gage
R_g	53.3448	Gas constant for air	$\text{ft-lb/lb}_m\text{-°R}$
R_1	R1	Rotor inlet radius, 4.70 in.	in
R_{20}	R20	Rotor outer discharge radius, 2.94 in	in
r	DR	Isentropic degree of reaction	- - - -
T	T	Torque measured by dynamometer	ft-lb
TCD	TCD	Torque calibration data	counts
TQ	TQ	Torque indicator reading	counts
T_E	- - - -	Equivalent rotor inlet temperature	°R
T_{ref}	TR	Referred torque output for no-loss case	ft-lb
T_{to}	T5	Total temperature ahead of turbine	°R
T_0	TO	Static temperature ahead of turbine	°R

Symbol	FORTRAN	Definition	Units
T_1	T1	Static temperature ahead of rotor	°R
T_1'	- - - -	Static temperature at rotor inlet for isentropic expansion from P_{t0} to p_1	°R
T_1^*	- - - -	Static temperature at rotor inlet resulting from rotor incidence losses	°R
T_2'	- - - -	Static discharge temperature resulting from isentropic expansion from p_E to p_2	°R
T_2''	- - - -	Static temperature at discharge resulting from isentropic expansion from P_{t0} to p_2	°R
T_4	T4	Total temperature ahead of flow orifice	°R
T_{20}	T20	Lubricating oil inlet temperature	°F
T_{21}	T21	Lubricating oil temperature at discharge from right bearing	°F
T_{22}	T22	Lubricating oil temperature at discharge from left bearing	°F
ΔT_{is}	DTIS	Isentropic temperature drop from P_{t0} to p_2	°R
ΔT_W	DTW	Temperature drop corresponding to actual work output of turbine	°R
t	A	Average temperature through turbine	°F
tare	STARE	Tare of precision scales	lb
t_{cj}	TCJ	Thermocouple reference cold junction temperature	°F
t_{rm}	TRM	Control room temperature	°F
U_1	U1	Peripheral speed of rotor at inlet	ft/sec
U_{20}	U20	Peripheral speed of rotor at outer discharge radius	ft/sec

Symbol	FORTRAN	Definition	Units
V	- - - -	Thermocouple reading	mv
V_O	VO	Velocity at turbine inlet	ft/sec
V_1	V1	Absolute flow velocity at rotor inlet	ft/sec
V_{u1}	VUL	Peripheral component of V_1	ft/sec
V_{m1}	VM1	Meridional component of V_1	ft/sec
V_{ith}	VITH	Theoretical absolute rotor inlet velocity for no losses	ft/sec
V_{20}	V20	Absolute discharge flow velocity at outer radius of rotor	ft/sec
V_{u20}	VU20	Peripheral component of V_{20}	ft/sec
V_{m20}	VM20	Meridional component of V_{20}	ft/sec
V_4	V4	Thermocouple reading ahead of flow orifice	mv
V_5	V5	Thermocouple reading at turbine inlet	mv
V_{20}	V20	Thermocouple reading at lube oil inlet	mv
V_{21}	V21	Thermocouple reading at lube oil discharge from right bearing	mv
V_{22}	V22	Thermocouple reading at lube oil discharge from left bearing	mv
W_1	W1	Relative flow velocity at rotor inlet	ft/sec
W_{u1}	WU1	Peripheral component of W_1	ft/sec
W_{20}	W20	Relative flow velocity at rotor discharge outer radius	ft/sec
W_{u20}	WU20	Peripheral component of W_{20}	ft/sec
W_{20th}	W20TH	Theoretical relative flow velocity at outer discharge radius, for isentropic expansion from p_E to p_2	ft/sec

Symbol	FORTRAN	Definition	Units
$\dot{W}$	WVC	Mass flow rate, for vena contracta taps	lb_m/sec
$\dot{W}_{ref}$	WVCR	Referred mass flow rate	lb_m/sec
$\dot{W}_{oil}$	- - - -	Mass flow rate of lubricating oil	lb_m/sec
Y_1	Y	Factor accounting for compressibility effects in flow measuring orifice	- - - -

Symbol	FORTRAN	Definition	Units
GREEK SYMBOLS			
α	A	Area multiplier accounting for thermal expansion of flow orifice	- - - -
α_1	ALPH1	Absolute rotor inlet flow angle	degrees
α_{20}	ALF2	Absolute rotor discharge flow angle at outer radius, for no bearing loss case	degrees
α_{20L}	ALF2L	Absolute rotor discharge flow angle at outer radius, bearing losses considered	degrees
β_1	BETA1	Relative rotor inlet flow angle	degrees
β_{20}	BET20	Relative rotor discharge flow angle at outer radius	degrees
γ	GAMMA	Ratio of specific heats based on T_{t0}	- - - -
$\gamma_{(avg)}$	GAM	Ratio of specific heats based on t	- - - -
$(\gamma-1)/\gamma$	EXP	Exponent	- - - -
δ	DEL	Referred pressure ratio, $P_{to}/14.7$	- - - -
ϵ	EPS	Factor which corrects flow rate through the turbine for varying values of γ	- - - -
η	ETA	Total-to-static turbine efficiency, bearing losses not considered	per cent
η_L	ETAL	Total-to-static turbine efficiency, including bearing losses	per cent
ϕ	PHI	velocity coefficient for scroll and guide vanes	- - - -
Ψ	PSI	Velocity coefficient for rotor, based on ratio of actual to theoretical relative discharge velocities, bearing losses not considered	- - - -

Symbol	FORTRAN	Definition	Units
Ψ_L	PSIL	Velocity coefficient for rotor, bearing losses included	- - - -
ρ_0	RHO	Density at turbine inlet	lb_m/ft^3
ρ_1	RHO	Density at rotor inlet	lb_m/ft^3
θ	THETA	Referred temperature ratio, $T_{to}/518.7$	- - - -
ω	ROSP	Rotational speed of rotor	radians/sec
ζ_N	ZETAN	Loss coefficient for scroll and guide vanes	- - - -
ζ_R	ZETR	Rotor loss coefficient, bearing losses not considered	- - - -
ζ_{RL}	ZETRL	Rotor loss coefficient, with bearing losses	- - - -

SECTION I

INTRODUCTION

As requirements for smaller more powerful turbines increase, to keep pace with the needs of the rapidly expanding aerospace industry, more and more attention is given to radial turbines. Since the radial turbine can extract more energy per stage than an axial turbine, it is more useful in applications where space limitations preclude the use of a staged axial turbine. Currently, it is therefore used extensively for aircraft electric power generation, in aircraft cockpit and equipment cooling systems, in cryogenic systems, and in missile auxiliary power systems.

As a consequence of the increasingly widespread use of the radial turbine, the establishment of performance parameters as an aid to the design of these turbines is of fundamental importance. It is the objective of this report to establish some of the performance parameters for a particular radial inflow, dual discharge turbine using air as an operating fluid and relating these parameters in such a way that they may be applied to geometrically similar turbines operating with different fluids and in different environments.

Although similar studies have previously been conducted on this machine, this investigation differs in two important aspects. First, several significant and necessary changes in the internal dimensions of the turbine were made, thus resulting in a somewhat different machine than that previously tested. Also, the method of analysis used is a considerably simplified one, which yields more significant results with less computational effort than those methods previously employed by referring all losses to the outer discharge radius rather than a computed average radius.

Additionally, this project had as an objective a significant expansion of the operating ranges examined beyond those previously considered.

Because the evaluation of turbine performance parameters involves a formidable computation requirement, the data obtained in the experiments were reduced by means of the computer programs described herein, which are written in FORTRAN IV language for the IBM 360 computer system used at the Naval Postgraduate School.

The author gratefully acknowledges the guidance and counsel of Professor Robert D. Zucker, of the Department of Aeronautics, Naval Postgraduate School, and of Professor Michael H. Vavra of the same department. Thanks are due also to Mr. James E. Hammer and his coworkers on the technical staff of the Turbopropulsion Laboratory for their many hours of hard work in modifying, repairing, and operating the turbine test rig.

SECTION 2

THE I.C.P. RADIAL TURBINE

The turbine used in this investigation is a dual discharge, radial inflow turbine installed at the Turbopropulsion Laboratory of the Department of Aeronautics, Naval Postgraduate School. It was originally designed and built by the Aerojet General Corporation, for application as the power supply for a missile propulsion combustion cycle. The original performance evaluation was conducted by Vavra (1), with subsequent investigations by Finn (2), Riley (3), and Boshoven (4).

2.1 Description of Turbine Assembly

The basic turbine test installations used are shown in Figures 1 and 2. The turbine assembly consists of: the wooden inlet casing, with its inner contour in the shape of a varying diameter torus, or scroll; a circular stainless steel guide vane assembly consisting of seven circular-arc blades and the rings themselves; the rotor assembly; and two plexiglass shrouds.

The inner contour of the inlet casing was formed by casing plaster of paris around a wooden insert of the desired scroll dimensions. The inner surface of the scroll was varnished to prevent erosion. The wooden insert used in this process is shown in Figure 3, and Figure 4 presents a cross-section of the wooden casing, showing the shape of the scroll and the locations of the various scroll pressure taps. It is worthy of note that the flow entry is not tangential, as is customarily the case in radial turbine installations. This characteristic is a result of design requirements in the originally proposed missile installation.

A cross-section of the turbine is shown in Figure 5. In this view are indicated the turbine dimensions and minimum clearance as they existed for the test runs. The clearance, or axial distance between the rotor and the shrouds, was increased during the tests by means of circular metal shims inserted between the shroud flanges and the aluminum rings on which they rest.

The series of tests conducted utilized two different rotors. The "dummy" rotor, so called because it does not rotate, is a special device designed to permit measurement of the torque generated by the incoming flow and thus provides a measure of scroll and guide vane performance. This rotor is shown in Figure 6. It has a diameter of 9.50 inches, an axial length of 8.50 inches, and 36 meridional blades. This diameter places the blade leading edges at the radius which corresponds to that of the annulus containing the static pressure taps ahead of the rotor, and the axial length extends the blade trailing edges beyond the shrouds.

The "active" rotor, or the power-producing rotating element, is shown in Figure 7. It is 9.40 inches in diameter and has an axial length of 5.00 inches. The rotor discharge radius is 1.76 inches at the hub and 2.94 inches at the tip. The fifteen blades have a spacing at the discharge varying from 0.737 to 1.232 inches, hub to tip respectively. The actual rotor discharge area on one side of the rotor is 6.43 square inches, including an effective flow area through the radial gap between the blades and the shroud taken at the discharge plane (1). A view of the left rotor discharge, showing the plexiglass shroud and several of the eight shroud pressure taps which measure static pressure at the rotor inlet, is given in Figure 8.

2.2 Modifications to Turbine Assembly

When the turbine assembly was dismantled in preparation for this series of tests, it was discovered that one of the plexiglass shrouds was deeply gouged. Since removal of enough material to eliminate this fault would have destroyed the contour of the shroud, it was decided to cut the contours of both shrouds so that they would exactly fit the rotor contour. Additionally, it was decided to correct several dimensional discrepancies noted in earlier reports.

Riley (3) indicates a distance of 0.943 inch between the inner extremities of the shrouds. Since the axial width of the blade tips is 0.894 inch, this indicates a basic (unshimmed) axial tip clearance of 0.025 inch on each side of the blade. Boshoven (4), however, determined the distance between shrouds to be 0.966 inch, with a resulting unshimmed clearance of 0.036 inch. Additionally, Boshoven discovered that the inside extremity of the left shroud (as viewed from the turbine inlet) was offset 0.016 inch more from the guide vane ring than the right shroud.

In order to correct these discrepancies, an extensive series of measurements was undertaken. The guide vane rings, which were found to be warped, were lapped until they were flat, and all rough edges, burrs, and high spots on the inner surfaces of the casing halves were carefully removed. This resulted in a consistency to within 0.0025 inch in the dimension between the shroud support rings, at all points around the periphery. Initial measurements showed a maximum variation of 0.01 inch in this dimension.

Measurements with the reworked shrouds installed then showed a minimum clearance of 0.0477 inch, with the left shroud offset axially outward 0.0056 inch more than the right. The shroud flange thicknesses were then reduced so as to compensate for this dissymmetry and to yield a final unshimmed clearance of 0.015 inch. Subsequent measurement of the axial travel of the active rotor, from contact at one shroud face to contact at the other, verified that all calculated clearances used in these tests were correct to within ± 0.002 inch.

Additional modifications were made to the dummy rotor in order to correct the axial stagger and unequal widths of the blades and to correct as much as possible the large gaps which were found to exist between the rotor blade contours and the shroud contours. By careful machining, the blade contours were made uniform, and a much closer fit was made to the shroud contours, even though it was not possible to completely correct this condition and still maintain the blade width.

It is thus apparent that the results obtained from the turbine after this series of modifications could differ to a marked degree from those previously obtained under identical operating conditions. It also seems to this author that both Riley (3) and Boshoven (4) were operating at clearances somewhat greater than stated in their respective studies. Based only on these modifications, the distance between the shroud inner extremities for their tests would have been approximately 0.989 inch, yielding a minimum clearance of 0.048 inch. This may be compared with the minimum clearance of 0.0245 inch reported by Riley and 0.036 inch reported by Boshoven.

Other modifications to the components of the test rig were made and are covered in the sections to which they apply. In this section only those modifications basic to the radial turbine itself are discussed.

SECTION 3

ANALYSIS OF SCROLL AND GUIDE VANE PERFORMANCE

In order to evaluate the performance parameters of a turbine, it is necessary to divide the losses into those which occur in the inlet guide vanes and those which occur in the rotor itself. Riley (3) and Boshoven (4) have used the special dummy rotor installation previously described (Figure 2) to determine the losses in the stator, or scroll and guide vane assembly. The installation determines the average conditions at the rotor inlet and thus provides an indication of scroll and guide vane efficiency as well as the absolute velocity (in both mangitude and direction) at the rotor inlet.

Riley (3) concluded that the velocity coefficient, which is a measure of the losses occurring in the inlet manifold and guide vanes, as well as the absolute inlet flow angle, was essentially constant in the range of turbine pressure ratios and axial clearances examined. The results obtained by Boshoven (4) indicate that this assumption is invalid; in fact, the velocity coefficients were found to increase with pressure ratio for a given clearance, and the absolute rotor inlet flow angles were found to decrease linearly with pressure ratio. Specific results of these earlier tests are discussed in detail in Section 3.3.

It was originally intended to utilize the dummy rotor test data of Boshoven (4) in this experiment. However, because of the extensive modifications previously discussed, it was necessary to repeat these tests. This repetition yielded the additional advantage of permitting testing over a wider range of clearances.

3.1 Instrumentation and Test Procedures

The dummy rotor shown in Figure 6 is mounted on self-aligning ball bearings and replaces the turbine rotor. Its purpose is to turn the flow from the guide vanes into the axial direction and to discharge it with no peripheral velocity component. If this condition is met, the losses in the scroll and guide vanes may be determined by measuring the torque exerted on the static dummy rotor, the flow rate, the conditions at the manifold inlet, and the static pressure at the dummy rotor inlet.

As was previously mentioned, the dummy rotor has an axial length of 8.50 inches, which extends the blade trailing edges beyond the shrouds. To insure that the discharge flow had no whirl components, flow straighteners, also shown in Figure 6, were used. These devices consist of aluminum caps containing a 1.00 inch depth of 0.125 by 0.0015 inch honeycomb material. The caps slide over the rotor shaft and cover the rotor blade trailing edges. The entire dummy rotor assembly is supported by brackets attached to the manifold casing, as shown by Figure 2.

Air for turbine operation was supplied by an Allis-Chalmers 12-stage axial compressor. Air from the main supply line passes through a four-inch pipe, a settling tank, a five-inch pipe, and then into the turbine. The flow rate was regulated by remotely controlled butterfly valves in the inlet line to the turbine and in the outside discharge line of the Allis-Chalmers compressor. (See Figure 9.) The controls for operating these valves are located in the control room (Figure 10).

The flow rate of the incoming air was measured with a sharp-edged orifice located in the four-inch inlet pipe. This orifice is also shown in Figure 9. The pressure ahead of the orifice and the pressure differential across the orifice were measured with standard vena contracta taps. The total temperature ahead of the orifice was measured with an iron-constantan thermocouple installed in a Kiel temperature probe. The orifice installation conforms to standards set forth by Stearns, et al. (5).

The total inlet conditions in the five-inch pipe just upstream of the turbine were measured with a Kiel probe, also incorporating an iron-constantan thermocouple. The static pressure at the same location was measured by two static pressure taps in the line. The static pressure at the rotor inlet was measured by pressure taps located at eight peripheral stations in each shroud. The axial location of these taps is depicted in Figure 5, and their peripheral locations are shown in Figure 4. These taps were moved to the positions shown from their original locations near the shroud inner extremities by Boshoven (4) in order to reduce the effects of local pressure perturbations experienced in previous tests.

The torque exerted on the dummy rotor by the flow was measured on a 25-pound capacity Toledo precision scale, shown in Figure 2. A twelve-inch lever arm was attached to the rotor shaft and incorporated a simple provision for leveling, so that the force was exerted on the scale through an exactly vertical link. This was done to preserve the direct relationship between scale reading and moment. A counter balance was added to the lever arm in order to extend the capacity of the scales to accommodate higher mass flow rates.

A general schematic of the instrumentation used in this and the subsequent active rotor tests is shown in Figure 11. From this schematic it may be seen that the pressure upstream of the flow measuring orifice, the total and static pressures at the turbine inlet, and the reference pressures 1 and 2 were read from an eleven column, 40-inch mercury manometer board located in the control room. This board was referenced to atmospheric pressure. Additionally, one arbitrarily selected scroll pressure tap was connected to the mercury board, and this pressure, together with the total inlet pressure, was used to set the pressure ratio across the scroll and guide vanes. The total inlet pressure displayed on the mercury board was used only for setting this pressure ratio since a more representative total pressure was computed in the data reduction.

The sixteen shroud pressure taps that measure the static pressure at the rotor inlet were read on a fifty-column, 96-inch water manometer board. Also displayed on this board were the pressures at various stations in the scroll itself, although these pressures were not used in the tests. These pressures were measured against atmospheric pressure for the entire series of dummy rotor runs. However, additional, controlled, pressures could have been imposed on the water board reservoirs by means of regulated house air if this had become necessary in order to avoid exceeding the limits of the manometer board. These pressures (the reference pressures 1 and 2 mentioned above) were displayed on the mercury manometer board. The first of these pressures, displayed on column 10 of the mercury board, was recorded as a test datum since it applied to the sixteen columns which indicated the rotor inlet pressures. The value of this pressure was thus zero for all dummy rotor runs.

The pressure differential across the flow orifice was measured on a 20-inch Meriam model 34FB2 mercury micro-manometer, which has a measuring accuracy of ±0.001 inch. A pair of these instruments is shown in Figure 12.

The potentials generated by the iron-constantan thermocouples were measured on a 48-channel Brown potentiometer, manufactured by Minneapolis-Honeywell. This potentiometer, shown in Figure 13, was located in the control room and used an ice bath in the test cell as a cold junction reference.

A series of eighteen test runs were made on the dummy rotor installation, of which eight are documented in this report. These eight runs represent clearances of 0.015, 0.024, 0.030, 0.041, 0.051, 0.061, 0.072, and 0.081 inches, respectively. For each clearance ten pressure ratios were sampled, ranging in value from 1.05 to 1.65. These pressure ratios represent the ratio of total turbine inlet pressure to the static pressure at the rotor inlet.

This large number of runs was necessitated by several factors. Data from the initial runs possessed an unacceptable degree of scatter. This was attributed to an unstable supply of source air from the Allis-Chalmers compressor. When this unsatisfactory trend was discovered, the speed control system was overhauled, and the subsequent test results were significantly improved.

Additionally, the stability of the system was improved by judicious use of the aforementioned butterfly control valve. Experimentation showed that if less of the excess air from the compressor were discharged to the outside, the compressor would be operating at a higher pressure ratio, (with a greater pressure drop across the valve feeding the turbine),and the pressurized air in the house plumbing would act as an additional plenum. The system fluctuations would then be substantially reduced. These improvements in equipment and operating technique, as well as the inevitable improvement in data taking technique, led to such improved results that many runs were repeated in order to obtain the best possible test data.

As first observed by Boshoven (4), it was noted that the pressure distribution around the shroud was very sensitive to the relative positions of the rotor blade leading edges. To eliminate this factor as a possible variable, it was arranged to permit the return of the rotor to the same location each time a new pressure ratio was set. This was accomplished by means of a wing nut on the end of the rod connecting the moment arm to the scale.

It was also observed that the pressures seemed to be higher by about 4 to 5 inches of water at the right side of the rotor inlet than at the left. This condition could be eliminated by moving the rotor approximately 0.001 inch axially to the left; but since the condition was also present in the scroll itself, it was attributed to scroll pressure distribution rather than to misalignment. The rotor was centered for all runs.

3.2 Theoretical Analysis

From the law of moment of momentum (6), the moment M exerted on the dummy rotor by the flow is given by

$$M = (\dot{W}/g)\, R_1 V_{u1} \tag{1}$$

where $\dot{W}$ is the mass flow rate, R_1 is the inlet radius of the dummy rotor, and V_{U1} is the peripheral velocity component at R_1. Equation (1) is valid for the case of steady flow in the dummy rotor because the pressures acting over the inlet and discharge areas cannot produce a moment about the axis, and because the flow straighteners insure an axial discharge velocity.

A measure of the performance of the scroll and guide vanes is given in the form of the velocity coefficient, ϕ, which is defined by

$$\phi \equiv V_1 / V_{1th} \tag{2}$$

where V_1 is the average velocity at the dummy rotor inlet and V_{1th} is the theoretical velocity at the dummy rotor inlet which would result from an isentropic expansion from the manifold inlet total conditions P_{t0}, T_{t0}, to the static pressure p_1 at the dummy rotor inlet. This process is shown on the T-s diagram of Figure 14. The component velocities may be seen on Figure 15.

From the energy equation for an adiabatic, no work process, the velocity V_1 at the dummy rotor inlet is

$$V_1 = \sqrt{2gJc_p(T_{t0} - T_1)} \tag{3}$$

If use is made of the isentropic pressure-temperature relation for a perfect gas and of Equation (2), V_1 may be alternately expressed as

$$V_1 = \phi \sqrt{2gJc_pT_{t0}\left[1-(p_1/p_{t0})^{\frac{\gamma-1}{\gamma}}\right]} \tag{4}$$

Application of the equation of continuity at the dummy rotor inlet yields the following expression for the average meridional velocity component:

$$V_{m1} = \dot{W}/\rho_1 A_1 \tag{5}$$

where ρ_1 is the density at the dummy rotor inlet, and A_1 is the cross-sectional area normal to the flow (meridional cross-section). The area A_1 is given by

$$A_1 = 2\pi R_1 B_1 \tag{6}$$

where B_1 is the distance between the shrouds at the rotor inlet. Using the equation of state for a perfect gas, ρ_1 may be expressed as

$$\rho_1 = p_1/RgT_1 \tag{7}$$

Substitution of this relation and Equation (6) into Equation (5) yields the resultant expression for V_{m1}:

$$V_{m1} = \frac{\dot{W} R_g T_1}{2\pi R_1 B_1 p_1} \tag{8}$$

From Equation (1), the peripheral velocity may be expressed as

$$V_{u1} = \frac{M g}{R_1 \dot{W}} \tag{9}$$

and V_1 may additionally be given by

$$V_1 = \sqrt{V_{u1}^2 + V_{m1}^2} \tag{10}$$

Thus, three equations expressing the velocity V_1 are established, these being Equations (3), (4), and (10). Upon substitution of Equations (8) and (9) into Equation (10), it may be seen that this set of three equations contains three unknowns. The unknown quantities to be determined are the velocity V_1, the velocity coefficient ϕ, and the temperature T_1, all other quantities being either constants or determined directly from measured data. Solution of this system of equations establishes the velocity components, which may then be used to calculate the absolute flow angle at the dummy rotor inlet, according to the relation

$$\alpha_1 = \tan^{-1}\left(V_{u1} / V_{m1}\right) \tag{11}$$

A nozzle loss coefficient, ζ_N, may be obtained from the relation

$$\zeta_N = 1 - \phi^2 = 1 - \eta \tag{12}$$

where η is an efficiency based on the ratio of the actual-to-isentropic temperature drop across the scroll and guide vanes. It is introduced here only to illustrate the significance of ζ_N and ϕ.

3.3 Reduction of Data: Program SCROLL

The computer program SCROLL, listed in Appendix A, determines the unknown quantities, V_1, ϕ, and T_1, and the absolute inlet angle, α_1, from the test data using an iterative procedure. The program makes temperature corrections to the physical properties of air and to the specific gravities of the water and mercury used as manometer fluids. It converts the manometer readings and thermocouple voltages into pressures and temperatures, as required, and then establishes the mass flow rate. The average conditions at the dummy rotor inlet are then calculated from the measured torque in accordance with the previously given relations.

Program SCROLL has been described in detail by Riley (3) and Boshoven (4). Except for conversion to the FORTRAN IV language, the program used in this experiment remains essentially the same; therefore, the details of the computational processes will not be repeated. However, certain minor changes were incorporated in the temperature corrections applied to the manometer fluids, in the thermocouple equations used, and in the pressure and flow rate solutions. These changes are briefly described in Appendix A, although they become evident if the program used in this report is compared with either of the two above-listed references.

3.4 Discussion of Results

The results of program SCROLL consist primarily of values of the velocity coefficient, ϕ, and the absolute flow angle at the rotor inlet, α_1. These values are plotted versus M_1, the Mach number at the rotor inlet, as opposed to the pressure ratio, P_{to}/p_1, because the Mach number is a more significant parameter in the application of test results to geometrically similar machines. Figure 16 shows ϕ as a function of

M_1 for each of the eight clearances tested, and Figure 17 is a similar plot for α_1 as a function of M_1. Each of the curves was fitted to the data obtained for that run by the least squares method. The tabulated results for each of the eight runs are given in Appendix A.

It may be seen from Figure 16 that the velocity coefficient increases with Mach number, the average increase being approximately 4.75 per cent over a Mach number range of 0.2 to about 0.8. This percentage increase is practically the same regardless of clearance. This increase is due, at least in part, to the decreasing coefficient of friction in the scroll and guide vanes, which results from the increasing Reynolds number.

The coefficient ϕ generally increases with decreasing clearance for a given pressure ratio with the maximum values of ϕ occurring at the minimum clearance of 0.015 inches. As clearance is increased beyond a value of about 0.070 inches, the incremental drop in ϕ per increment of clearance increase appears to become much larger. An explanation for this occurrence is that as clearance is increased, an increasing amount of flow escapes around the blade tips. This flow loses angular momentum by wall friction and subsequently strikes the dummy rotor blades at some lesser radius, thus imparting a reduced amount of torque to the rotor. The cumulative effect of this energy loss would logically become more pronounced at increased clearances. The overlapping of certain of the curves in Figure 16 at the lower Mach numbers occurred because of the relative insensitivity of the instrumentation at low pressures.

Figure 17 shows that the absolute rotor inlet flow angle, α_1, increases with increasing Mach number up to a Mach number of approximately 0.4. Beyond that point, α_1 decreases with increasing Mach number. These changes are small, although they appear to be significant because of the highly expanded scale of Figure 17. In fact, the average maximum change in α_1 over the range of Mach numbers is approximately 0.52 degrees. In general, increasing the mass flow rate will increase V_1 and, of course, the components V_{u1} and V_{m1}. The variations in the magnitudes of these two quantities as the Mach number is increased determine the variations of α_1, as shown by Equation (11).

It is also shown on Figure 17 that the angle α_1 increases as clearance increases. This is primarily because V_{m1} is inversely proportional to the meridional cross section, which increases with clearance since it depends on the distance between the shrouds. By Equation (11), the smaller values of V_{m1} result in larger inlet flow angles.

It was concluded by Riley (3) that the velocity coefficient ϕ was essentially independent of the pressure ratio P_{to}/p_1, and that a constant representative value of 0.889 was sufficiently accurate. Although he determined that α_1 decreases with increasing pressure ration, he also assumed a representative value of 80.0 degrees for α_1.

Boshoven (4) subsequently investigated the scroll and guide vane performance in greater detail and obtained results that agree in a qualitative sense with those described above. Because of the many modifications made to the machine components, both in preparation for this experiment and during the course of Boshoven's, a more precise comparison is not warranted. It is worthy of note, however, that Boshoven did not obtain the continuous decrease in ϕ with increasing clearance which is apparent from Figure 16. Further, the increase in ϕ with Mach number found in the present tests is more pronounced than Boshoven's, his increase being on the order of 2 per cent for a given clearance, over the range of Mach numbers. It is felt that these changes have occurred because of the machining of the rotor so that it more closely fits the shroud contours, thus minimizing flow loss around the blades and permitting closer minimum clearances.

An examination of the data points given in Figure 16 for ϕ as a function of Mach number shows that some scatter exists. This scatter may be attributed to fluctuations in the air supply from the Allis-Chalmers compressor. The presence of this problem and methods undertaken to alleviate it have been discussed previously in Section 3.1. This scatter of data is also present in the curves of α_1 as a function of Mach number given in Figure 17, but to a lesser extent.

In order to use the results of the dummy rotor tests in later data reduction programs, it was necessary to obtain equations representing ϕ and α_1 in the form

$$\alpha_1 = \text{Constant } [f_1 \text{ (clearance)}][f_2 \text{ (Mach number)}]$$

The function f_1 was obtained by first taking the ratio of α_1 to α_1 maximum at each Mach number, for each clearance. The values of this ratio were then plotted versus clearance. From this plot an average curve was obtained, and its equation was computed by the least squares technique. The resulting equation expressed α_1 / α_{1max} as a dimensionless function of clearance.

The function f_2 was obtained by computing the ratio of α_1 to the value of α_1 at a Mach number of 0.5, and plotting this ratio versus Mach number for each clearance. Again, an average curve was determined, and its equation was computed. This equation, again dimensionless, expresses $\alpha_1 / \alpha_{1(M=.5)}$ as a function of Mach number.

The appropriate scaling factor was determined for each test point. An average of all of these factors, which did not differ greatly in value, was taken as the constant in the above expression. The equation for ϕ was determined in the same manner.

The final equations resulting from this procedure were

$$\alpha_1 = (81.762)[.98267 + .26958\,(\mathrm{Clnc}) - .65080\,(\mathrm{Clnc})^2]\;[.99624 + .02223(M_1) - .02940\,(M_1)^2] \qquad (13)$$

$$\phi = (.92473)[1.01433 - 1.24601\,(\mathrm{Clnc}) + 24.06839\,(\mathrm{Clnc})^2 - 180.36258\,(\mathrm{Clnc})^3]\;[.93149 + .18292(M_1) - .09202\,(M_1)^2] \qquad (14)$$

Families of curves produced by these equations are given in Figures 18 and 19, for ϕ and α_1 respectively. These curves agree well with those of Figures 16 and 17 when consideration is given to the approximations introduced in the derivations of Equations (13) and (14). For the velocity coefficient, ϕ, the maximum difference which exists at any point between the curves of Figure 16 and those of Figure 18 is 0.0052. A similar comparison for α_1 yields a maximum difference of 0.06 degrees. Because of the manner in which Equations (13) and (14) were derived, the most significant discrepancies occur near the extremes of the Mach number range.

SECTION 4

ANALYSIS OF OVERALL TURBINE PERFORMANCE

The turbine overall performance tests, when combined with the results of the dummy rotor tests, provided data from which detailed performance parameters of the turbine could be evaluated. The specific parameters evaluated were: the total-to-static overall efficiency; velocity and loss coefficients for the rotor and guide vanes; rotor inlet and outlet flow angles; referred speed, moments, and flow rates; the head coefficient; and the degree of reaction. Calculations were made assuming no bearing losses and also for the case of "maximum" bearing losses. Bearing loss values were determined from equations given by Vavra (1), which were established from coast-down tests. The analysis was made using a "mean" streamline approach, which is defined as utilizing a representative streamline along which the measured flow conditions are assumed to exist. This streamline was taken as that at the outer discharge radius of the turbine for this analysis, and thus all losses are referred to that outer radius.

4.1 Instrumentation

The "active" rotor shown in Figure 7 was installed for this series of tests, and the rotor and wooden casing were placed in an aluminum test stand. Figure 1 shows the test installation. Alignment of the scroll with respect to the rotor was accomplished by the use of the dummy alignment shaft and dial micrometers shown in Figure 20. Precise alignment was found to be quite difficult because the massive wooden casing and scroll assembly had to be positioned relative to the rotor. Positioning was accomplished by means of four adjusting bolts located at the bottom of the casing and by four angle-irons attached to the casing and resting on the bearing supports. In spite of the difficulty involved, alignment of the concentric aluminum rings which serve as supports for the shrouds was obtained to within ± 0.001 inch in the radial direction from the dummy alignment shaft. These rings were found to deviate from a plane perpendicular to the rotor axis by less than 0.002 inch at a radius of 4.7 inches.

The power developed by the turbine was absorbed by a Vortec Products Company air dynamometer, model 20.075, shown in Figure 1. Lubrication of the dynamometer was accomplished by an oil mist generated by air pressure. The torque output was measured with a torque capsule having a maximum rated capacity of 400 inch-pounds. This capsule utilized strain gages arranged on an internal flexure and was additionally instrumented with an iron-constantan thermocouple to provide a means of monitoring the capsule temperature. The signal generated by the strain gages was read on a Daytronic model 700 digital indicator located in the control room (Figure 10).

The dynamometer shroud was modified from the configuration used by Riley (3) so as to discharge the hot exhaust air radially outward, rather than back onto the torque capsule and housing, in order to minimize thermal effects on the torque capsule. The circular aluminum ring visible in Figure 1 was used to accomplish this modification. Additionally, a wooden baffle, not shown on Figure 1, was used to protect the capsule from the cold turbine discharge air, and to prevent any interference between the dynamometer discharge and the right rotor discharge.

Figure 21 shows the inner face of the torque capsule, the steel quill shaft used to connect the dynamometer to the turbine, and the magnetic pick-up and six-lobe flux cutter used to measure turbine speed. The turbine speed was read from a Hewlett-Packard electronic counter located in the control room (Figure 22). Speed was regulated by means of a remotely controlled motor on the dynamometer itself, which changes the load capacity of the dynamometer. The remote control unit is shown in Figure 10, and the drive motor is shown in Figure 1.

Lubrication of the turbine bearings was provided by a dry-sump system utilizing a gear-driven oil pump and an upper and a lower oil mist injector for each bearing. The lubricating fluid used was 1010 jet engine oil. The cart containing the pump, oil reservoir, heat exchanger, and system pressure gages is shown in Figure 23, and the lubrication system is shown schematically in Figure 24. For these tests the previously existing system was changed to that shown in Figure 24 to permit measurement of the oil temperature into the bearings and at the point of discharge from both bearings. This was accomplished with iron-constantan thermocouples installed as shown on the schematic.

Figure 24 also shows the iron-constantan thermocouples used to measure the bearing outer race temperatures. Vibration signals from the bearings were detected by a piezo-quartz accelerometer mounted on the upper left bearing cap and monitored on a Panoramic vibration analyzer manufactured by the Singer Metrics Company. The accelerometer is visible in Figure 8, and the analyzer is shown in Figure 22.

The pressures and flow rates were measured in the same manner as for the dummy rotor test previously described. The signals from the thermocouples were initially read from the Brown potentiometer shown in Figure 13. During the latter part of the testing period, however, they were read from a new automatic data acquisition system manufactured by B & F Instruments, Inc. This system is shown in Figure 25.

4.2 Test Procedures

Test runs were conducted at five different axial clearances: 0.081, 0.061, 0.041, 0.024, and 0.015 inches. For each clearance, runs were made at total inlet to static discharge pressure ratios of 1.2, 1.3, 1.4, 1.5, 1.6, and 1.7. At each pressure ratio, turbine speed was varied from the minimum speed (maximum load condition) for that pressure, to the highest speed attainable, in increments of about 1,500 rpm. Maximum speed was restricted to 18,000 rpm for reasons of safety.

Measurement of the torque at zero speed was also made for each pressure ratio at each clearance. This was accomplished by engaging the dynamometer rotor lock and measuring the resulting torque.

As turbine speed was increased during the first run, a point was reached at which the bearings overheated and started to seize, causing a rapid drop in speed. The turbine was dismantled and carefully examined. No apparent damage had been incurred by the ball bearings. The oil system was flushed and refilled, and the unit was reassembled. This condition repeated itself in several subsequent runs, occurring whenever the bearing temperature reached approximately 135°F. Additionally, considerable amounts of oil were being lost from around the shaft and bearing caps at higher speeds. Apparently neither of these conditions had existed in previous tests.

Since the bearings themselves did not appear to be at fault, extensive tests were made to determine whether changing the amount of lubricating oil flow would alleviate these problems. It was found that varying the oil system pressure from 10 pounds per square inch to 50 pounds per square inch would reduce the bearing temperature a maximum of six degrees, but this variation did not significantly reduce leakage. A solution was ultimately found to both problems by carefully positioning the oil injectors so that they discharged directly into the balls of the bearing and did not strike the race and by slightly enlarging the injector orifices so as to increase the mass flow rate of the oil. The bearing temperatures could then be kept below a maximum of about 125°F at 18,000 rpm, and oil leakage was negligible.

The fact that the bearings experienced a maximum temperature increase of about 50° over the range of speeds tested, whereas in previous tests the increase had been only about half as much (7), created a question as to the applicability of the bearing loss information obtained from the coast-down tests conducted by Vavra (1). It was therefore decided to attempt to evaluate the bearing losses by measuring the oil flow rate and the amount of heat absorbed by the oil as it flowed across the bearings. If the constant pressure specific heat, C_p, of the oil were known, the energy lost in the bearings could be obtained from the relation

$$\mathrm{BFM} = \frac{\dot{W}_{oil} \, c_{p_{oil}} \, \Delta T_{bearings}}{\omega} \qquad (15)$$

where BFM is the bearing friction moment in foot-pounds and ω is the turbine rotational speed.

Numerous tests were made in order to calibrate the mass flow rate of the oil with the system pressure, and the lubrication system was modified to include the previously discussed thermocouples ahead of and after the bearings. Flow rate calibration was accomplished by weighing the amount of oil discharged by the injectors on each side in a given time interval.

In attempting to evaluate bearing losses by this technique, the results obtained from several test points indicated losses on the order of 20 per cent of the minimum losses predicted by Vavra (1). In fact, it was discovered that the exposure of the inlet lines, the bearing block itself, and the sumps to the cold discharge air sometimes produced cooler temperatures on the discharge side of the bearings than existed ahead of the injectors. Since insulation of the oil lines and the bearing blocks to the extent necessary to overcome this deficit was not feasible, this attempt to determine the bearing losses was abandoned. The oil temperatures were recorded as data for future use, however, and appear in Appendix B.

The dynamometer torque capsule was calibrated both before and after each day's runs in order to permit consideration of any variations during the course of the runs. Calibration was accomplished by use of the device shown in Figure 26. An aluminum plug was fabricated to fit into the torque ring of the capsule. Torque was applied by loading the weight pans on the moment arm, which was attached to the plug. Riley (3) attached the moment arm directly to the inlet side of the dynamometer; thus, a moment was introduced due to the axial distance between the capsule and the point of application of the load. The apparatus used in these tests reduced this potential source of error almost entirely.

Loads of 0 to 400 inch-pounds were applied to the capsule in 100 inch-pound increments. The span of the digital readout was set at 0 to 1000 counts, the latter approximately corresponding to 400 inch-pounds. Calibration readings were taken for both increasing and decreasing loads in order to evaluate the amount of hysteresis present in the readout. As each load was applied, the capsule housing was tapped gently with a mallet to overcome any drag in the capsule itself and to eliminate errors caused by lag in the servomechanism of the digital counter. This procedure is valid, because a like amount of vibration was observed to exist under the dynamic load conditions of an actual test run. Using this technique, the amount of hysteresis present between the loading and unloading cycles was found to be negligible.

The torque readouts for calibrations performed both before and after the test runs were found to vary linearly with applied torque. However, the data obtained after the run were generally higher, by 2 to 3 counts at zero load, to 13 to 15 counts at 400 inch-pounds, than the original calibration. This was felt to be due to the thermal effects of the higher capsule temperatures which existed during the run. A thermocouple was installed in the capsule in an attempt to establish some correlation between this temperature rise and the torque count increase. Tests in which the capsule was heated from the outside with a strip heater were inconclusive, because similar increase in torque counts for given torque loadings could not be produced, even though the temperatures indicated by the thermocouple were considerably higher than those recorded during the actual test runs.

When the turbine is in operation, the capsule is heated from within by heat from the dynamometer bearings. This is modified by the dynamometer water cooling system and by the cold turbine discharge air. A method of reproducing the interaction of all of these conditions in static calibration tests was not found, and so the torque calibration data ultimately used represented an average of the data obtained before and after the test runs. This accounts for some increase due to thermal effects and is felt to be a reasonable representation. In some instances, the capsule temperature was observed to increase immediately following shut-down, while at other times the reverse effect occurred. It is felt that more representative temperature data could be obtained by relocating the thermocouple on the flexure closer to the strain gages.

The compressor which provides house air failed after two clearances, 0.081 and 0.061 inches, had been tested. This compressor provides air to the speed controls of the Allis-Chalmers compressor and also provides the air which is used as a reference pressure for the water manometer board. The remaining three clearances were tested using a smaller auxiliary compressor, which introduced considerable fluctuations into the house air system.

4.3 Theoretical Analysis

The known quantities necessary for the turbine analysis as performed in this project are: mass flow rate; total inlet temperature and pressure; static inlet pressure; turbine speed and torque output; atmospheric pressure and temperature; and the absolute rotor inlet flow angle and velocity coefficient based on the results of the scroll and guide vane analysis.

The working fluid is assumed to undergo an adiabatic process, since the quantity of heat passing through the casing is negligible compared to the enthalpy change undergone by the fluid as it passes through the turbine. It is additionally assumed that the fluid behaves as a perfect gas.

The flow is assumed to have axisymmetric stream surfaces; thus, in effect, the analysis is one-dimensional, based on the determination of the flow properties along a particular streamline lying on a chosen surface of revolution. Vavra (8) states that the major portion of the rotor losses is due to secondary flow phenomena, tip leakage losses, and the loss that occurs because of the motion of the blade tips in the wall boundary layers. Thus is would appear that the majority of the losses occur near the shrouds, and the representative streamline was accordingly chosen as that existing at the outer radius of the rotor discharge. It was felt that this approach would yield a better correlation of results than that obtained from use of a calculated mass-averaged mean radius at the rotor discharge (7).

It is assumed that the relative flow angle β_{20}, calculated from the blade dimensions, is very nearly equal to the actual relative flow angle at the outer discharge radius (where β_{20} assumes its maximum value). This implies that the so-called slip factor may be neglected. Verification of the validity of this assumption is given by the flow surveys taken at the rotor discharge by Riley (3). Accordingly, β_{20} was calculated from Equation A2(4) of (1) and found to be equal to -69.85 degrees at the outer radius. This value was used in all calculations.

The thermodynamic process of a fluid passing through a turbine is given in Figure 14. The resulting flow velocities are shown in Figure 15. The derivations which follow are based on these two diagrams.

Referring to Figure 14, for a reversible, adiabatic process,

$$\frac{T_2''}{T_{t_o}} = \left(\frac{P_2}{P_{to}}\right)^{\frac{\gamma-1}{\gamma}} \tag{16}$$

where T_2'' represents the static temperature at the rotor discharge for an isentropic expansion through the turbine to p_2. The isentropic temperature drop which would occur for such an expansion is

$$\Delta T_{is} \equiv T_{to} - T_2'' \tag{17}$$

and may therefore be expressed as

$$\Delta T_{is} = T_{to}\left[1 - (P_2/P_{to})^{\frac{\gamma-1}{\gamma}}\right] \tag{18}$$

Similarly, for an isentropic expansion across the inlet guide vanes

$$\frac{T_1'}{T_{t_o}} = \left(\frac{P_1}{P_{to}}\right)^{\frac{\gamma-1}{\gamma}} \tag{19}$$

and

$$(\Delta T_{is})_{\text{guide vanes}} \equiv T_{to} - T_1' = T_{to}\left[1 - (P_1/P_{to})^{\frac{\gamma-1}{\gamma}}\right] \tag{20}$$

The isentropic, or theoretical degree of reaction, r, represents that portion of the overall isentropic enthalpy drop which occurs in the rotor, or

$$r \equiv \frac{T_1' - T_2''}{\Delta T_{is}} \tag{21}$$

Therefore,

$$r = 1 - \frac{(\Delta T_{is})_{\text{guide vanes}}}{\Delta T_{is}} \tag{22}$$

and, from Equations (18) and (20),

$$r = 1 - \frac{\left[1 - (P_1/P_{t_0})^{\frac{\gamma-1}{\gamma}}\right]}{\left[1 - (P_2/P_{t_0})^{\frac{\gamma-1}{\gamma}}\right]} \tag{23}$$

The total-to-static efficiency of the turbine is defined as the ratio of the work actually produced by the turbine to that work which could ideally be accomplished by isentropic expansion from total inlet to static outlet conditions. For this case, the efficiency may be expressed by the ratio of the corresponding temperature drops,

$$\eta = \Delta T_w / \Delta T_{is} \tag{24}$$

The change in total enthalpy across the turbine is

$$\Delta H_w = c_p \, \Delta T_w = \frac{M \omega}{J \dot{W}} \tag{25}$$

where M is the net torque produced, ω is the rotational speed, and $\dot{W}$ is the mass flow rate. Therefore, ΔT_w may be expressed as:

$$\Delta T_w = \frac{M \omega}{J c_p \dot{W}} \tag{26}$$

The efficiency given by Equation (24) was computed both for the case where bearing friction was considered and for the case where it was not. Bearing friction was calculated based on the results of coast-down tests performed by Vavra (1). The friction horsepower is expressed by

$$HP_f = -0.6 + (N/1000)(.17143) \tag{27}$$

for N $\leq$ 10,500 rpm, and by

$$HP_f = -0.6 + (N/1000)(.17143) - (4.898 \times 10^{-3})(N/1000 - 10.5)^2 \tag{28}$$

for N $>$ 10,500 rpm. The bearing friction moment is then given by

$$M_f = \frac{HP_f \times 550}{\omega} \tag{29}$$

The net moment is then the sum of T, the moment measured by the dynamometer, and the bearing friction moment:

$$M = T + M_f \tag{30}$$

The velocity C_0 corresponding to the isentropic enthalpy drop through the turbine is given by the expression

$$C_0^2 \equiv 2gJc_p \Delta T_{is} \tag{31}$$

and the peripheral speed of the rotor at the rotor inlet is

$$U_1 = \frac{\pi N D_1}{720} \tag{32}$$

where D_1 is the rotor inlet diameter in inches. By Equations (31) and (32), the isentropic head coefficient is given by

$$K_{is} \equiv (C_0/U_1)^2 \tag{33}$$

The absolute velocity V_1 is expressed by Equation (4). An alternate expression, obtained by substitution of Equation (23) into Equation (4), is

$$V_1 = \phi \sqrt{2gJc_p\,(1-r)\,\Delta T_{is}} \tag{34}$$

The temperature T_1 may then be obtained from

$$T_1 = T_{to} - \frac{V_1^2}{2gJc_p} \tag{35}$$

and M_1, the Mach number at the rotor inlet, is

$$M_1 = \frac{V_1}{\overline{2gJc_p T_1}} \tag{36}$$

The results of the dummy rotor tests can now be used by introducing Equation (14) to obtain ϕ by an iterative procedure which is discussed in Appendix B. Equation (12) gives the nozzle loss coefficient as

$$\varphi_N = 1 - \phi^2 \tag{37}$$

Values for α_1 can now be taken from Equation (13) to determine the peripheral and meridional velocity components of V_1.

$$V_{u1} = V_1 \sin \alpha_1 \tag{38}$$

$$V_{m1} = V_1 \cos \alpha_1 \tag{39}$$

From Figure 15 it is apparent that the peripheral component of the relative rotor inlet velocity W_1 is

$$W_{u1} = V_{u1} - U_1 \tag{40}$$

and W_1 is then found from

$$W_1 = \sqrt{V_{m1}^2 + W_{u1}^2} \tag{41}$$

The relative inlet flow angle β_1 is

$$\beta_1 = \sin^{-1}\left(W_{u1} / W_1 \right) \tag{42}$$

At this point all conditions at the entrance to the rotor are known.

It is assumed that only the kinetic energy $V_{m1}^2/2gJC_p$ is useful in the rotor (since it has radial blades), and that the incidence loss at the rotor inlet is taken as $W_{U1}^2/2gJC_p$ (8). Thus, the effective relative velocity head is reduced, and static conditions at the rotor inlet are really those at T_1* on Figure 14.

The equivalent state point E shown on Figure 14 is established from the energy equation for a rotating system in the following manner (6):

$$H_R = \text{constant} = h_1 + \frac{W_1^2}{2gJ} - \frac{\omega^2 R_1^2}{2gJ} = h_2 + \frac{W_2^2}{2gJ} - \frac{\omega^2 R_2^2}{2gJ} \tag{43}$$

where H_R is the relative total enthalpy. This equation may be rearranged in the form

$$H_E \equiv h_1 + \frac{W_1^2}{2gJ} - \left(\frac{U_1^2 - U_2^2}{2gJ}\right) = h_2 + \frac{W_2^2}{2gJ} \tag{44}$$

where the left side is equal to H_E, the total enthalpy at the state point E. Equation (44) clearly shows that state point E is the proper reference point from which to view the expansion process through the rotor in an analogous manner to that of the stator. The peripheral speed at the outer discharge radius, U_{20}, is given by Equation (32) with D_1 replaced by D_{20}, the outer diameter of the rotor discharge.

The work output of the turbine, represented by the change in total enthalpy, may be represented by Euler's turbine equation (6):

$$\Delta H_W = C_p \Delta T_W = \frac{U_1 V_{u1} - U_{20} V_{u20}}{gJ} \tag{45}$$

where U_{20} and V_{U20} occur at the outer discharge radius. Manipulating this equation and Equations (24) and (31), an expression for the peripheral component of the absolute discharge velocity, V_{U20}, is

$$\frac{V_{u20}}{U_1} = \frac{R_1}{R_{20}}\left[\frac{V_{u1}}{U_1} - \frac{\eta}{2}\left(\frac{C_o}{U_1}\right)^2\right] \tag{46}$$

Using the velocity diagram of Figure 15, it can be shown that the relative velocity at the outer discharge radius, W_{20}, may be expressed by

$$\frac{W_{20}}{U_1} = \frac{(V_{u20}/U_1) - (R_{20}/R_1)}{\sin\beta_{20}} \tag{47}$$

where, in keeping with the stated assumptions,

$$\beta_{20} = -69.85° \tag{48}$$

If the divergence of the pressure lines on the entropy diagram of Figure 14, in the direction of increasing entropy, is neglected, there is

$$T_1^* - T_2' = T_1' - T_2'' \tag{49}$$

By Equations (21) and (31), the right side of the expression is equivalent to

$$T_1' - T_2'' = r\,\frac{C_o^2}{2gJc_p} \tag{50}$$

From Figure 14, the left side may be expressed in terms of the velocities:

$$T_1^* - T_2' = \frac{W_{20th}^2}{2gJc_p} + \frac{U_1^2 - U_{20}^2}{2gJc_p} - \frac{V_{m1}^2}{2gJc_p} \tag{51}$$

Manipulation of Equations (50), (51), and (32) yields a relation for W_{20th}, the theoretical relative velocity at the rotor discharge:

$$\frac{W_{20th}}{U_1} = \left[\frac{r}{(U_1/C_o)^2} + \left(\frac{R_{20}}{R_1}\right)^2 + \left(\frac{V_{m1}}{U_1}\right)^2 - 1\right] \tag{52}$$

Using Equations (47) and (52) it is now possible to define a velocity coefficient Ψ for the rotor, which is analogous to the velocity coefficient ϕ for the scroll and guide vanes given by Equation (2).

$$\Psi \equiv W_{20} \Big/ W_{20\,th} \tag{53}$$

The rotor loss coefficient, which is a measure of the kinetic energy loss through the rotor, is, then

$$\zeta_R \equiv 1 - \Psi^2 \tag{54}$$

The meridional velocity component of the absolute discharge velocity can be expressed by

$$V_{m20} = W_{20} \cos \beta_{20} \tag{55}$$

from Figure 15. The absolute discharge flow angle is then

$$\alpha_{20} = \tan^{-1} \left(V_{u20} \Big/ V_{m20} \right) \tag{56}$$

If consideration is given to the case where bearing losses are assumed to exist, the resulting efficiency will obviously be different from that for no bearing losses. Examination of the foregoing analysis shows that, correspondingly, different values for V_{U20}, V_{M20}, W_{20}, Ψ and ζ_R will result.

Thus, from the measured items of test data specified at the beginning of this section, the following performance parameters are obtained by the analysis technique: flow rate, head coefficient, degree of reaction, absolute and relative rotor inlet flow angles, velocity and loss coefficients for the scroll and guide vanes, the net torque produced, the absolute discharge flow angle, the rotor velocity and loss coefficients, and the total-to-static efficiency.

In this experiment the above parameters are referred to standard air in accordance with the NASA method, as described in (1). This method utilizes a total inlet pressure of 14.7 pounds per square inch absolute, a total inlet temperature of 518.7 degrees Rankine, a specific heat ratio of 1.4, and a constant pressure specific heat of 0.24 BTU per pound mass-degree Fahrenheit. The referral parameters are

$$\delta \equiv P_{to} / 14.7 \tag{57}$$

$$\theta \equiv T_{to} / 518.7 \tag{58}$$

and

$$\epsilon = \frac{0.810}{\gamma} \left(\frac{\gamma+1}{2} \right)^{\frac{\gamma+1}{2(\gamma-1)}} \tag{59}$$

The factor ϵ, which corrects the flow rate through the turbine for varying values of γ, is that given by Vavra (1) and is supposed to give a better correlation than the expression for ϵ used by NASA.

The referred speed is then given by

$$N_{ref.} \equiv N / \sqrt{\theta} \tag{60}$$

The referred flow rate is

$$\dot{W}_{ref.} \equiv \dot{W} \left(\sqrt{\theta} \, \frac{\epsilon}{\delta} \right) \tag{61}$$

Finally,, the referred moment is

$$M_{ref} \equiv M \left(\frac{\epsilon}{\delta} \right) \tag{62}$$

4.4 Data Reduction: Programs RADIAL and NOSPD

The computer program RADIAL, listed in Appendix B, determines the turbine performance parameters described in Section 4.3 from the test data. In general, the specific techniques used by the computer in these computations are apparent from the program itself. However, Appendix B describes each subroutine briefly and elaborates on specific computational procedures which are not immediately obvious.

Program NOSPD, listed in Appendix C, was written to compute the desired performance parameters from the locked rotor test data.

4.5 Discussion of Results

The input data and results of program RADIAL are listed in Tables B4 through B13, with input and output for a given clearance appearing in adjacent tables. The input data and results of program NOSPD appear in Table C2.

Figure 27 shows the degree of reaction, r, as a function of head coefficient, k_{is}, for the clearances tested in this analysis as well as those of Riley (3) and Vavra (1). For each clearance, the degree of reaction was found to be a unique function of head coefficient, independent of turbine pressure ratio. This is in agreement with the findings of both Riley and Vavra. Riley further concluded that the degree of reaction is independent of axial clearance. The results of the present tests verify this for all clearances except for 0.081 inch. At this clearance, the values of r obtained were found to be approximately 1 to 1.5 per cent lower than those for the other clearances. This is shown on Figure 27, where the resulting curves for all clearances except 0.081 inch are represented by that for 0.061 inch, and the curve for 0.081 inch is plotted separately. This discrepancy implies that, for a given overall pressure ratio, the pressure p_1 can no longer be maintained at a clearance of 0.081 inch.

It may be seen from the representative curve of Figure 27 that r decreases with increasing k_{is} (decreasing speed), from a value of approximately 0.75 at a k_{is} of 1.05 to 0.30 at a k_{is} of 6. This drop occurs because, with decreasing speed, a smaller pressure drop is required to pass the flow through the rotor.

The degree of reaction curves obtained in earlier tests by Vavra (1) and Riley (3) are superimposed on the curve of Figure 27. Vavra states that the value of r at design k_{is} of 2.3 should be approximately 0.486, as compared with the value of 0.395 obtained by him and with Riley's value of 0.402. The current tests yielded a value of 0.440 at design k_{is}, except for a clearance of 0.081 inch, for which the corresponding value of r was 0.434. This apparent increase in degree of reaction is due primarily to a more accurate determination of p_1 than was used by either Vavra or Riley. Boshoven (4) relocated the shroud pressure taps, which measure the pressure p_1, to a position axially outward in the annulus around the periphery of the shroud. This was done to reduce the effects of local perturbations on the pressure readings and greatly improved the uniformity of the pressure distribution around the shrouds. This improvement in the accuracy of p_1 yields a more accurate value of r since degree of reaction is directly dependent on p_1.

The degree of reaction remains lower than the design value because the guide vane exit area is too small to permit discharge of the design mass flow (1).

Significant plots resulting from the overall turbine efficiency calculations are given in Figures 28 through 31. Figure 28 depicts turbine efficiency as a function of referred speed for the case of no bearing losses and a clearance of 0.081 inch. Figure 29 is a corresponding plot of efficiency versus head coefficient. Figures 30 and 31 represent these same respective parameters, also at a clearance of 0.081 inch, for the case where bearing losses are considered.

Efficiency was found to be essentially independent of clearance over the range of clearances tested. Figures 28 through 31 are therefore representative of the results for all clearances between 0.015 and 0.081 inch.

Values of turbine efficiency were obtained from measurements of the torque at the turbine shaft made with the air dynamometer and from the bearing loss values as determined from the results of coast-down tests conducted by Vavra (1). Because of the previously discussed problem of excessive bearing temperatures and seizing experienced during these tests, the bearing losses are probably greater than the maximum losses determined by Vavra. However, since time did not permit a repetition of the coast-down tests, Vavra's equations for maximum bearing losses [Equations (27) and (28)] were used.

A comparison of Figures 28 and 29 and of Figures 30 and 31 shows the advantage derived from representing efficiency as a function of head coefficient instead of referred speed. Use of the head coefficient effectively reduces a family of curves to a single curve. However, if the bearing losses are ignored, as in Figure 29, the resulting plot depends significantly on pressure ratio. In this figure only those curves representing the pressure ratios for maximum and minimum efficiencies are shown to avoid clutter.

Figure 31 shows that the efficiencies are nearly independent of pressure ratio in the case where allowance is made for bearing losses. If these bearing losses were accurately known, it would appear that the influence of pressure ratio would be completely eliminated from a plot of efficiency versus head coefficient.

In general, if bearing losses are not considered, a pressure ratio of 1.7 yields a maximum efficiency of 81.1 per cent at a k_{is} of 2.35 and an axial clearance of 0.015 inch. Minimum efficiencies are obtained for a pressure ratio of 1.2 and are in most cases 10 to 12 per cent lower than maximum efficiencies in the vicinity of the design k_{is} of 2.3. Vavra (1) reported a maximum efficiency of 81 per cent for the case of no bearing losses at a pressure ratio of 1.616, k_{is} of 2.37, and clearance of 0.062 inch. Riley (3) obtained a corresponding maximum efficiency of 82.52 per cent at a k_{is} of 2.26, pressure ratio of 1.678, and clearance of 0.027 inch.

For the case where bearing losses are taken into account, the maximum efficiency, η_L, was found to be 84.6 per cent at a pressure ratio of 1.7, head coefficient of 2.28, and clearance of 0.081 inch. This compares favorably with the design efficiency of 85.5 per cent at a pressure ratio of 1.7 and head coefficient of 2.3, as given by Vavra (1). Riley (3) obtained a maximum efficiency of 86.04 per cent at a pressure ratio of 1.678, head coefficient of 2.259, and clearance of 0.027 inch, based on the maximum values of bearing losses.

At minimum speed (maximum k_{is}) for a given pressure ratio and clearance, the efficiency in general is about 65 per cent. As speed is increased (k_{is} decreased), the efficiency increases to a maximum of about 84 per cent in the vicinity of a k_{is} of 2.3 and then falls off rapidly to 30 to 40 per cent at a k_{is} of about 1.05. Initially, then, the efficiency increases with speed because, by Equation (26), an increase in ω and decrease in $\dot{W}$ offset the decrease in torque, resulting in increased turbine work and efficiency. As speed is further increased, the decreasing torque begins to predominate, causing the efficiency curve to peak and then rapidly decrease.

It was expected that, as the clearance was varied over the range encompassed by these tests, a "critical" clearance would be reached beyond which turbine efficiency would deteriorate rapidly. Riley (3) observed this to occur at a clearance of 0.052 inch. Such an occurrence was not observed in these tests over the range of clearances from 0.015 to 0.081 inch. Thus, it appears that axial clearance has no appreciable effect on turbine efficiency over this range of clearances.

It has been previously stated that Riley (3) was in all likelihood operating at a considerably greater clearance than he believed himself to be. This is substantiated to a degree by the fact that Vavra (1) did not experience this efficiency drop at a clearance of 0.062 inch. Since gaps also existed between the rotor and shrouds during Riley's tests, the blades would have left the wall boundary layer at a lesser axial clearance than in these tests where the blade and shroud contours were matched. Thus, it is reasonable to assume that the critical clearance is at some value greater than 0.081 inch.

That such a drop in efficiency should occur as clearance is increased to some critical value is explained in part by Csanady (9). The rotating blades "scrape up" the shroud boundary layer and produce vortices in the vicinity of the tips of the blades which, in turbines, tend to nullify the tip vortices themselves. At a particular tip clearance, then, these two vortices would neutralize each other, leaving only the passage vortex which causes secondary flow losses. This neutralization should produce a pronounced increase in efficiency at that clearance at which it occurs. For the subject turbine, it would appear that if this condition does exist, it occurs at a clearance less than 0.015 inch.

The efficiency is essentially independent of clearance because, although the tip vortices become more predominant as clearance increases, there is also a buildup of the boundary layer. This buildup maintains a reasonably even relative balance between the tip vortices and the "scraped up" vortices. As clearance is extended beyond some critical value, however, the blades begin to operate near the edge of the wall boundary layer, and the countering vortices quickly cease to be effective in neutralizing the increasing tip vortices. The result is a pronounced increase in rotor loss and a corresponding decrease in turbine efficiency. It is also worthy of note that, for the test turbine, although the axial tip clearance is increased, the radial clearance between the shrouds and the rotor blades in the vicinity of the discharge remains essentially unchanged.

The rotor velocity coefficient, Ψ , is plotted as a function of the head coefficient in Figure 32, for the case where bearing losses are neglected. The clearance represented is 0.024 inch. Figures 33 through 37 show the curves of Ψ_L versus k_{is}, with bearing losses considered, for each of the five clearances tested. Again, it may be seen that if bearing losses are ignored, there is considerably more variation of the curves with pressure ratio than in the case where bearing losses are considered.

The only variation in rotor velocity coefficient with axial clearance which can be established is that values of Ψ for a clearance of 0.081 inch seem to be generally higher than for all other clearances. This variation is evident for both bearing loss cases, with values of Ψ_L being generally 10 to 15 per cent higher at a clearance of 0.081 inch. Because of the negligible effect of axial clearance and the doubtful significance of the case where bearing losses are neglected, Figure 32, for a clearance of 0.024 inch, is the only curve included for the case where bearing losses are not considered.

Figures 33 through 37 show that maximum values of Ψ_L do not always occur at the higher pressure ratios, although Ψ_L is more nearly constant over the range of k_{is} values for the higher pressure ratios.

At the design k_{is} of 2.3, a value for Ψ_L of 0.960 was produced at a pressure ratio of 1.2 and clearance of 0.081 inch. The maximum value of Ψ_L was found to occur at the same pressure ratio and clearance and at a k_{is} of 3.35. Its value is 0.990.

It can be seen from the curves for Ψ_L given in Figures 33 through 37 that Ψ_L remains relatively constant over a range of k_{is} between about 2.3 and the maximum value. As k_{is} is decreased below 2.3, Ψ_L first decreases, with a minimum occurring at a k_{is} of 1.7 to 1.9. It then increases to a peak at a k_{is} of about 1.5, and falls off sharply as the head coefficient is further decreased. Examination of the tabulated performance data in Appendix B shows that the relative rotor inlet flow angle β_1 is positive at values of k_{is} greater than about 2.3, so that the relative flow strikes the pressure side of the blades. This produces the accompanying incidence losses, and further losses occur as the flow is turned through a relatively large angle to follow the flow channel.

As U_1 is increased (k_{is} decreased), β_1 becomes negative, so that impingement of the flow on the blades acts opposite to the direction of rotation. The incidence losses are not significantly changed; however, the flow must now be turned by a considerably smaller amount in order to follow the flow channel. Thus, the resultant sum of these three losses appears to be less, and an increase in Ψ_L occurs at a k_{is} of about 1.5. Below this point, as β_1 becomes increasingly negative, the relative flow becomes almost perpendicular to the blades. Thus, the advantage is lost, and the rotor efficiency deteriorates rapidly.

A plot of referred moment with bearing losses included, as a function of referred speed, is shown in Figure 38 for data obtained at a clearance of 0.081 inch. The values of the torque at zero speed resulting from the locked rotor tests are also shown. The effects of clearance on this parameter were also found to be negligible over the range of clearances from 0.015 to 0.081 inch, there being only slight random variations present in the resulting data. Therefore, Figure 38 is a representative plot for all clearances.

As expected, the maximum moment of about 16.1 foot-pounds was found to occur at zero speed and at a pressure ratio of 1.7. For the maximum speed of about 18,000 rpm, this pressure ratio yielded 6.3 foot-pounds for zero bearing losses and 6.8 foot-pounds for maximum bearing losses. The lowest pressure ratio, 1.2, consistently yielded the lowest values of moment. The moment curves of Vavra (1) and Riley (3) are almost identical to those obtained in these tests, except for the results obtained by Riley beyond the "critical" clearance.

In general, the torque produced by the flow energy at a given pressure ratio is a maximum at zero speed and decreases with increasing turbine speed. This may be explained by the law of angular momentum, which, by reference to the velocity diagram of Figure 15, can be written as

$$M = \dot{W} R_{2o} \left[\left(\frac{R_1}{R_{2o}} \right) V_{u1} - V_{u2} \right] \tag{63}$$

For a given pressure ratio, V_{u1} is nearly constant with speed, and the mass flow rate $\dot{W}$ decreases with increasing speed. From Figure 15, V_{u2} also increases with speed. Thus, it is seen that the torque produced, M, decreases with increasing turbine speed.

After completion of the test runs previously described, an informal trial run was made at a clearance of 0.100 inch in an attempt to determine the critical clearance. Although not conclusive, the results indicated no significant change in the values of the performance parameters. This implies that a reasonable overall efficiency may be maintained at clearances which might considerably exceed those tested in this analysis. Since these additional tests were not complete, the resulting data are not included in this report.

SECTION 5

CONCLUSIONS AND RECOMMENDATIONS

At a pressure ratio of 1.7, a clearance of 0.081 inch, and a head coefficient of 2.28, a maximum total-to-static overall efficiency of 84.6 per cent was obtained for the case where bearing losses were considered. The efficiency, referred moment, and degree of reaction were found to be independent of clearance over the range of clearances between 0.015 and 0.081 inch. A clearance tolerance of this sort is very important in small turbines and in turbines where thermal expansion must be considered. It is recommended that additional testing be performed in order to determine the precise clearance beyond which turbine performance deteriorates. Tests might also be conducted in which the clearance at the rotor discharge is varied in addition to the tip clearance, although this would require cutting the shrouds or the manufacture of additional shrouds with various annular openings.

The results of this investigation show that computations based on flow conditions at the outer discharge radius are simpler and more straightforward than those obtained by referring the losses to a calculated mass-average radius, and that this simplicity does not compromise the quality of the results. On the contrary, a correlation of the rotor velocity coefficient is obtained by this method, whereas previous efforts to obtain meaningful loss parameters were not successful (7).

There is strong evidence that the bearing loss data used in this investigation are no longer applicable. Correct data should be obtained either through new coast-down tests or through some implementation of the lubricating oil temperature differential across the bearings, as previously described. The latter method would be highly preferable since it would provide accurate loss information on a current basis and would correctly reflect any change in the mechanical condition of the bearings. Successful implementation of such a method would probably be contingent on a complete redesigning of the test rig, so that the oil lines are routed outside of the discharge flow as much as possible and are thoroughly insulated.

Since any inaccuracies in torque measurement introduce considerable error into the calculations as performed herein, additional effort is required in order to determine how to properly compensate the torque capsule output for thermal effects. An alternative solution would be to utilize a force (reluctance) capsule and a moment arm arrangement. This capsule could be remotely located and shielded so as to be free of the effects of the dynamometer bearing heat and the cold turbine discharge air.

It is recommended that the modifications described by Vavra (1) be performed in order to improve the component matching of the turbine and that further tests be carried out in order to determine the effects of these modifications on the performance parameters. Specifically, the enlarging of the guide vane discharge area or the reduction of the rotor discharge area would ultimately increase the relative rotor discharge velocity W_2, which would reduce the peripheral velocity V_{u2}. Greater turbine work, and thus higher efficiencies, should result.

It is felt that the turbine test rig is now in much better operating condition than for any previous tests. The instrumentation has been proven; and, for the first time, the axial clearances may be accurately set. Accordingly, further testing to verify and expand on the performance parameters obtained in this investigation is recommended.

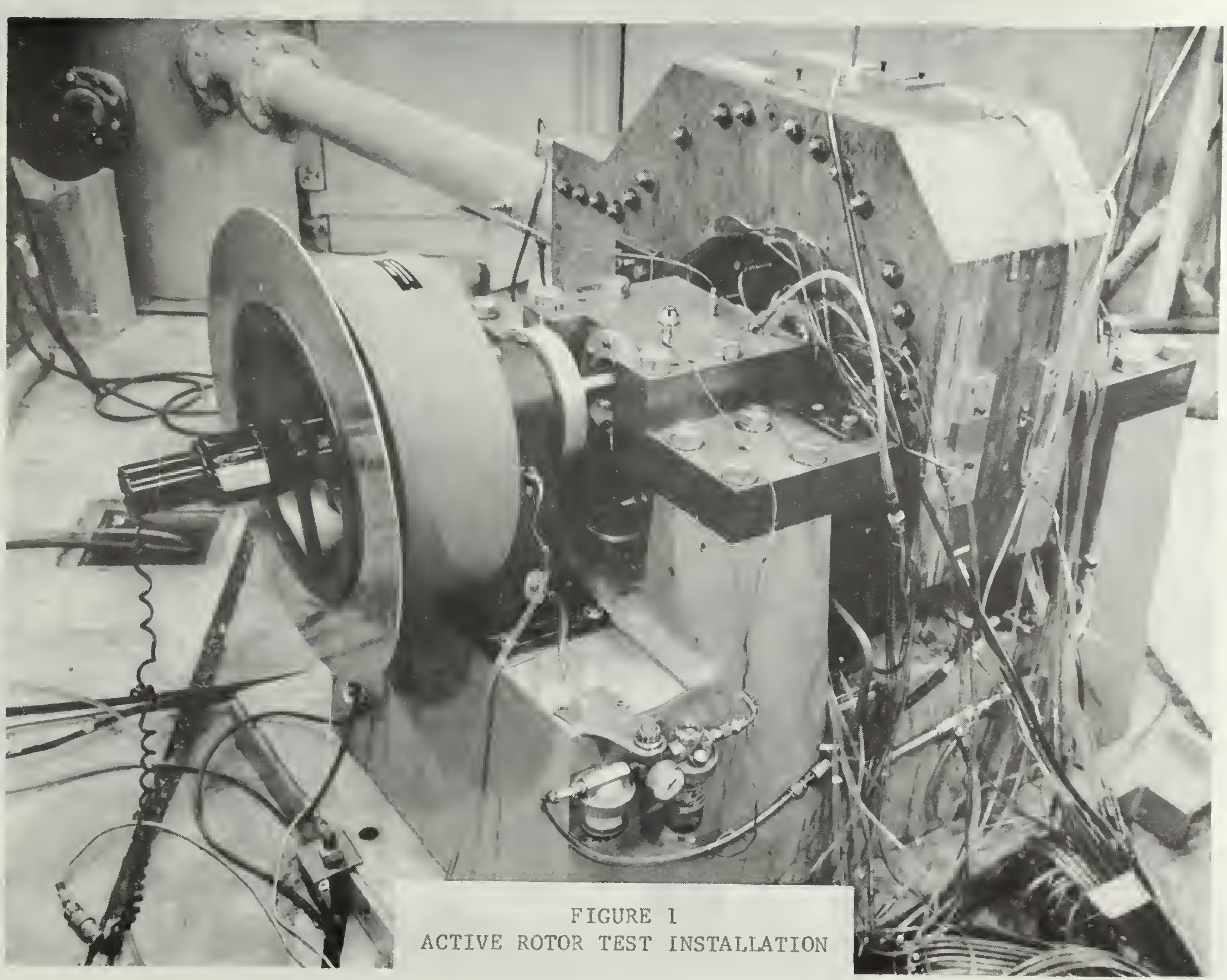

FIGURE 1
ACTIVE ROTOR TEST INSTALLATION

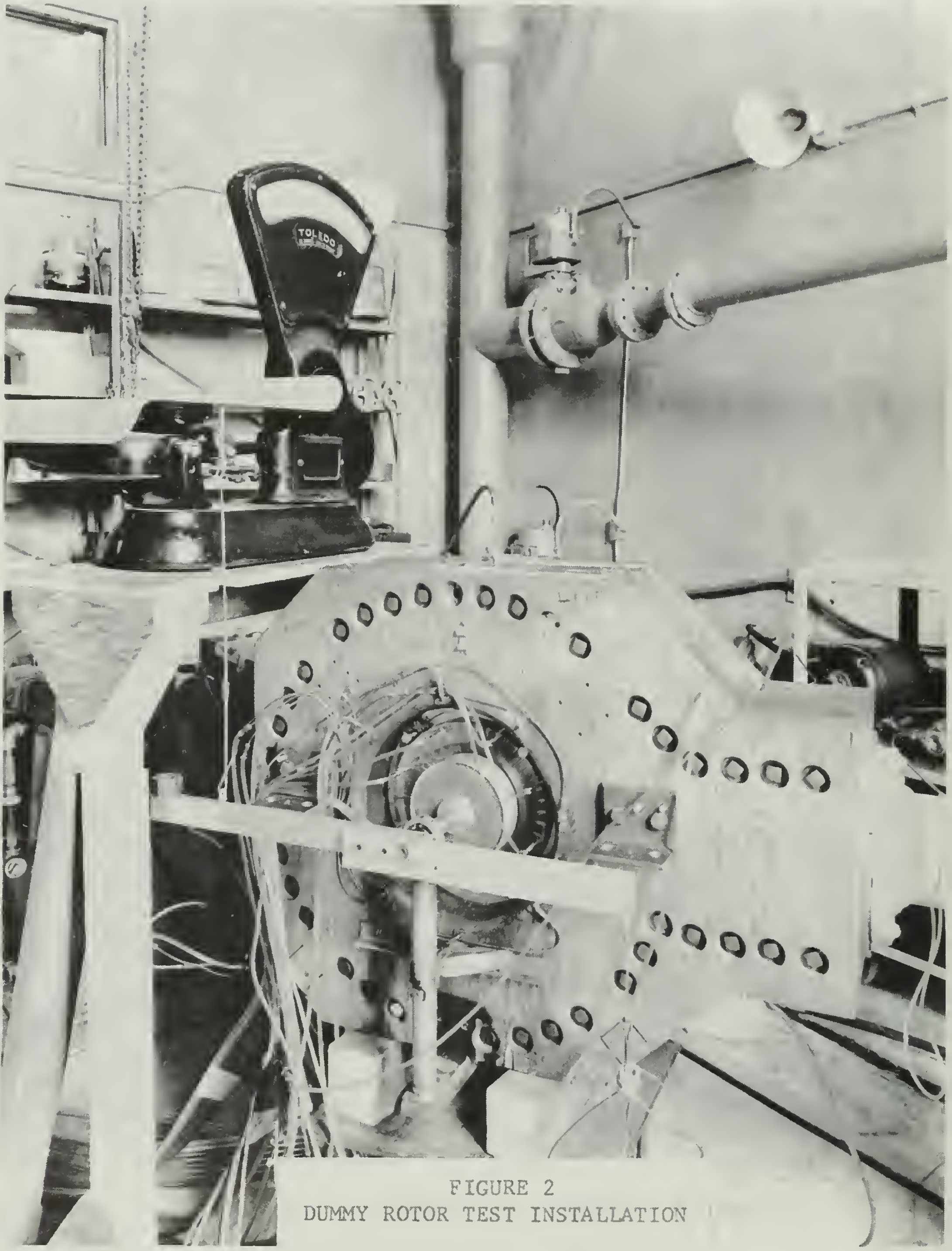

FIGURE 2
DUMMY ROTOR TEST INSTALLATION

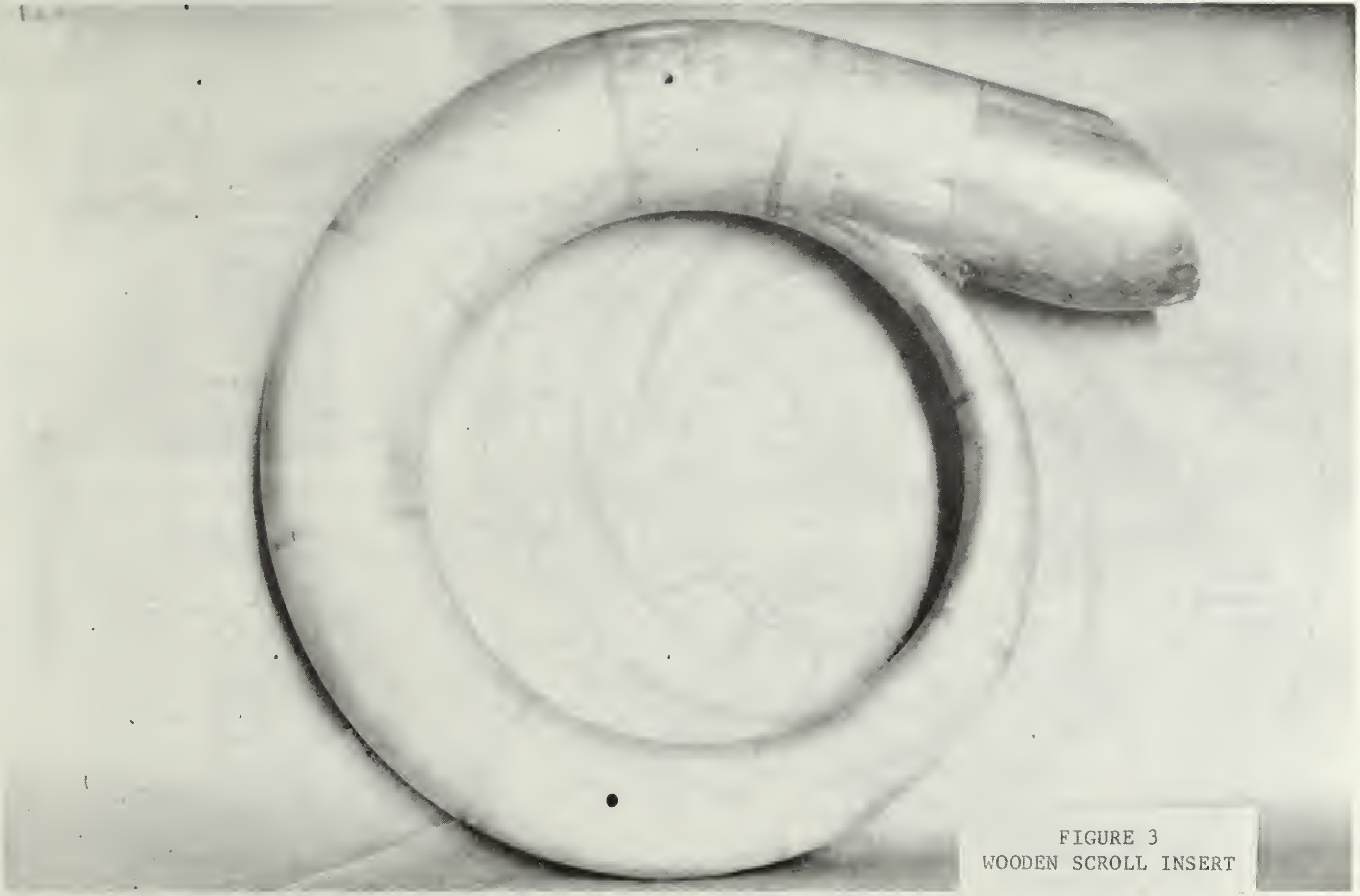

FIGURE 3
WOODEN SCROLL INSERT

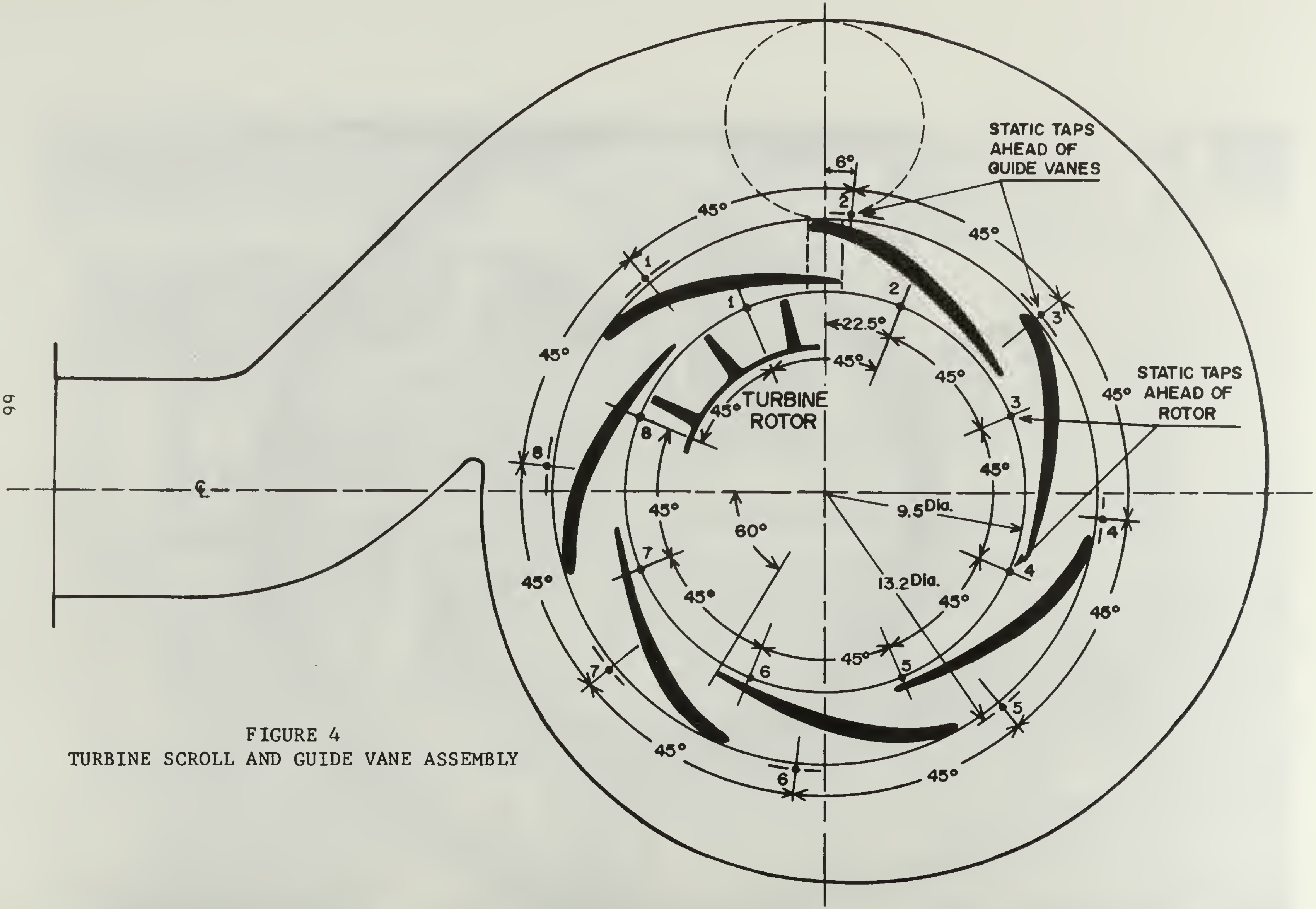
STATIC TAPS AHEAD OF GUIDE VANES
STATIC TAPS AHEAD OF ROTOR
TURBINE ROTOR
6°
22.5°
60°
45°
9.5 Dia.
13.2 Dia.
℄
1
2
3
4
5
6
7
8

FIGURE 4
TURBINE SCROLL AND GUIDE VANE ASSEMBLY

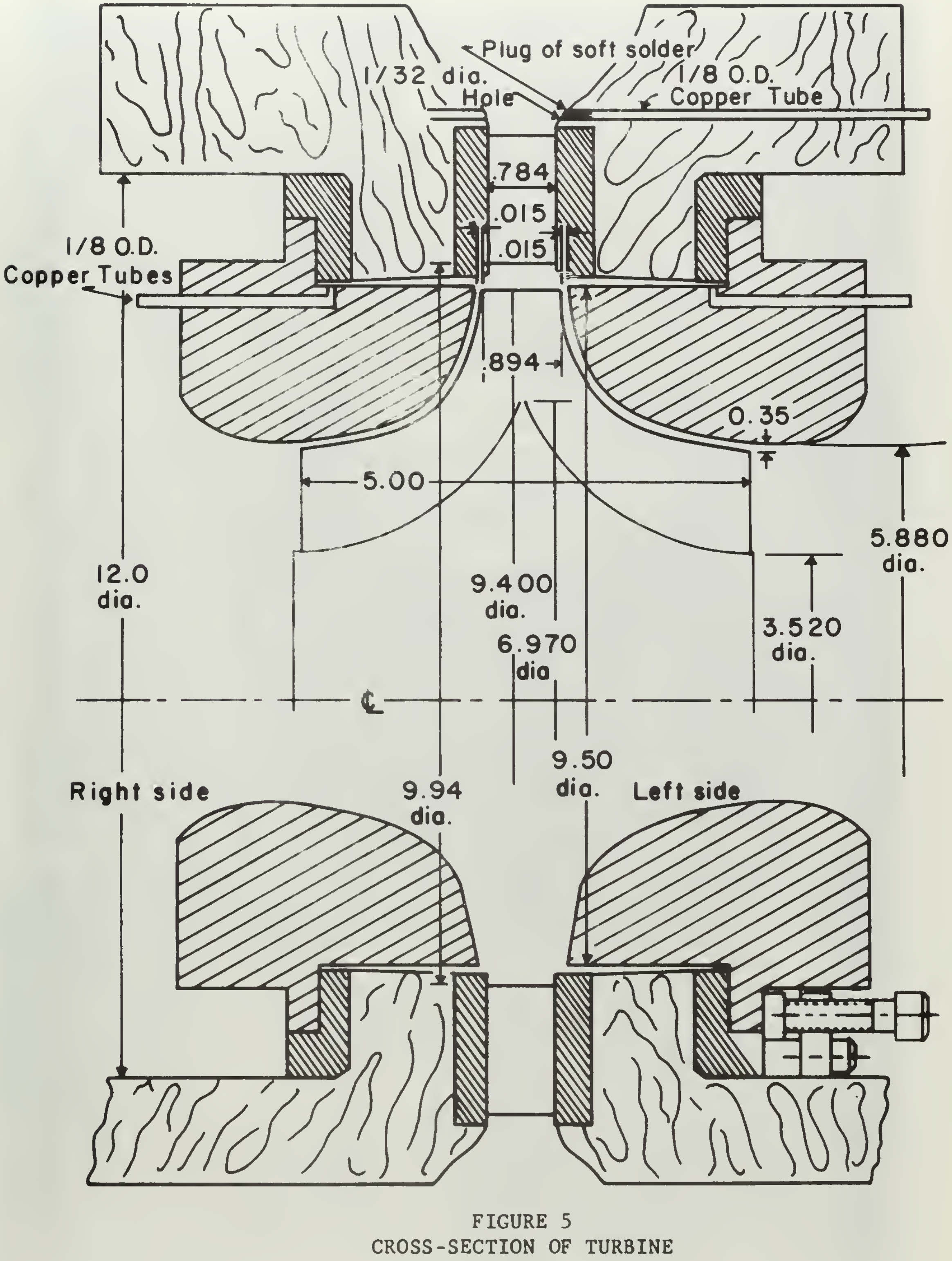
Plug of soft solder
1/32 dia. Hole
1/8 O.D. Copper Tube
.784
.015
.015
1/8 O.D. Copper Tubes
.894
0.35
5.00
5.880 dia.
12.0 dia.
9.400 dia.
3.520 dia.
6.970 dia
℄
9.50 dia.
Right side
9.94 dia.
Left side

FIGURE 5
CROSS-SECTION OF TURBINE

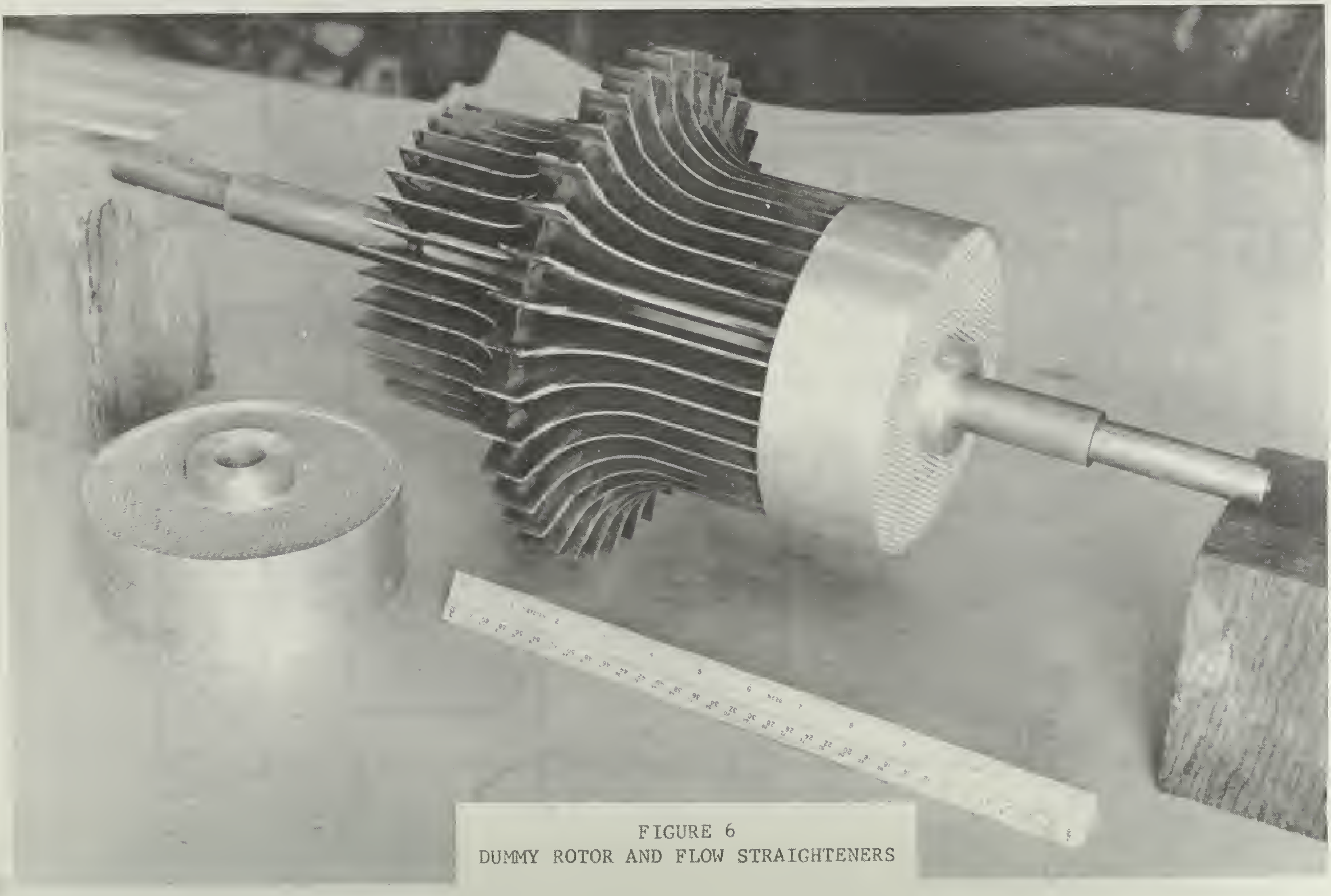

FIGURE 6
DUMMY ROTOR AND FLOW STRAIGHTENERS

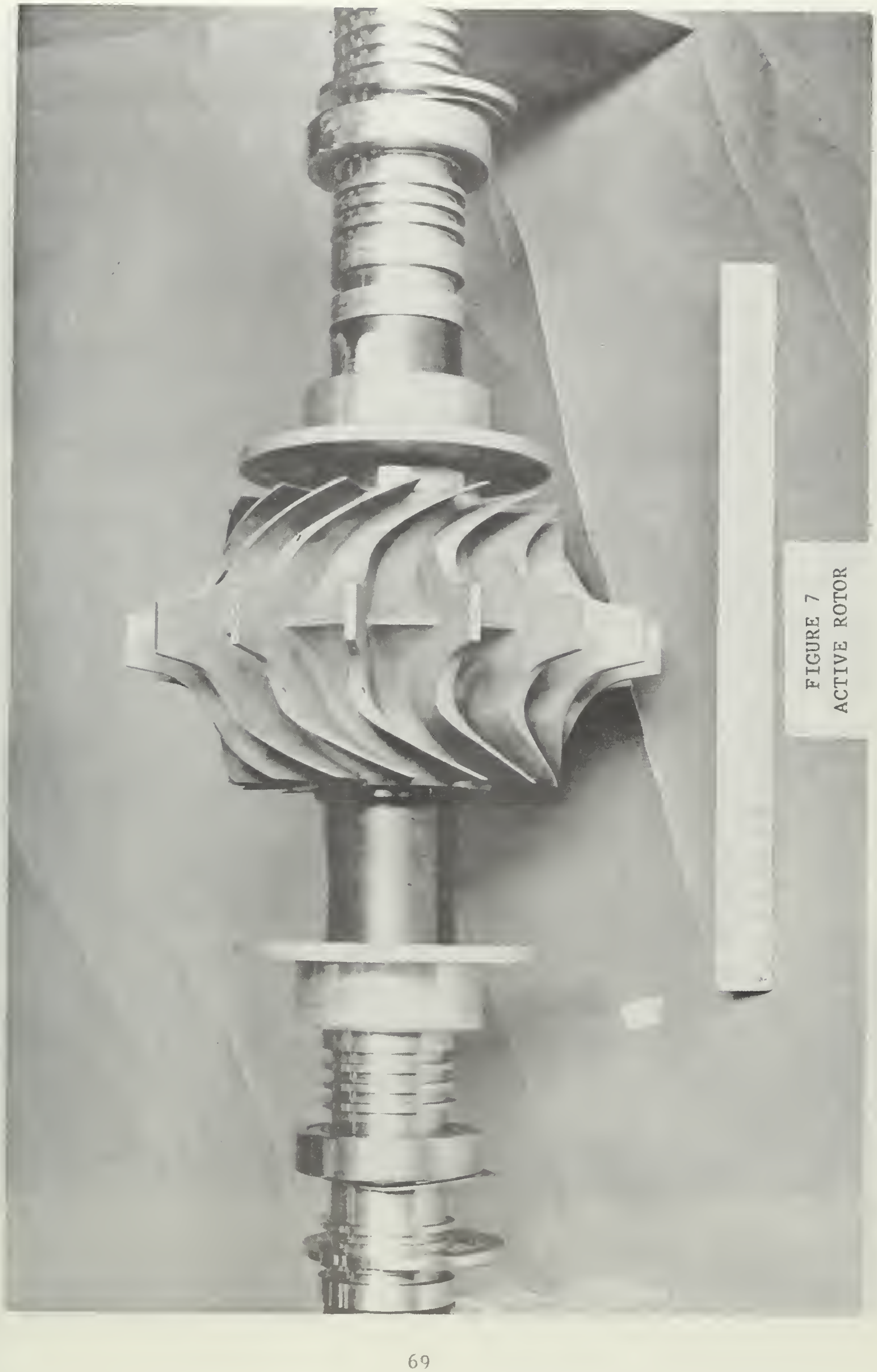

FIGURE 7
ACTIVE ROTOR

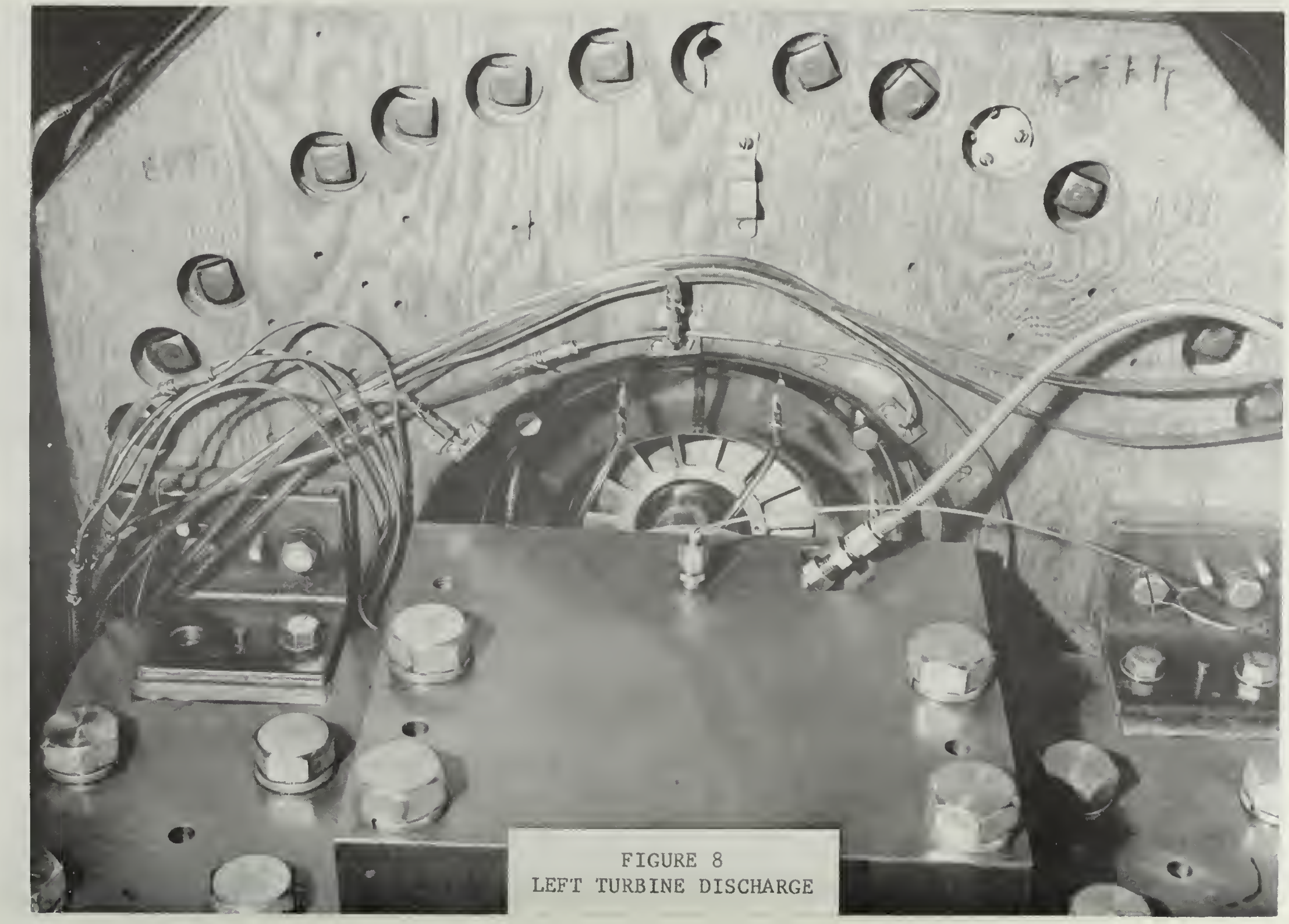

FIGURE 8
LEFT TURBINE DISCHARGE

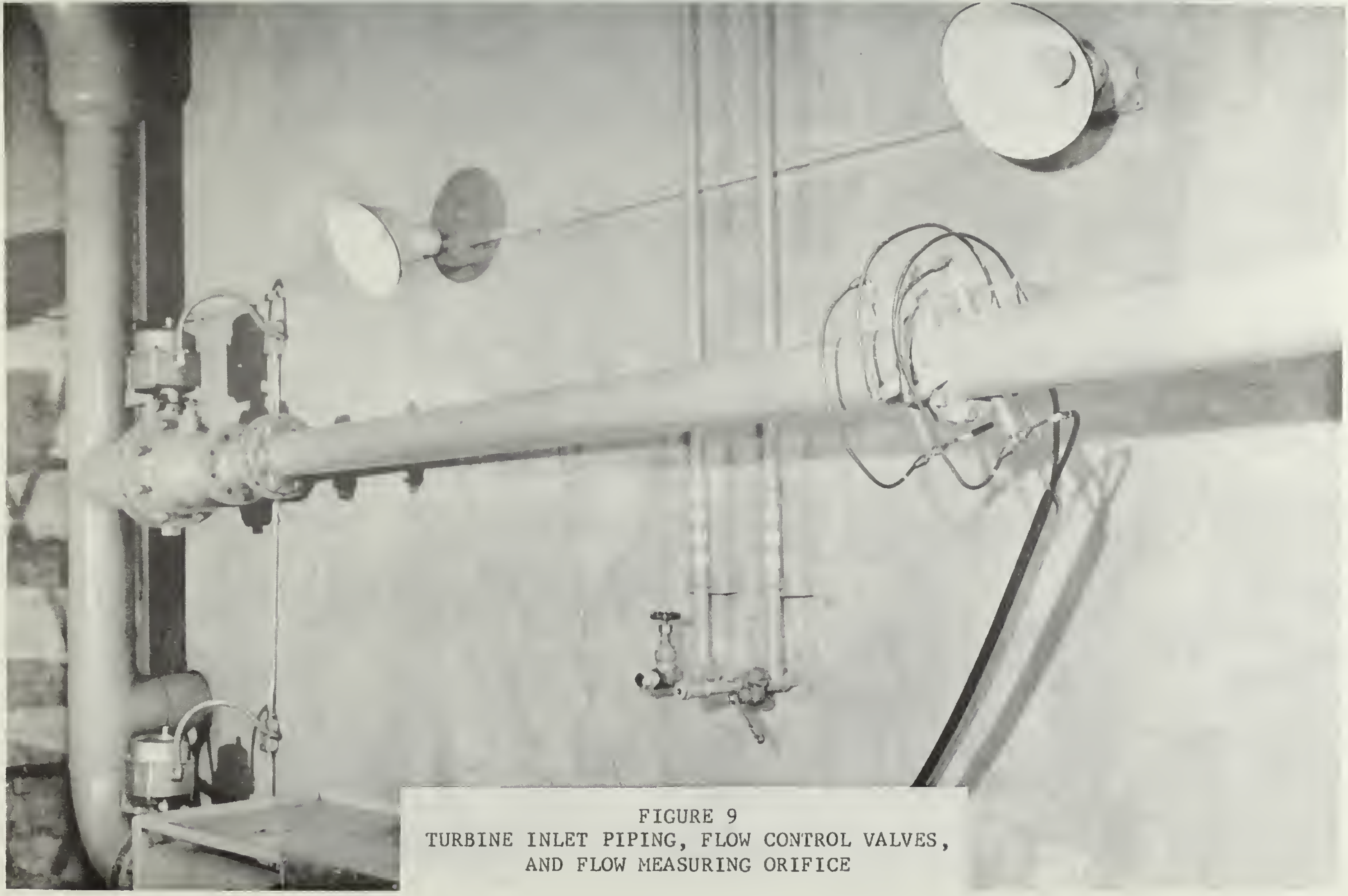

FIGURE 9
TURBINE INLET PIPING, FLOW CONTROL VALVES,
AND FLOW MEASURING ORIFICE

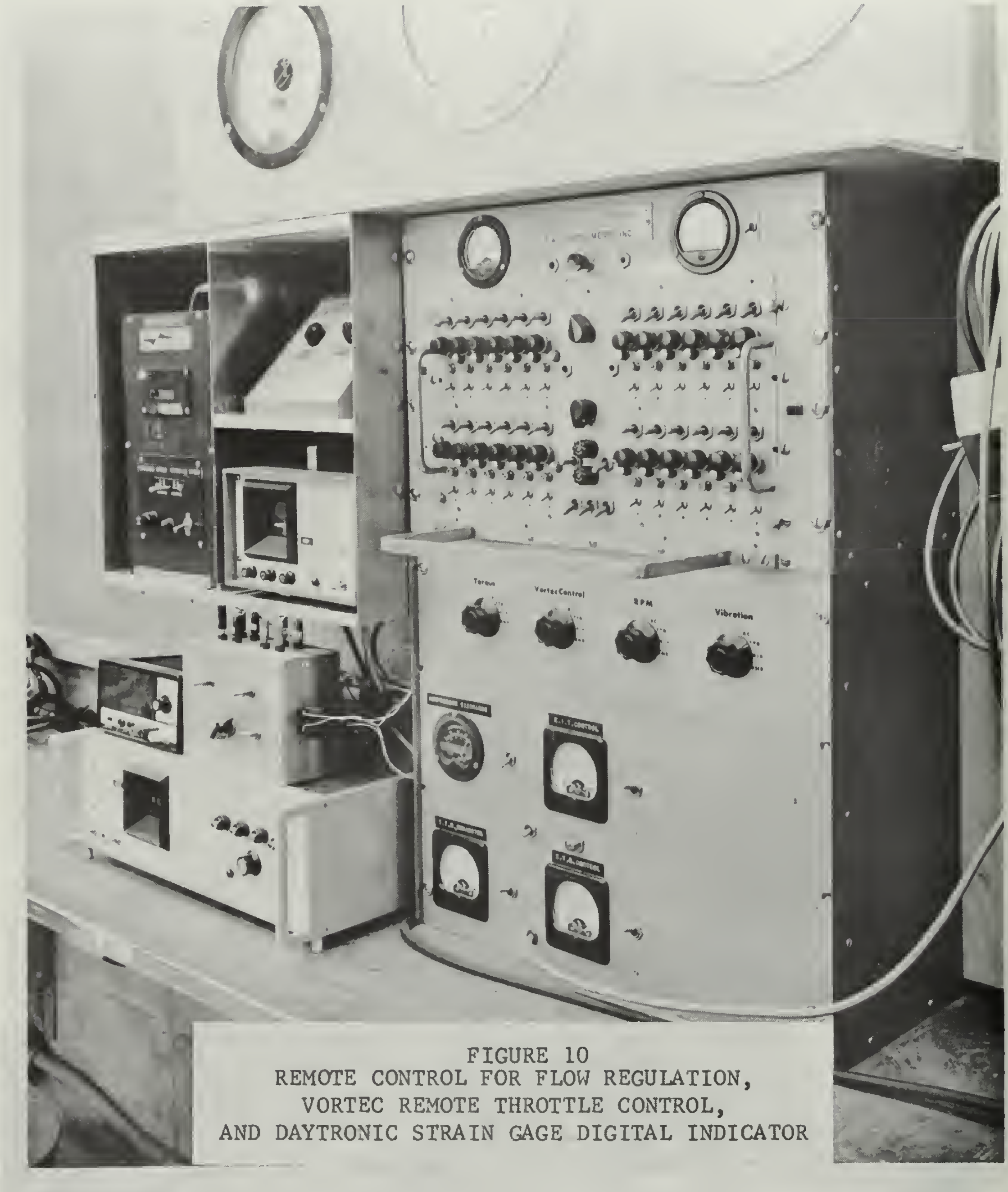
Torque
Vortec Control
RPM
Vibration

FIGURE 10
REMOTE CONTROL FOR FLOW REGULATION,
VORTEC REMOTE THROTTLE CONTROL,
AND DAYTRONIC STRAIN GAGE DIGITAL INDICATOR

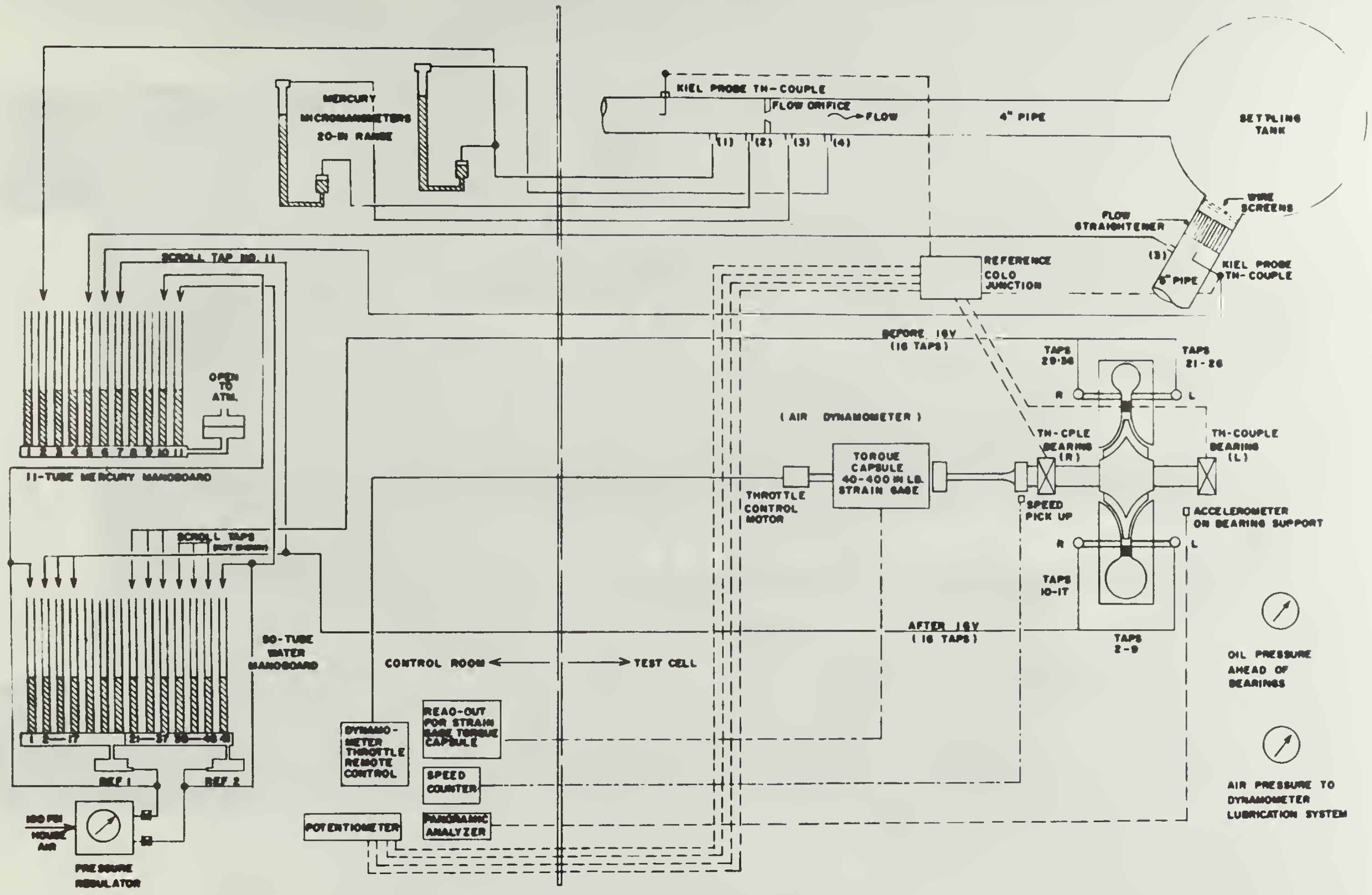
MERCURY MICROMANOMETERS 20-IN RANGE
KIEL PROBE TH-COUPLE
FLOW ORIFICE
FLOW
4" PIPE
SETTLING TANK
(1)
(2)
(3)
(4)
WIRE SCREENS
FLOW STRAIGHTENER
(3)
KIEL PROBE TH-COUPLE
8" PIPE
REFERENCE COLD JUNCTION
SCROLL TAP NO. 11
OPEN TO ATM.
11-TUBE MERCURY MANOBOARD
BEFORE IGV (16 TAPS)
TAPS 29-36
TAPS 21-26
R
L
(AIR DYNAMOMETER)
TORQUE CAPSULE 40-400 IN LB. STRAIN GAGE
THROTTLE CONTROL MOTOR
TH-CPLE BEARING (R)
TH-COUPLE BEARING (L)
SPEED PICK UP
ACCELEROMETER ON BEARING SUPPORT
TAPS 10-17
TAPS 2-9
AFTER IGV (16 TAPS)
SCROLL TAPS (NOT SHOWN)
50-TUBE WATER MANOBOARD
CONTROL ROOM
TEST CELL
OIL PRESSURE AHEAD OF BEARINGS
AIR PRESSURE TO DYNAMOMETER LUBRICATION SYSTEM
1 2—17
21—37 38—48 49
REF 1
REF 2
100 PSI HOUSE AIR
PRESSURE REGULATOR
DYNAMOMETER THROTTLE REMOTE CONTROL
READ-OUT FOR STRAIN GAGE TORQUE CAPSULE
SPEED COUNTER
POTENTIOMETER
PANORAMIC ANALYZER

FIGURE 11
SCHEMATIC OF RADIAL TURBINE INSTRUMENTATION

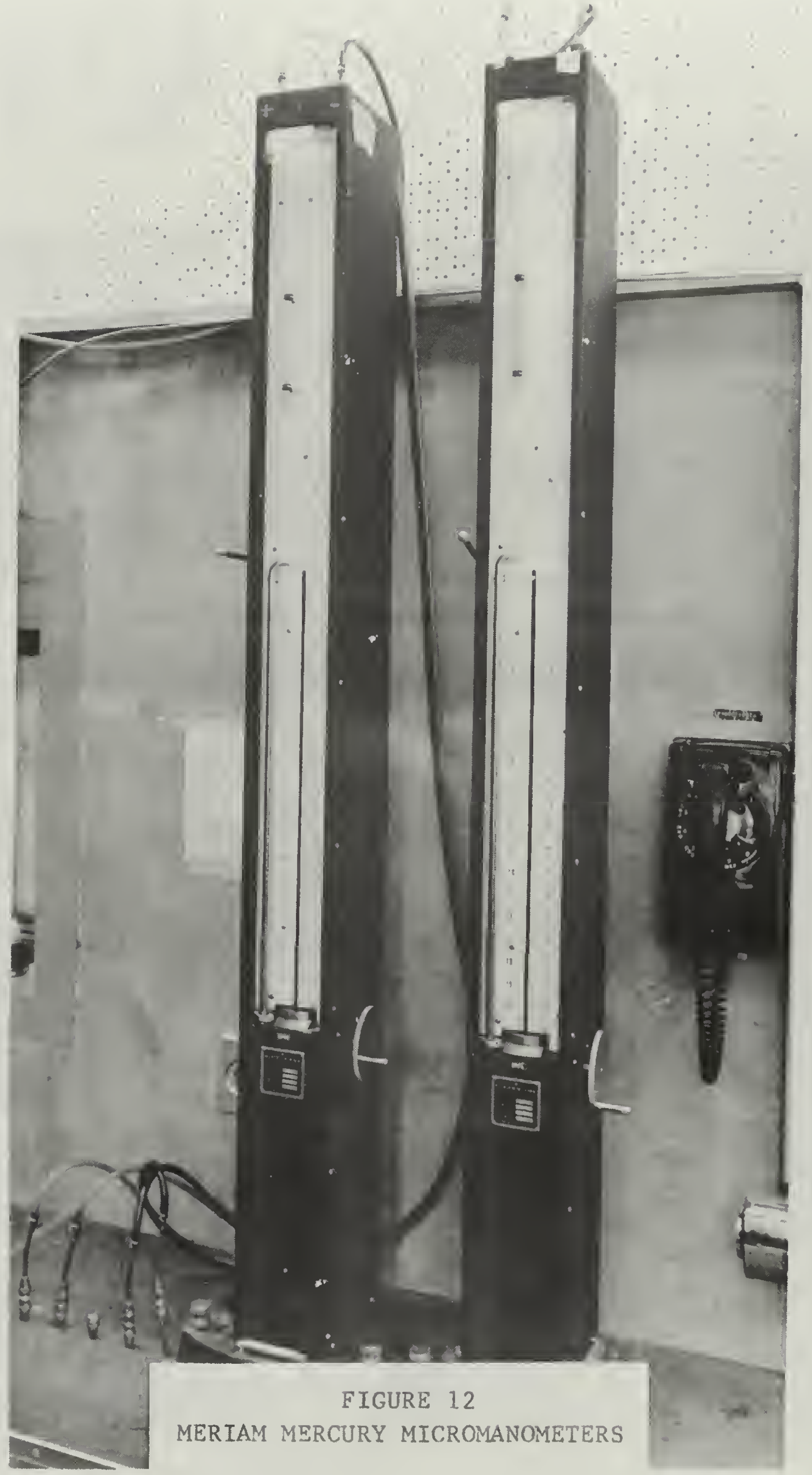

FIGURE 12
MERIAM MERCURY MICROMANOMETERS

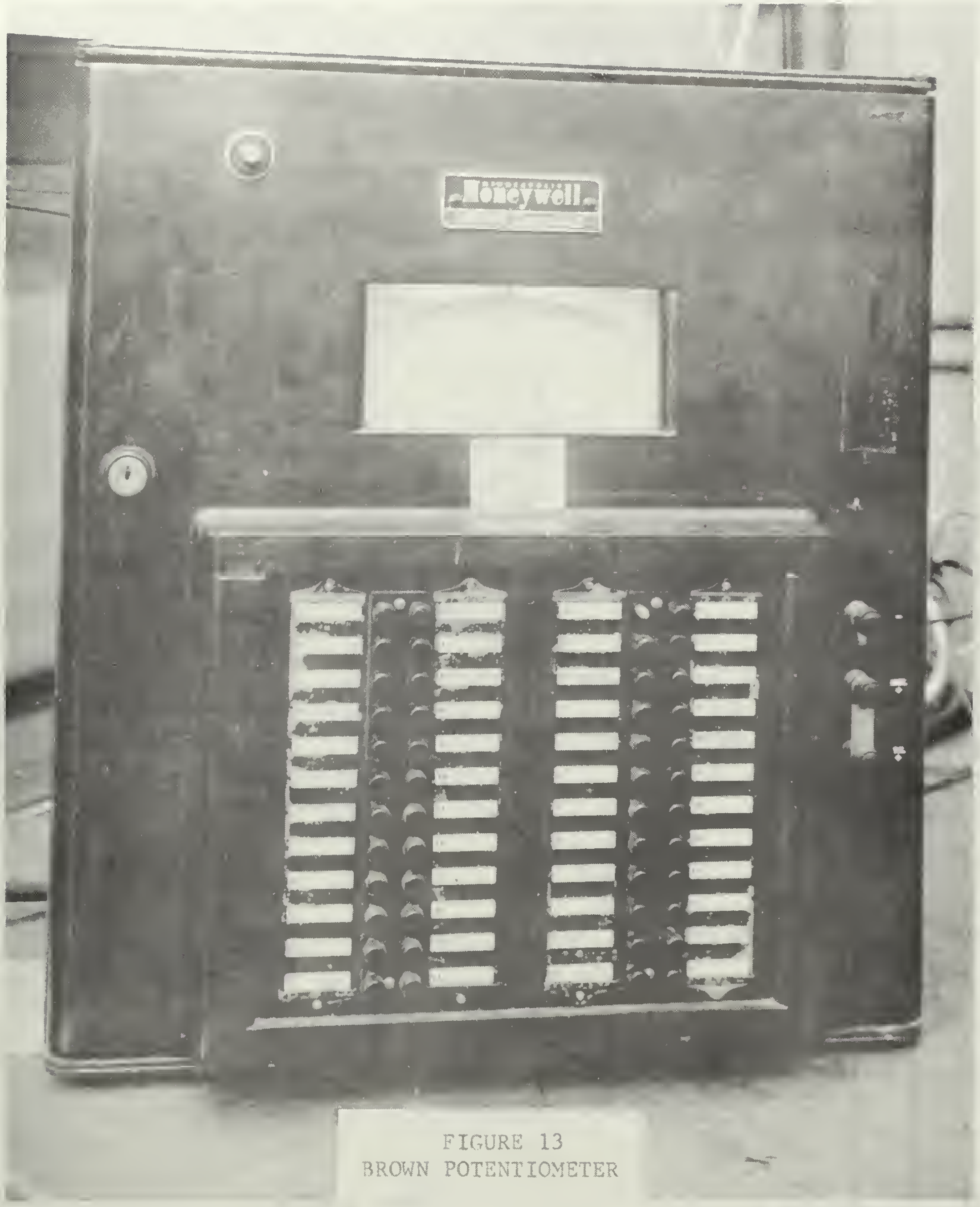

FIGURE 13
BROWN POTENTIOMETER

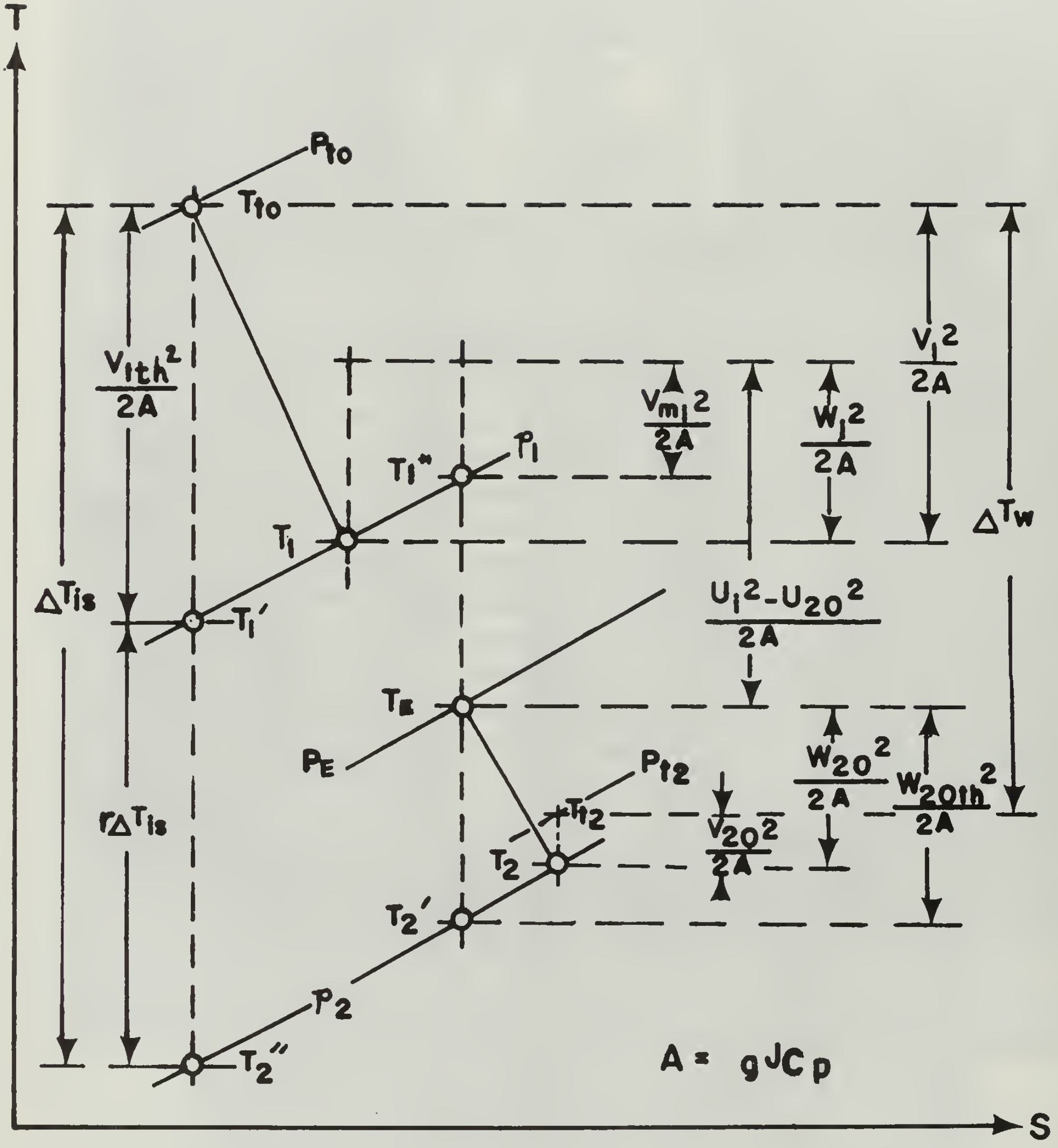
T
S
P_{t0}
T_{t0}
$\frac{V_{1th}^2}{2A}$
ΔT_{is}
$r\Delta T_{is}$
T_1'
T_1
T_1^*
P_1
$\frac{V_{m1}^2}{2A}$
$\frac{W_1^2}{2A}$
$\frac{V_1^2}{2A}$
ΔT_w
$\frac{U_1^2-U_{20}^2}{2A}$
T_E
P_E
P_{t2}
T_{t2}
T_2
$\frac{V_{20}^2}{2A}$
$\frac{W_{20}^2}{2A}$
$\frac{W_{20th}^2}{2A}$
T_2'
P_2
T_2''
$A = gJC_p$

FIGURE 14
TEMPERATURE-ENTROPY DIAGRAM FOR RADIAL TURBINE

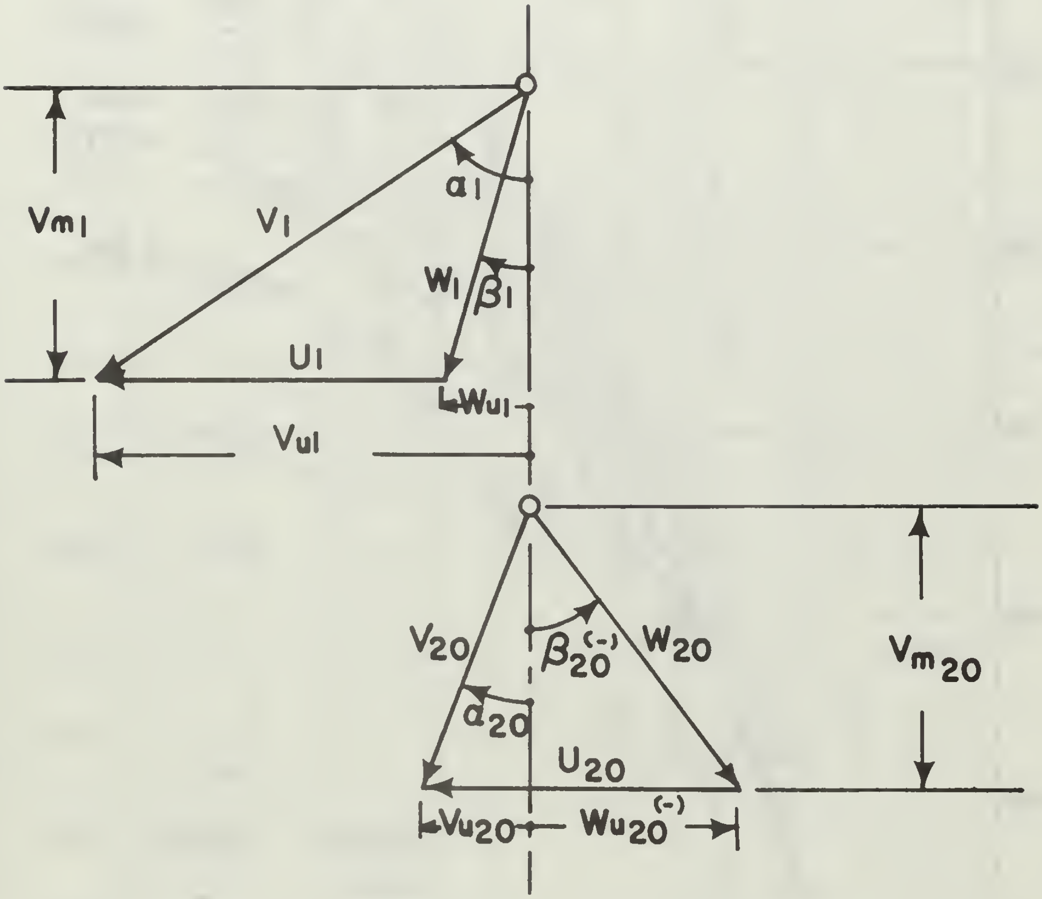

Vm1
V1
α1
W1
β1
U1
Wu1
Vu1
V20
β20 (-)
W20
Vm20
α20
U20
Vu20
Wu20 (-)

FIGURE 15
VELOCITY DIAGRAMS FOR RADIAL TURBINE

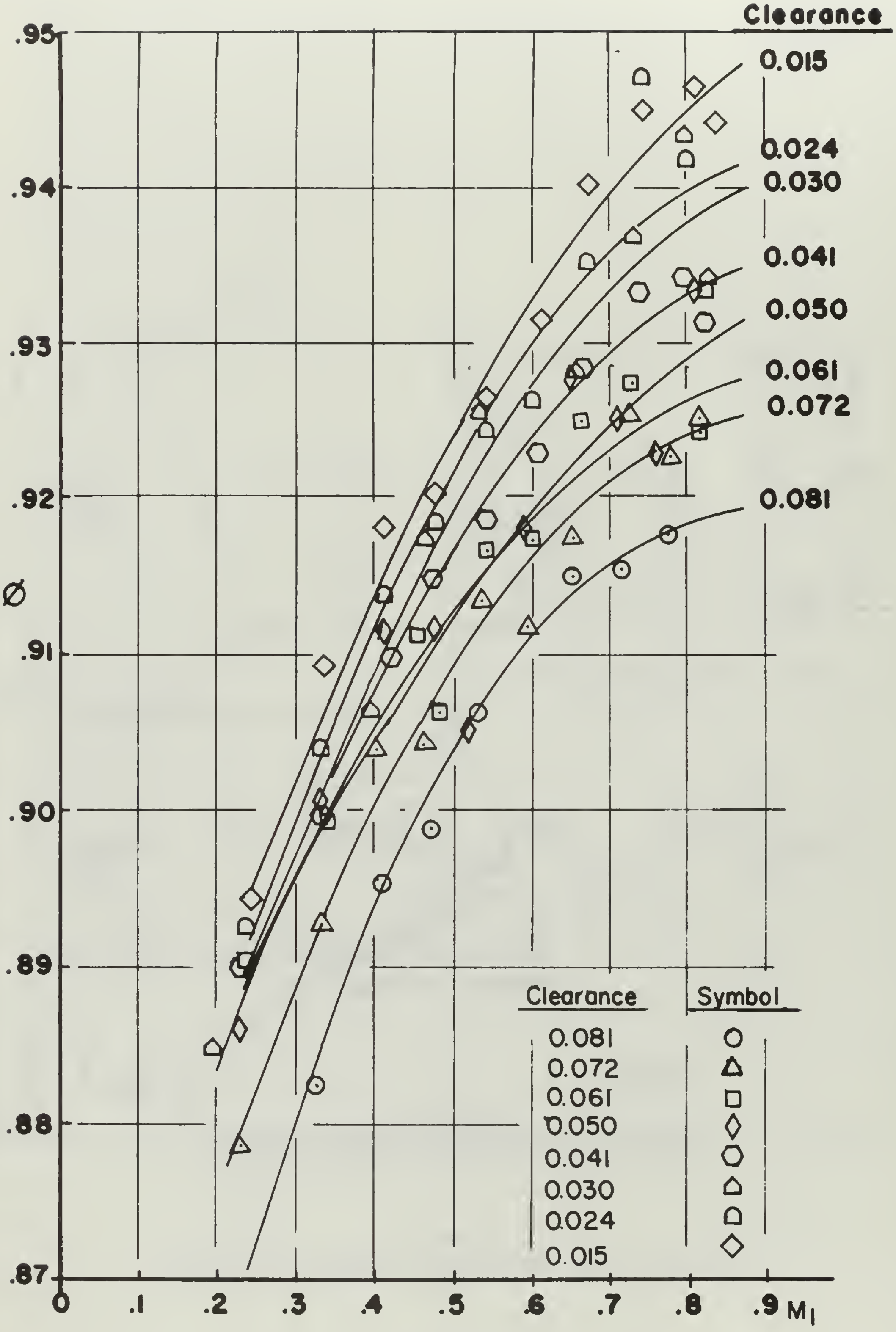

FIGURE 16
VELOCITY COEFFICIENT VS. MACH NUMBER

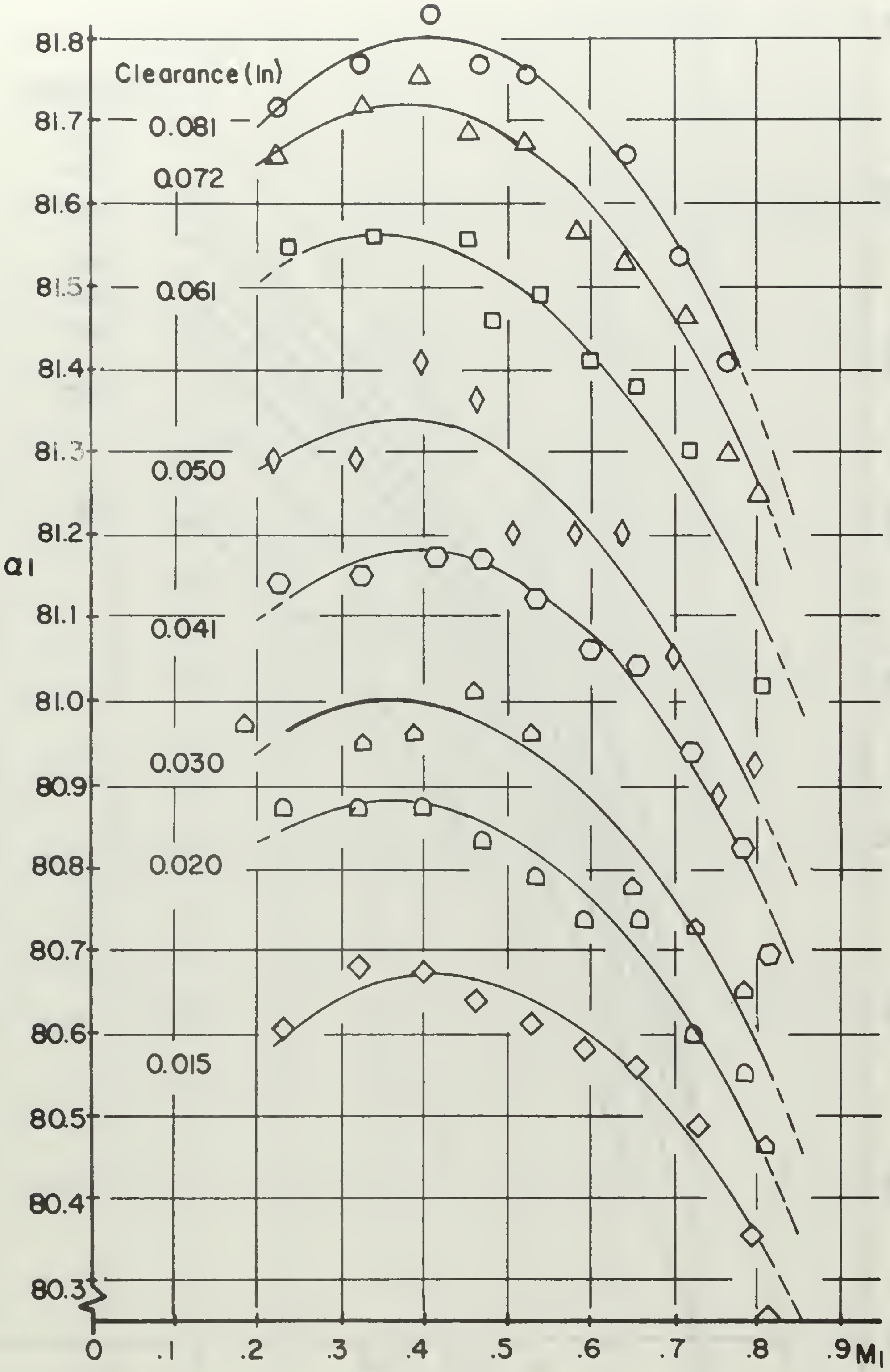

FIGURE 17
ABSOLUTE ROTOR INLET FLOW ANGLE VS. MACH NUMBER

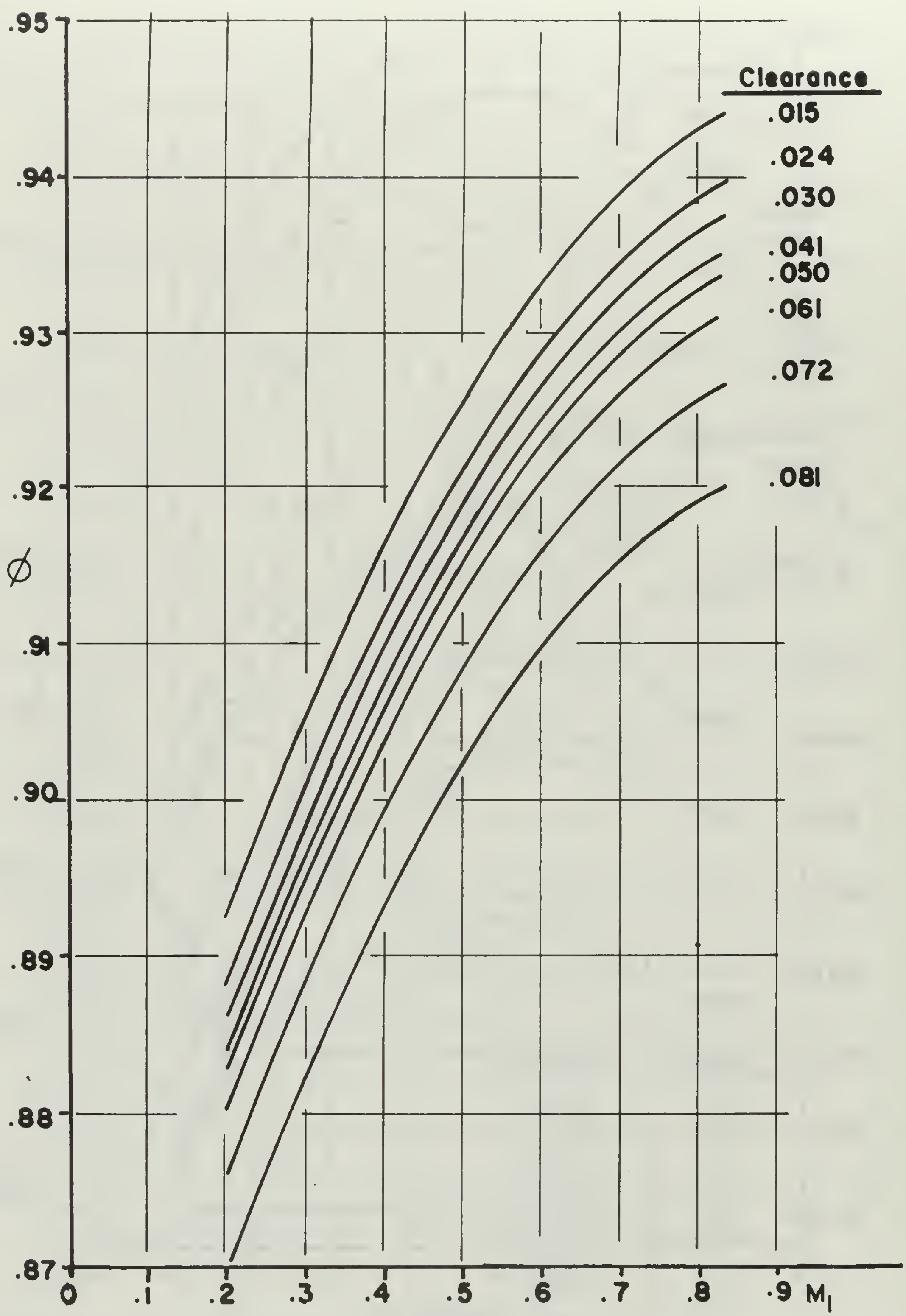

FIGURE 18
VELOCITY COEFFICIENT VS. MACH NUMBER
FROM DERIVED EQUATION

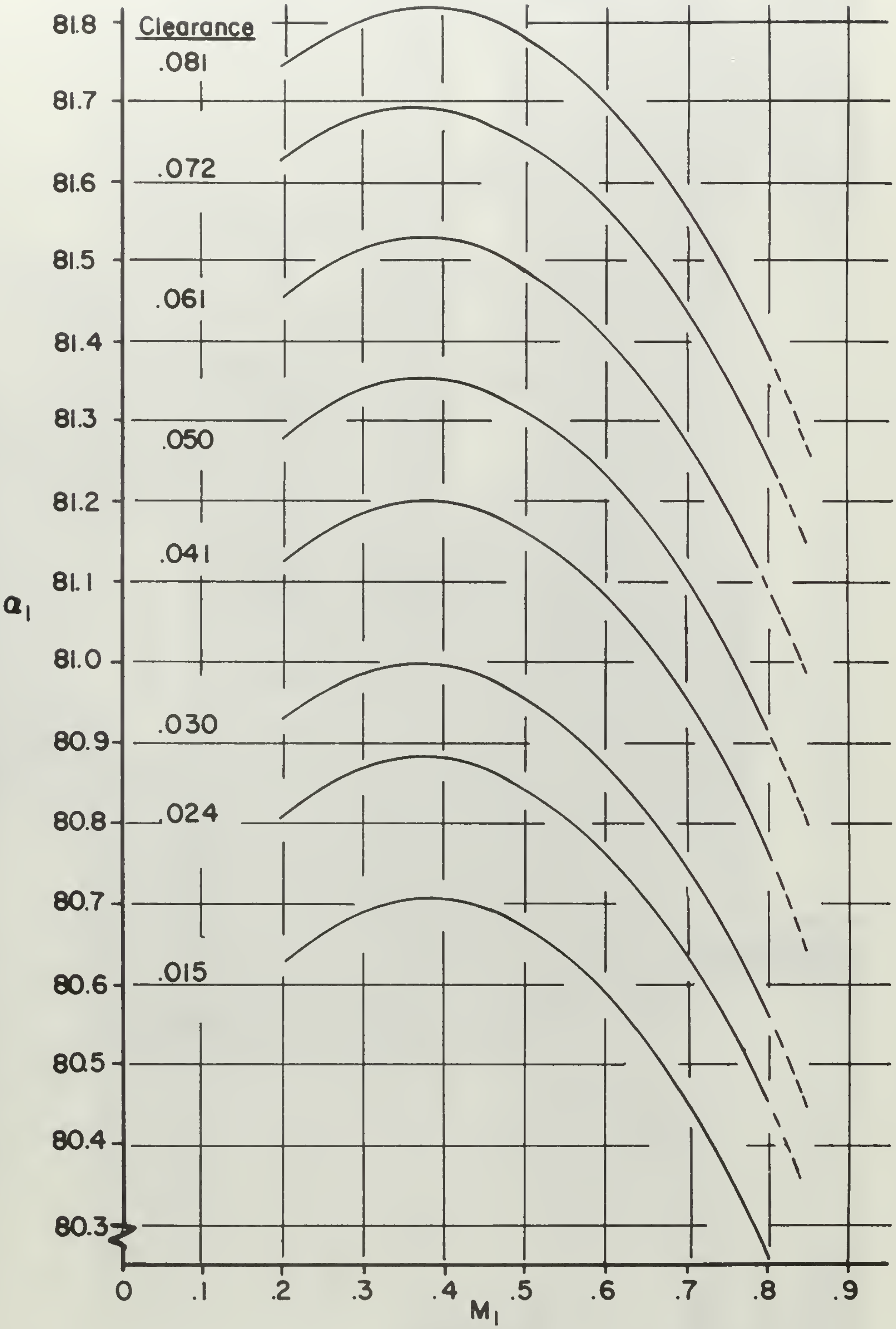

FIGURE 19
ABSOLUTE ROTOR INLET FLOW ANGLE VS. MACH NUMBER
FROM DERIVED EQUATION

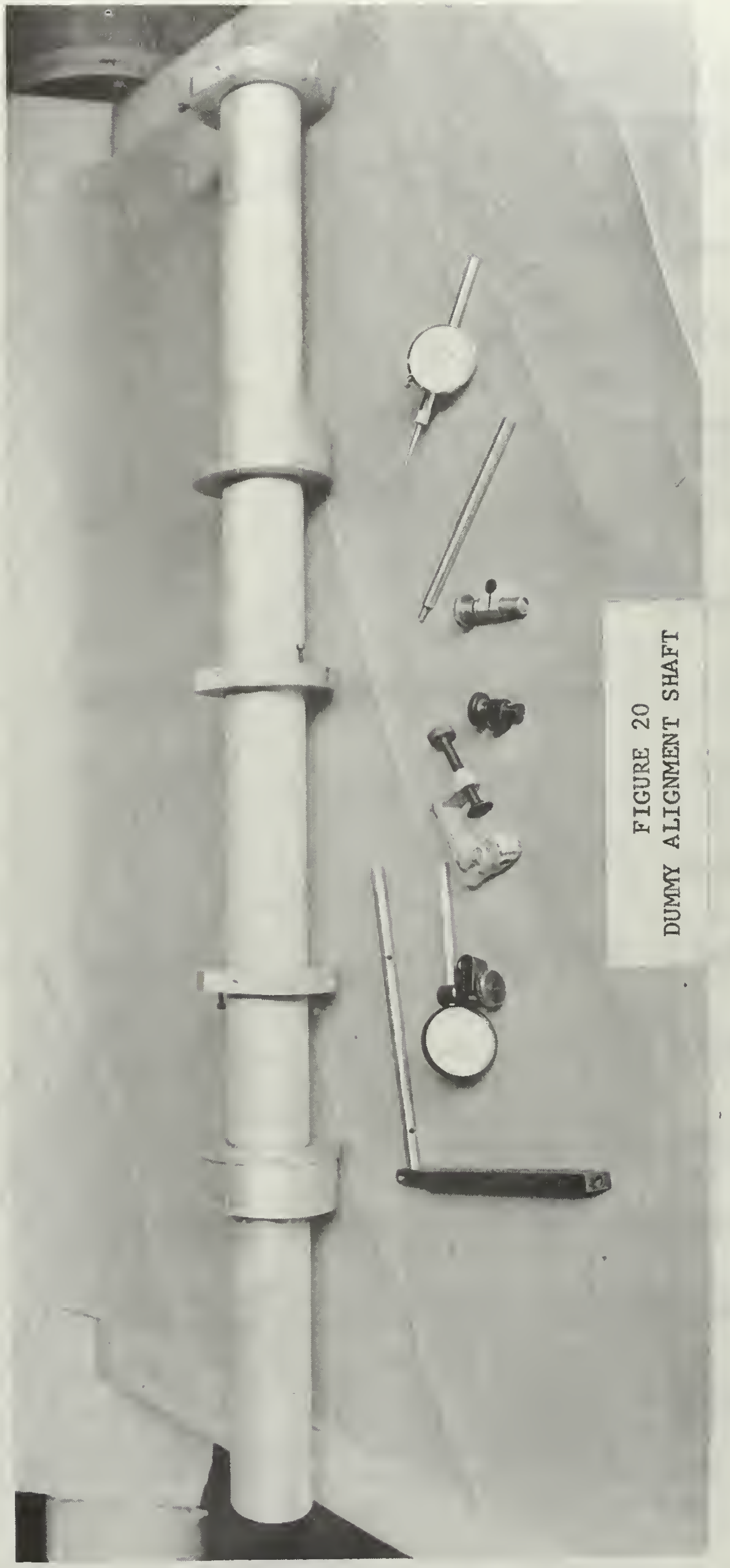

FIGURE 20
DUMMY ALIGNMENT SHAFT

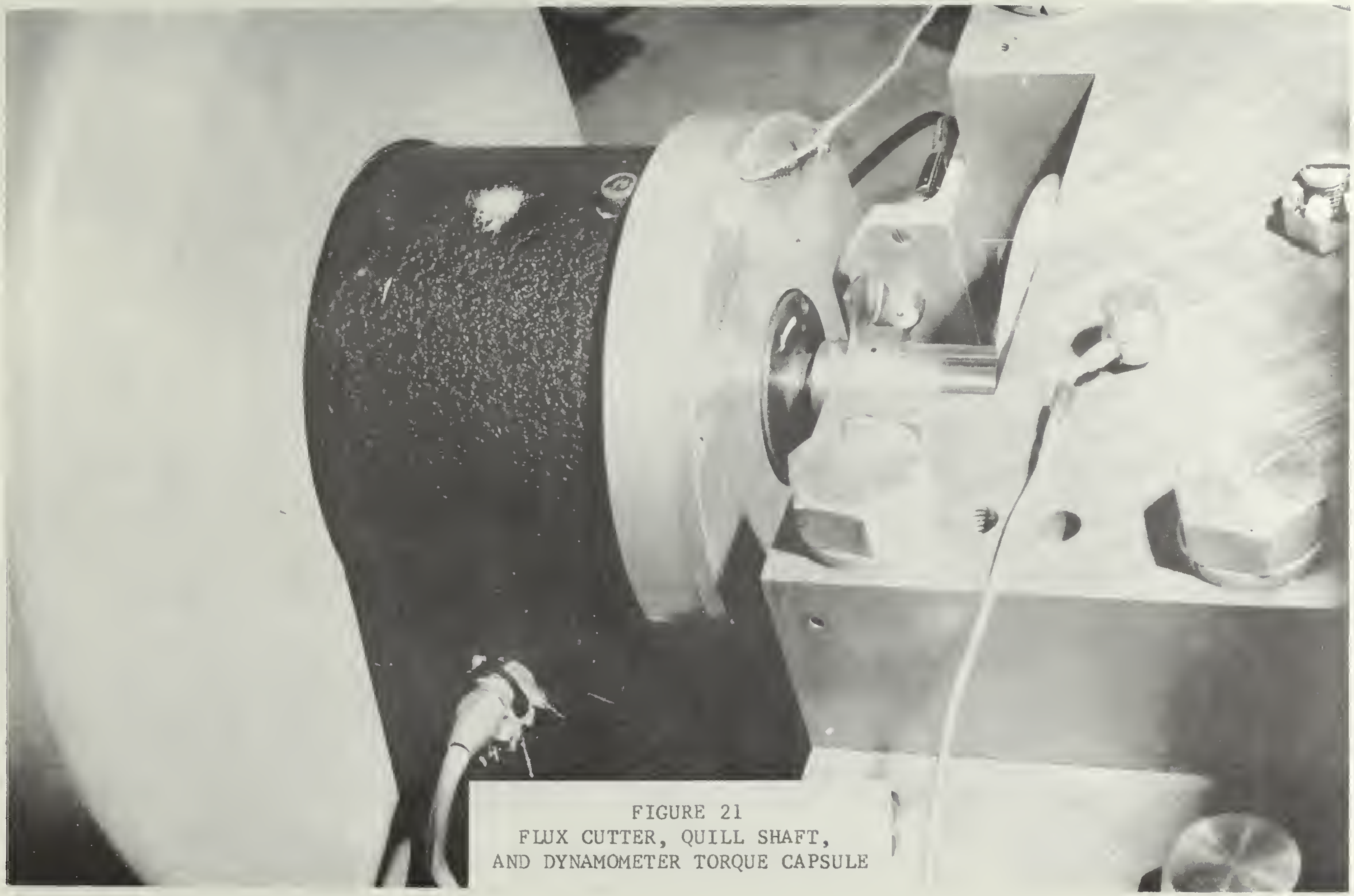

FIGURE 21
FLUX CUTTER, QUILL SHAFT,
AND DYNAMOMETER TORQUE CAPSULE

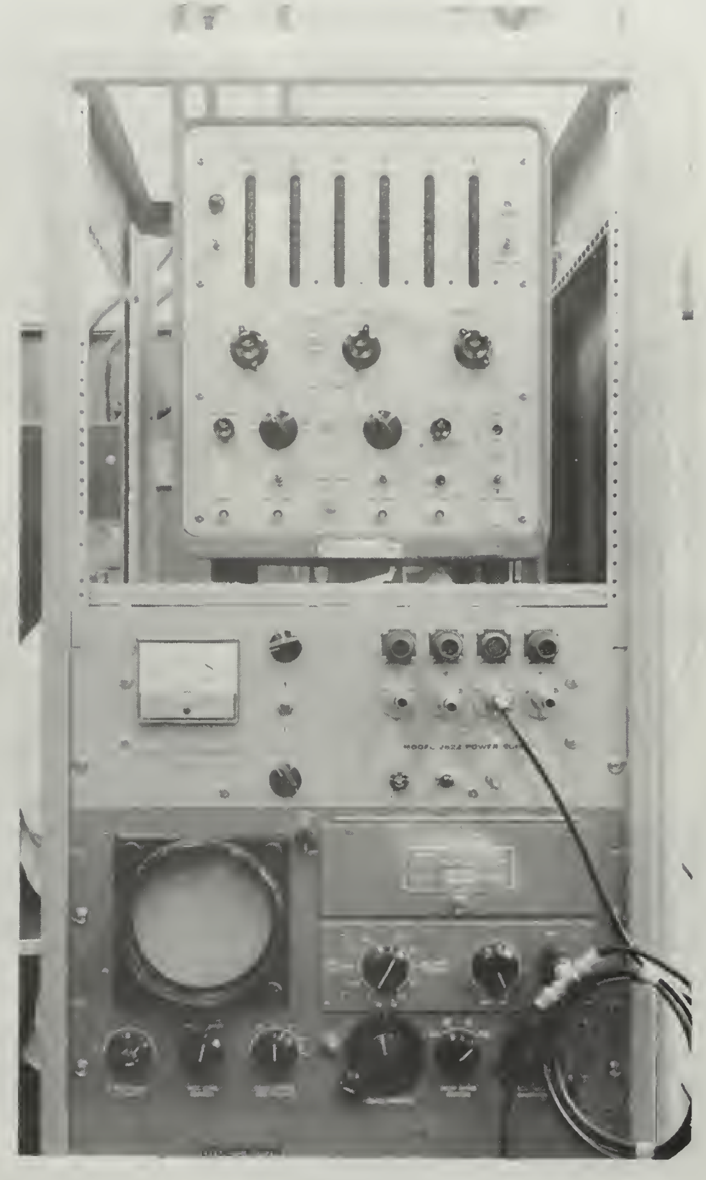

FIGURE 22
ELECTRONIC SPEED COUNTER
AND VIBRATION ANALYZER

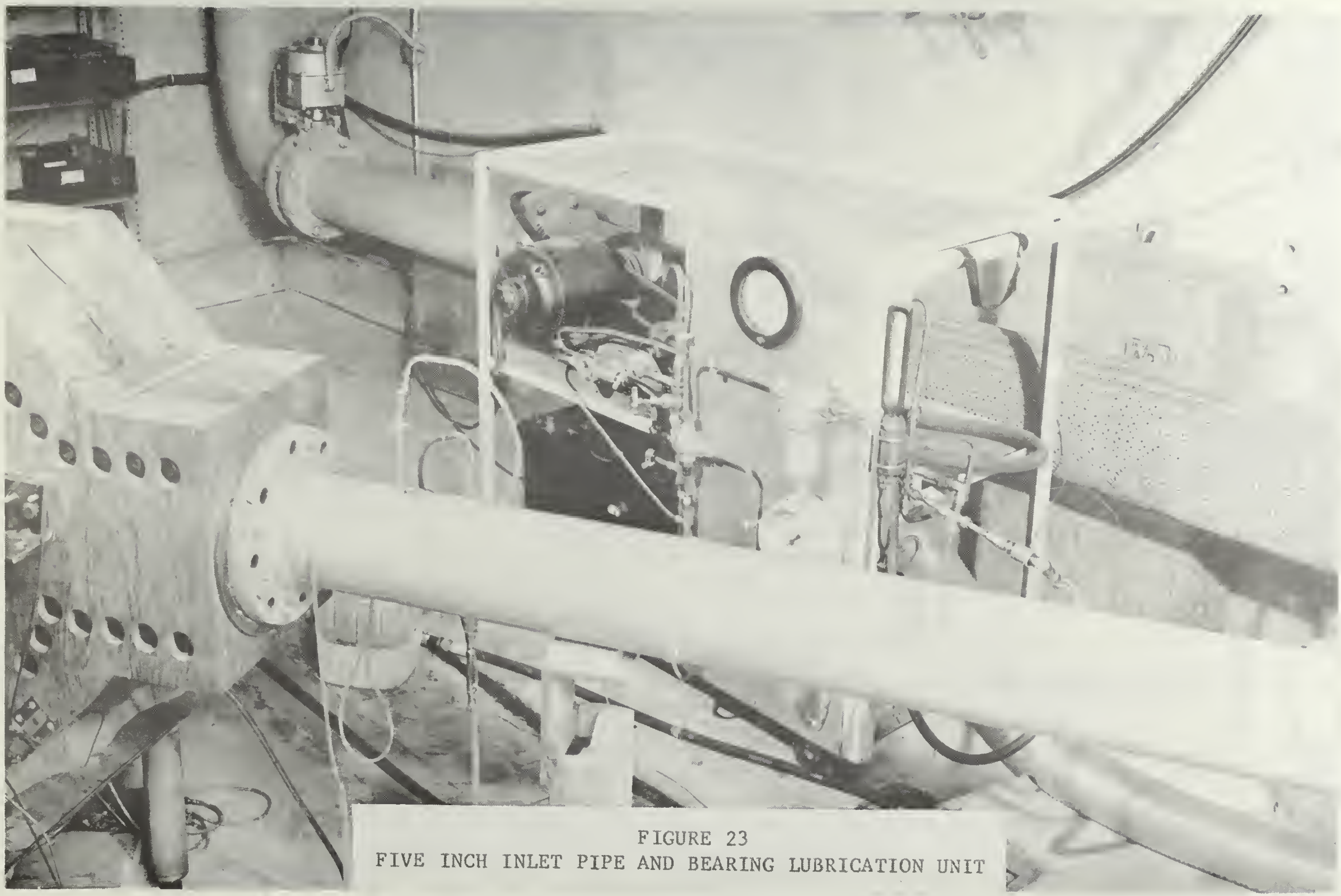

FIGURE 23
FIVE INCH INLET PIPE AND BEARING LUBRICATION UNIT

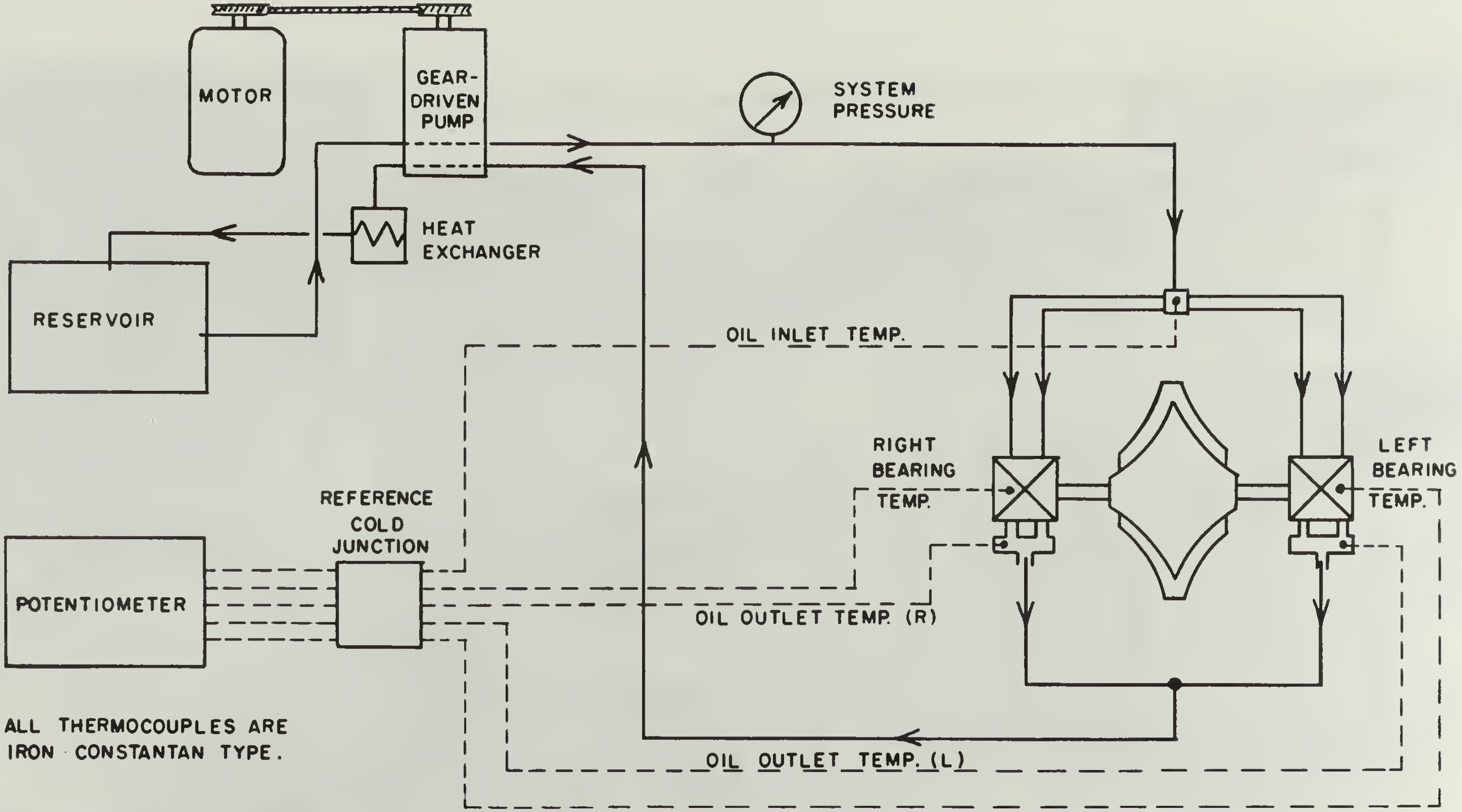
MOTOR
GEAR-DRIVEN PUMP
SYSTEM PRESSURE
HEAT EXCHANGER
RESERVOIR
OIL INLET TEMP.
RIGHT BEARING TEMP.
LEFT BEARING TEMP.
REFERENCE COLD JUNCTION
POTENTIOMETER
OIL OUTLET TEMP. (R)
OIL OUTLET TEMP. (L)

ALL THERMOCOUPLES ARE
IRON · CONSTANTAN TYPE.

FIGURE 24
SCHEMATIC OF TURBINE LUBRICATION SYSTEM

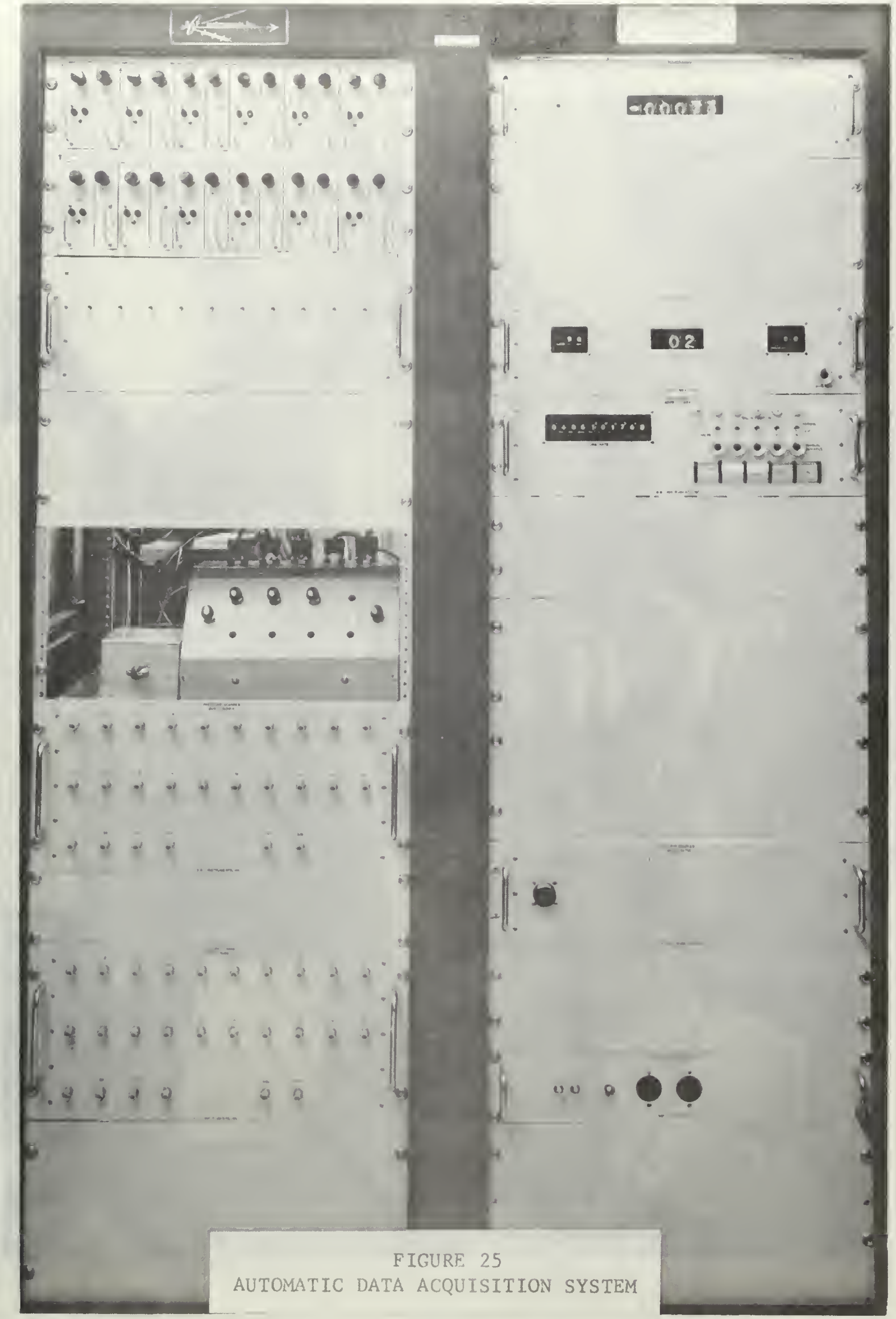

FIGURE 25
AUTOMATIC DATA ACQUISITION SYSTEM

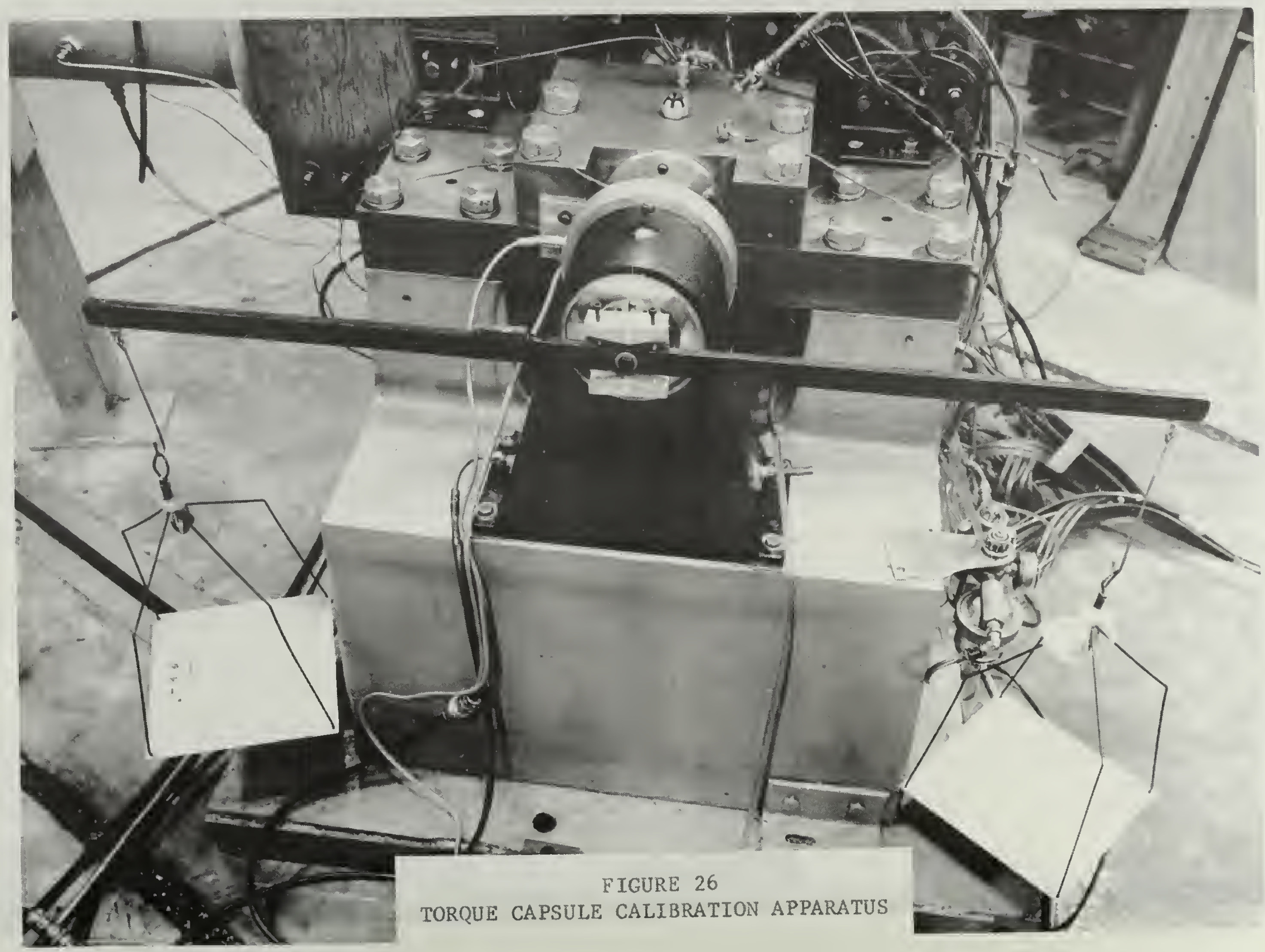

FIGURE 26
TORQUE CAPSULE CALIBRATION APPARATUS

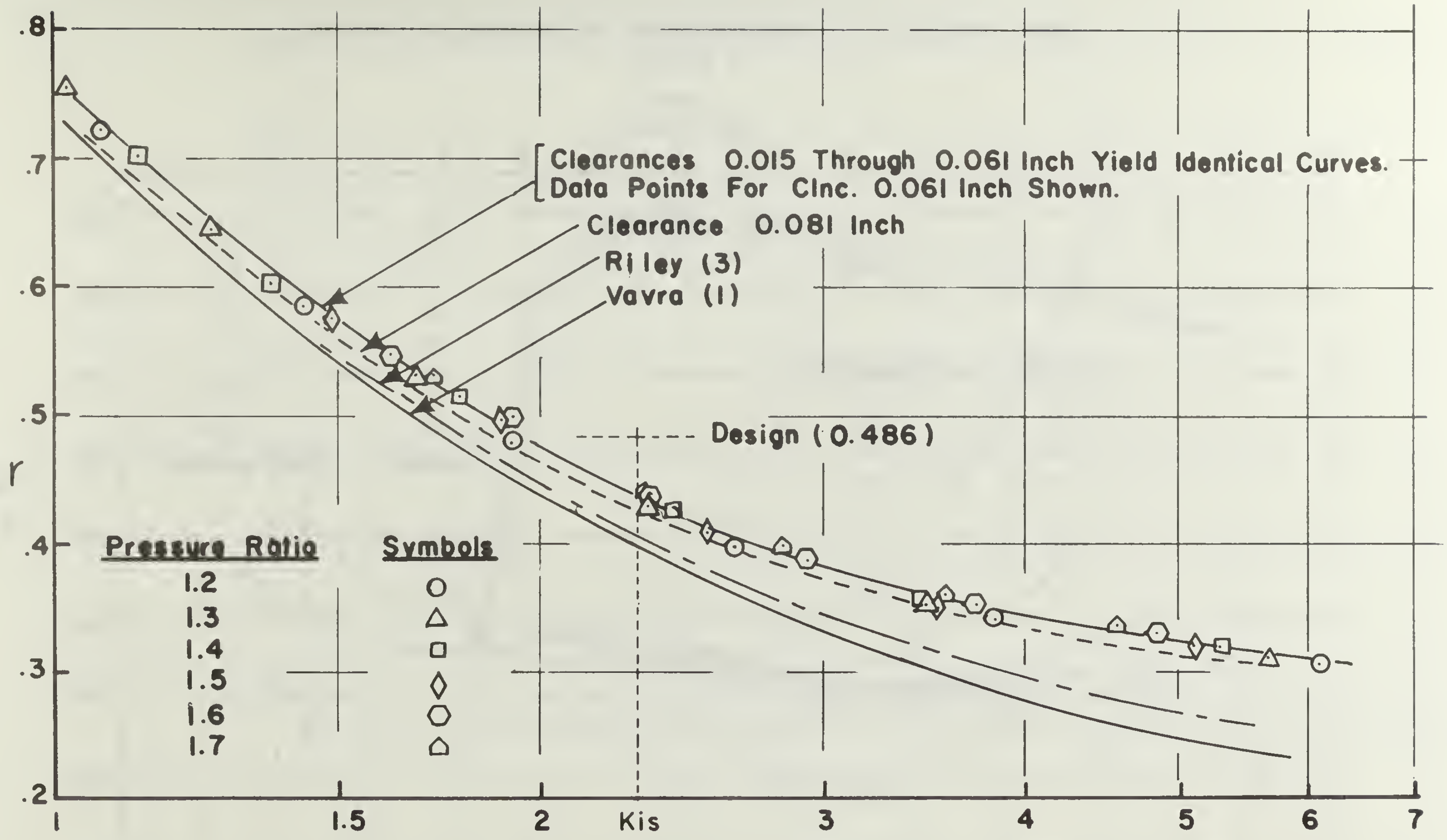

FIGURE 27
DEGREE OF REACTION VS. HEAD COEFFICIENT

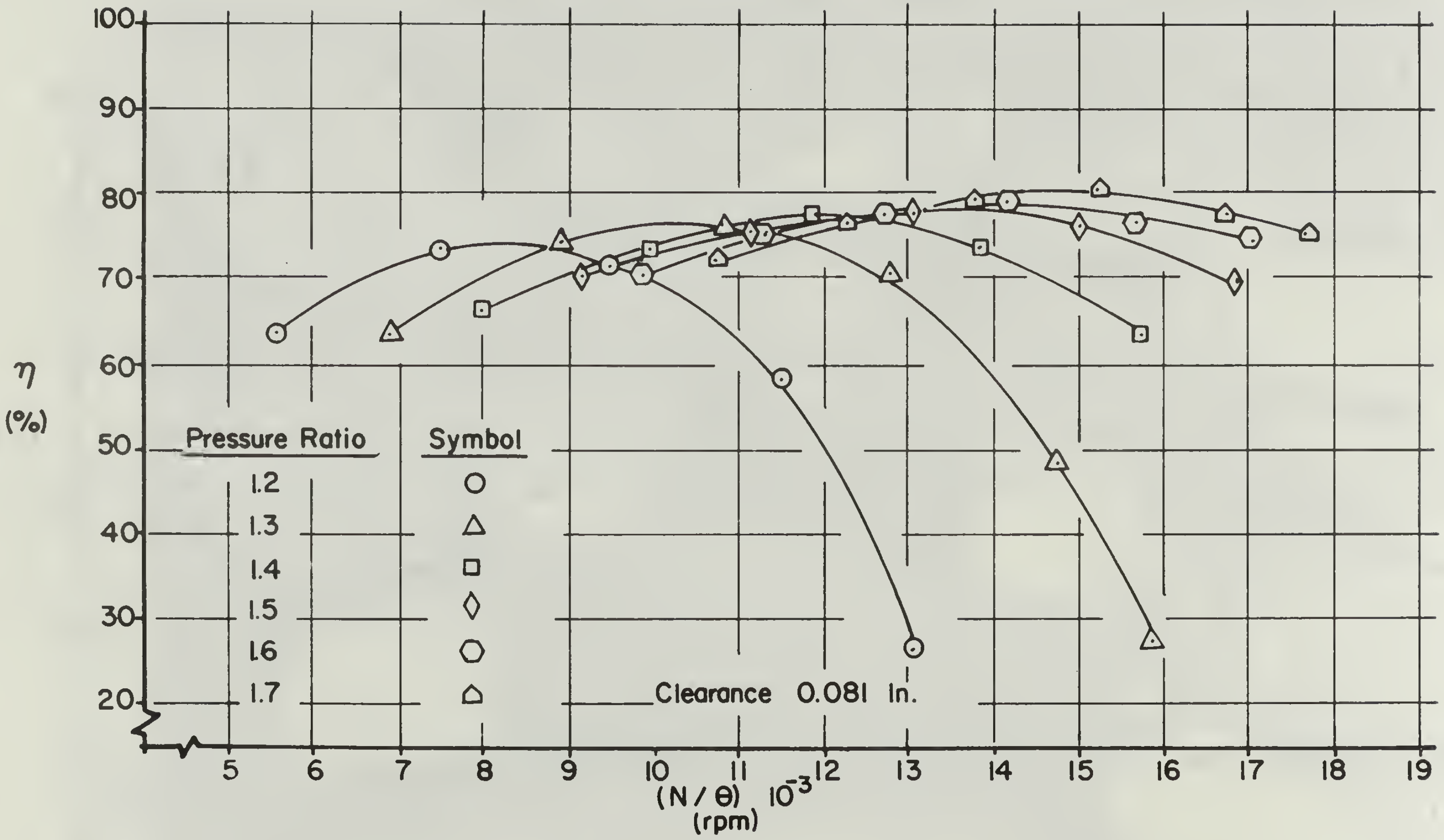

FIGURE 28
OVERALL EFFICIENCY (NO BEARING LOSSES) VS. REFERRED SPEED

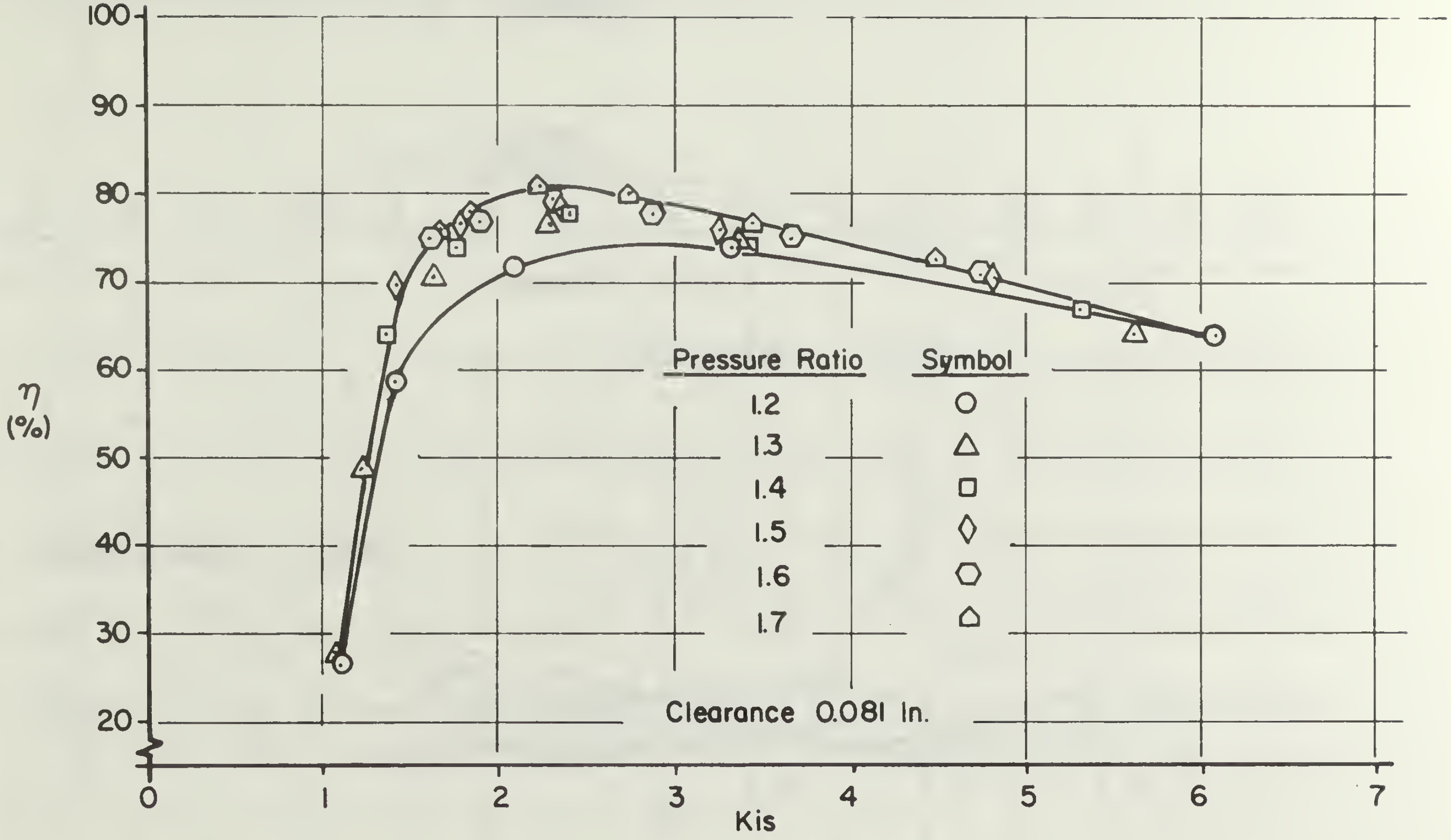

FIGURE 29
OVERALL EFFICIENCY (NO BEARING LOSSES) VS. HEAD COEFFICIENT

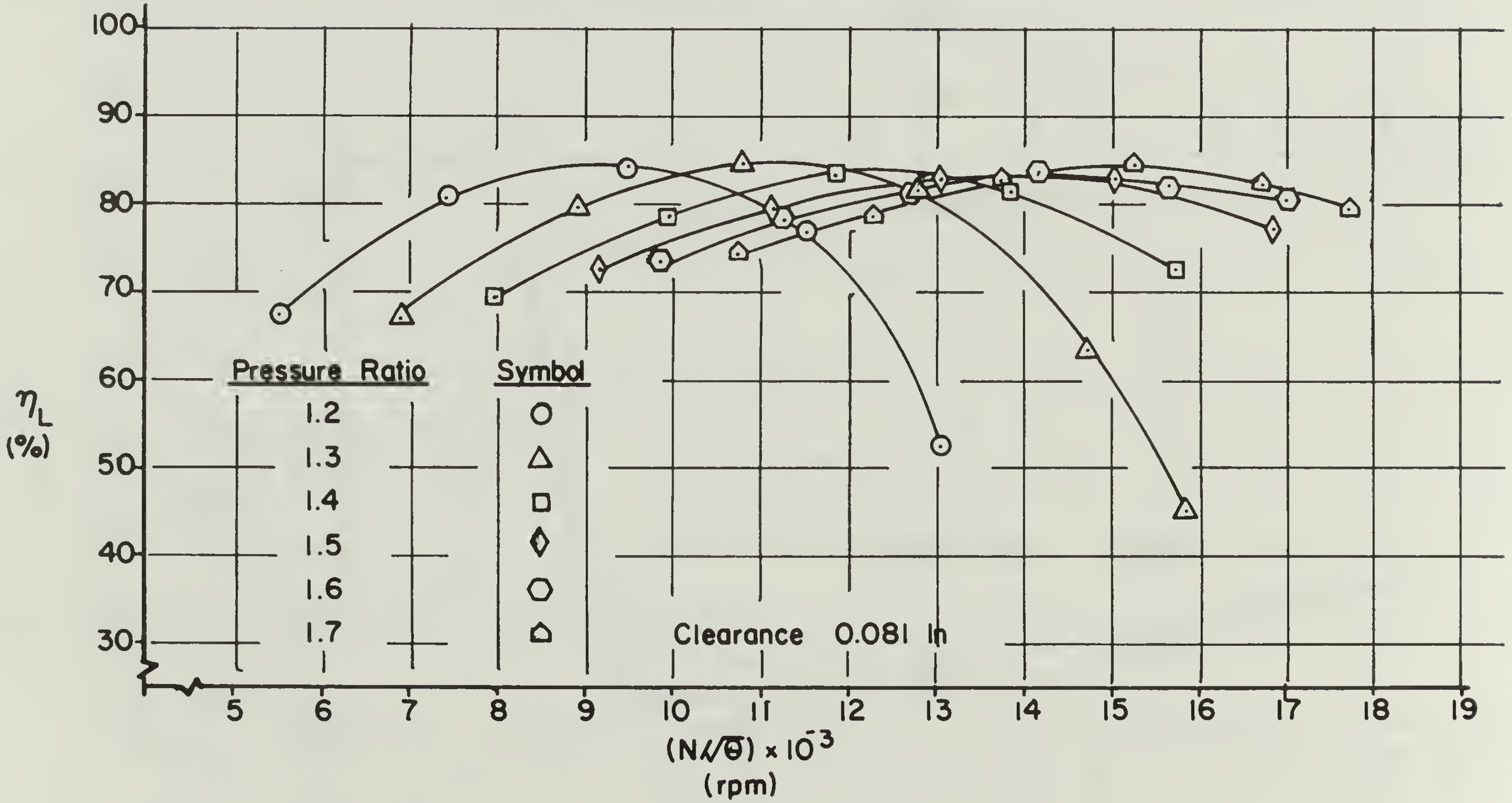

FIGURE 30
OVERALL EFFICIENCY (WITH BEARING LOSSES) VS. REFERRED SPEED

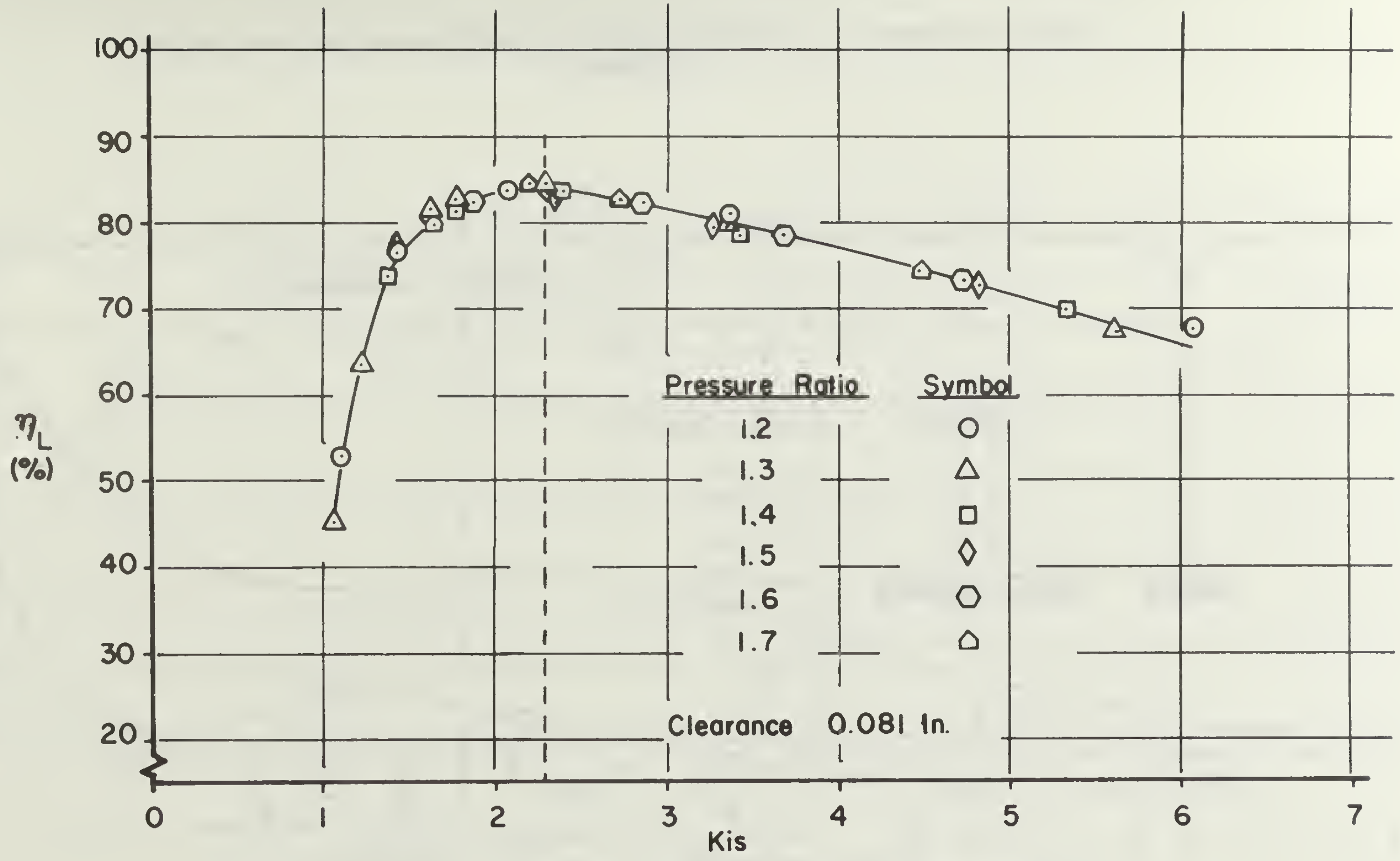

FIGURE 31
OVERALL EFFICIENCY (WITH BEARING LOSSES) VS. HEAD COEFFICIENT

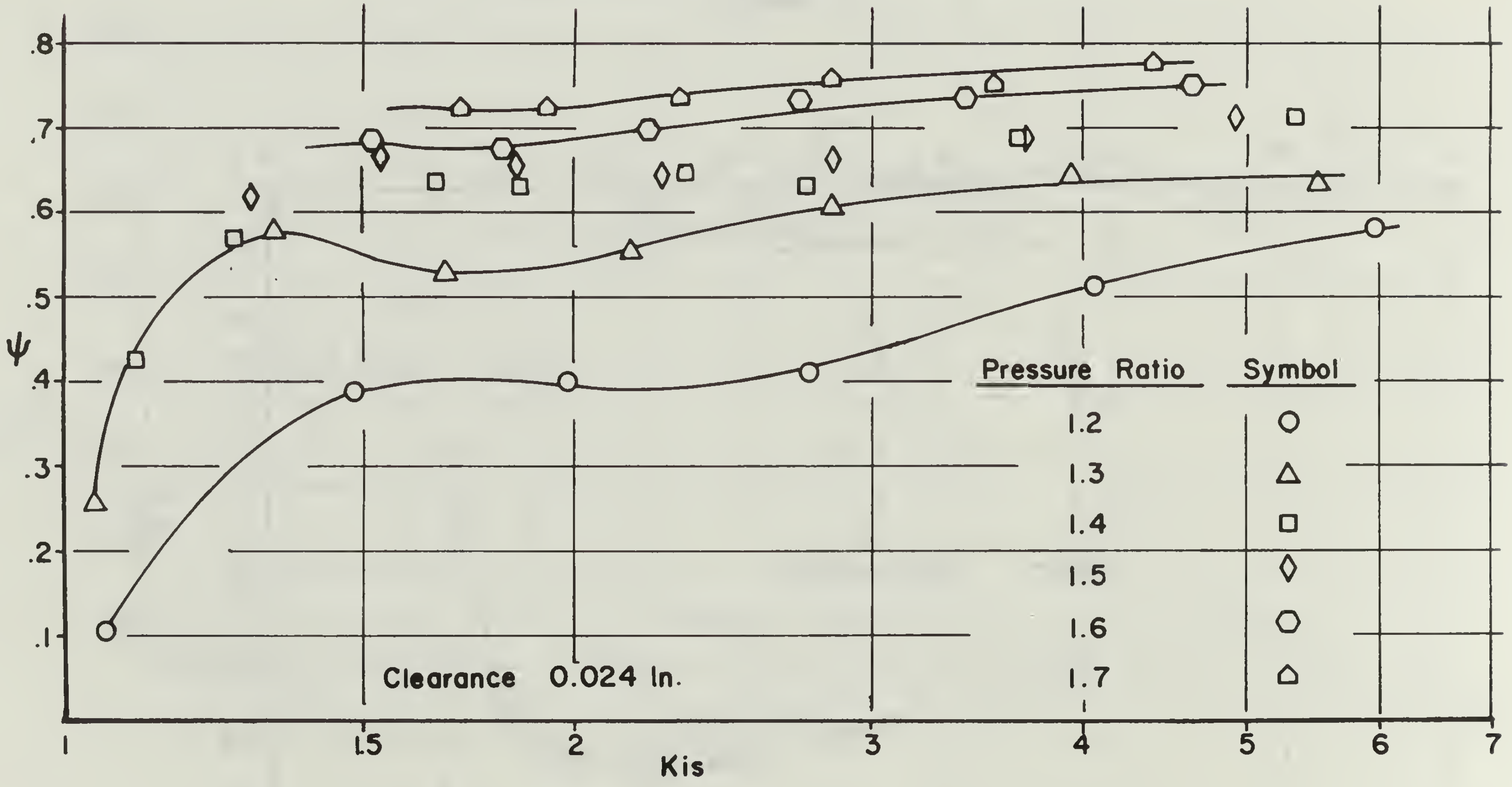

FIGURE 32
ROTOR VELOCITY COEFFICIENT (NO BEARING LOSSES) VS. HEAD COEFFICIENT

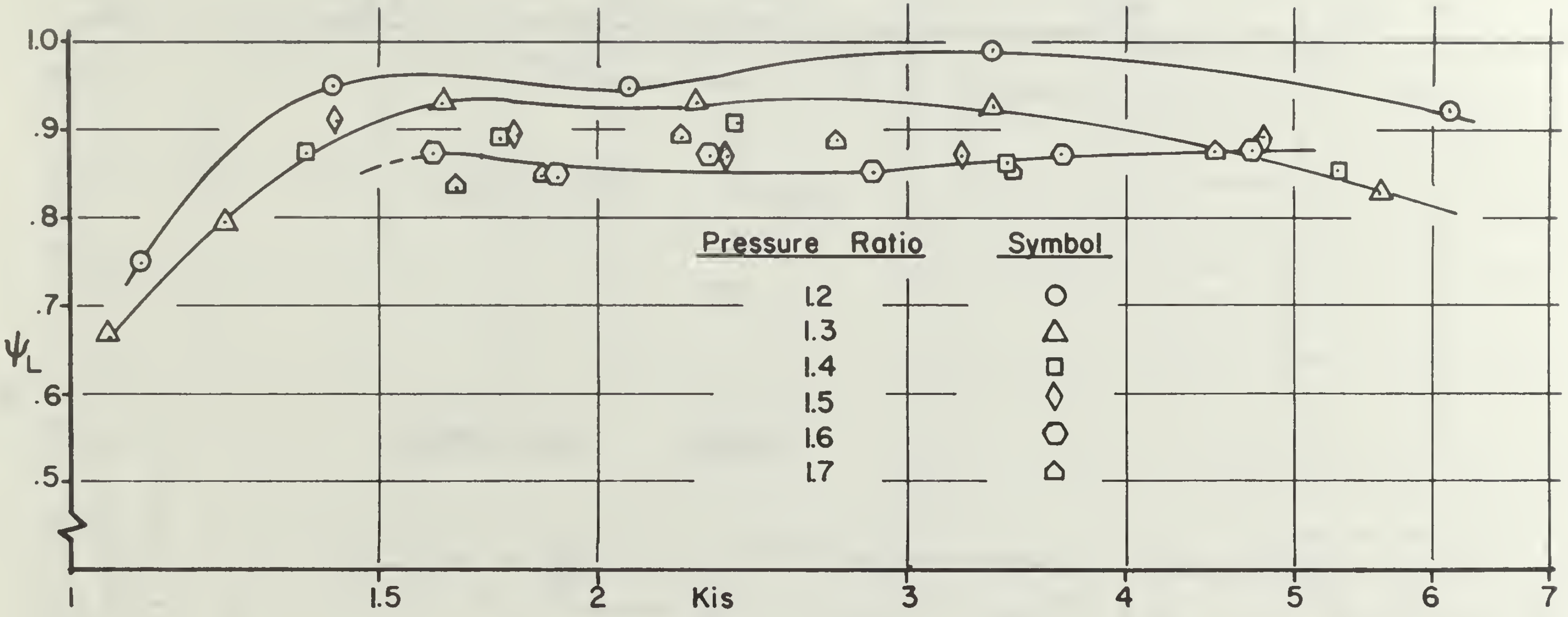

FIGURE 33
ROTOR VELOCITY COEFFICIENT (WITH BEARING LOSSES) VS. HEAD COEFFICIENT
CLEARANCE 0.081 IN.

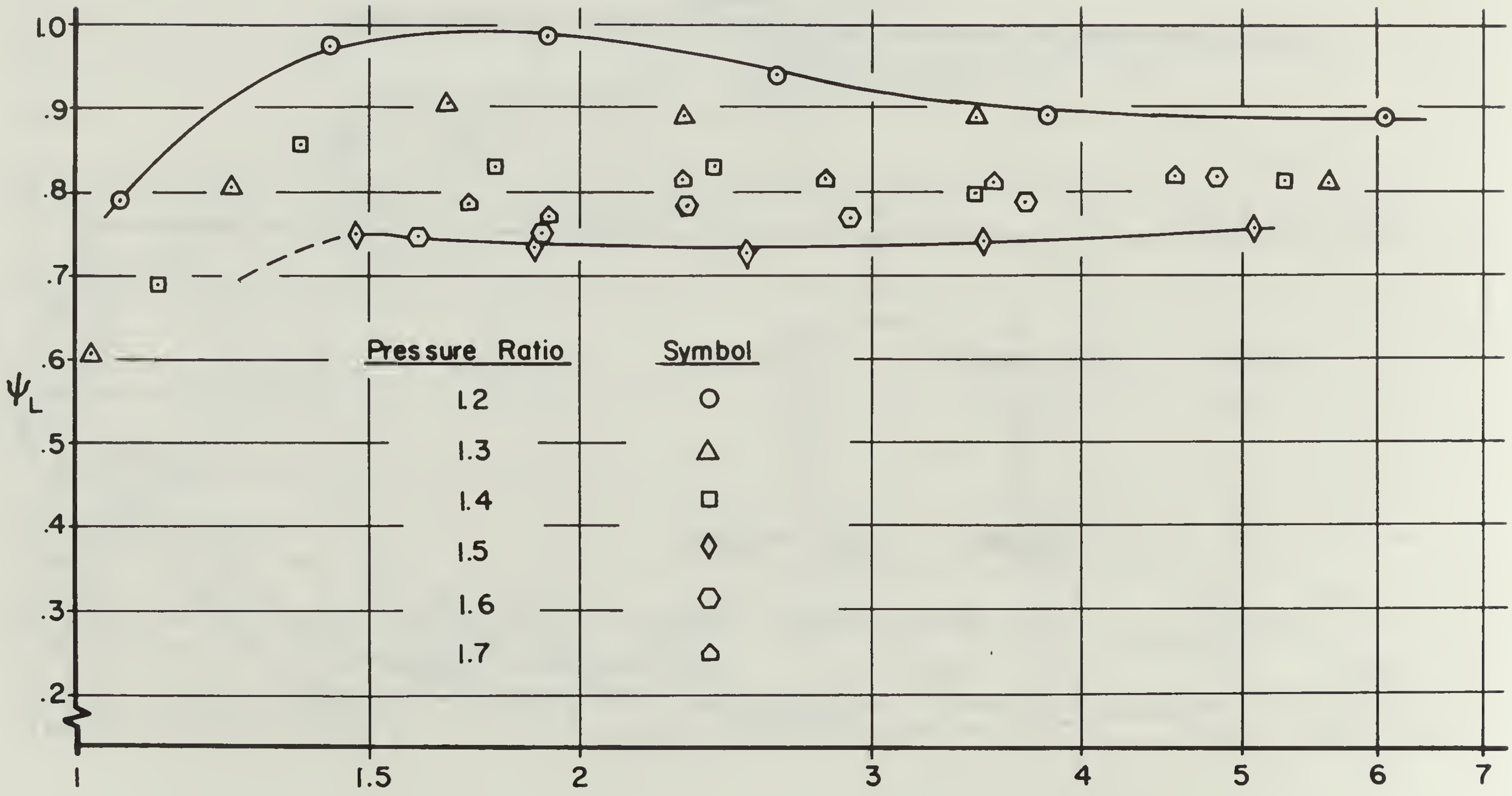

FIGURE 34
ROTOR VELOCITY COEFFICIENT (WITH BEARING LOSSES) VS. HEAD COEFFICIENT
CLEARANCE 0.061 IN.

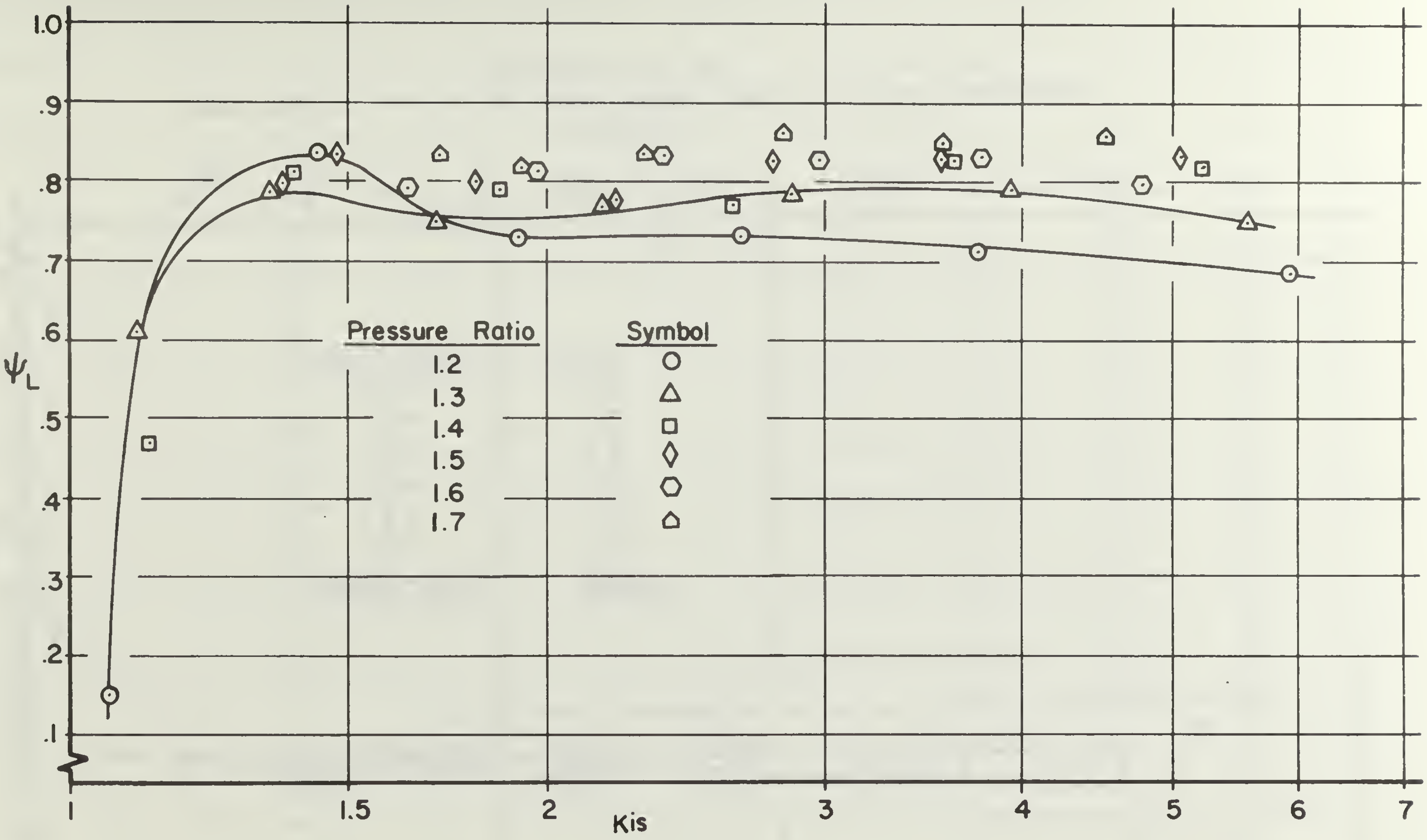

FIGURE 35
ROTOR VELOCITY COEFFICIENT (WITH BEARING LOSSES) VS. HEAD COEFFICIENT
CLEARANCE 0.041 IN.

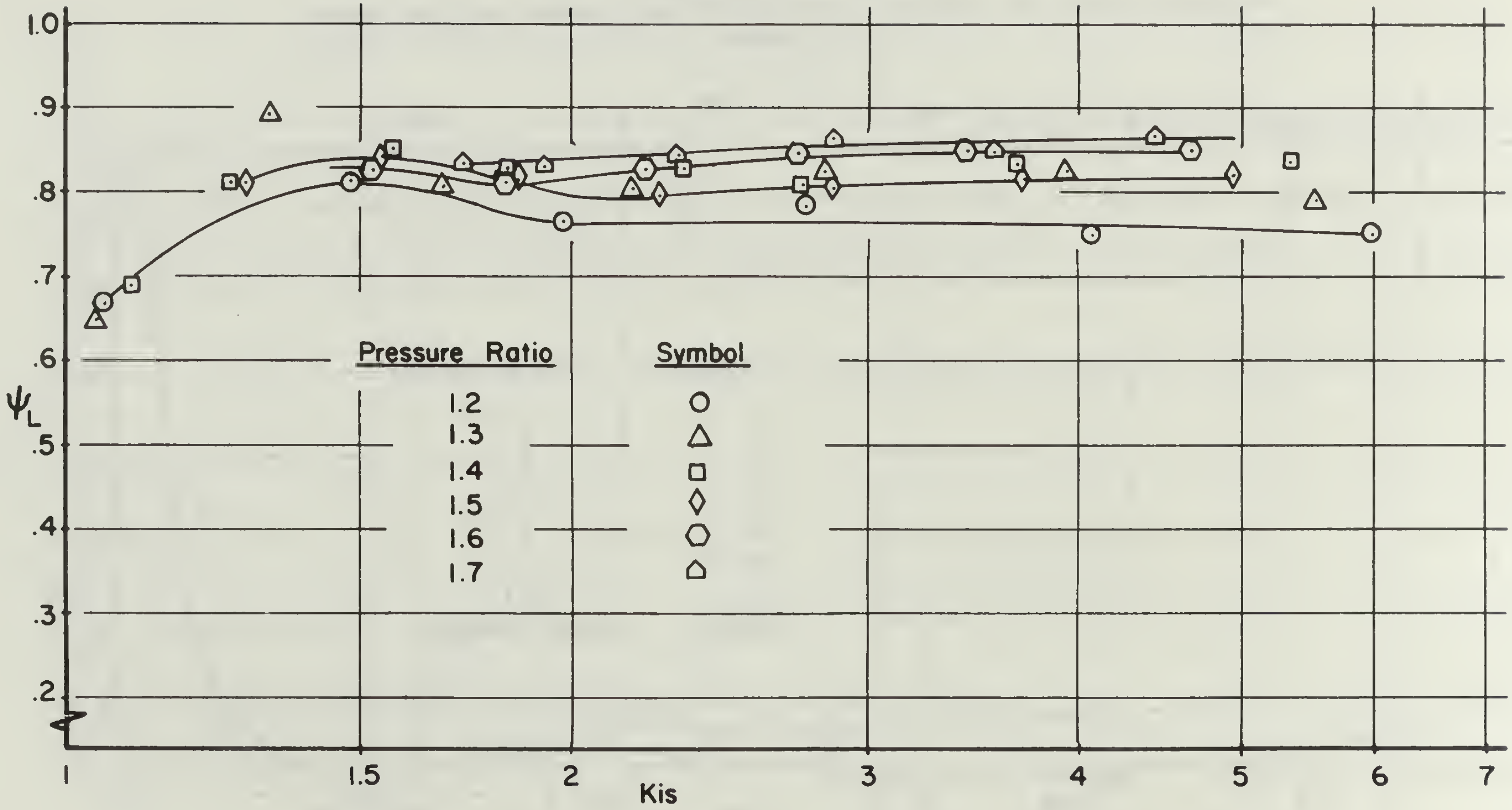

FIGURE 36
ROTOR VELOCITY COEFFICIENT (WITH BEARING LOSSES) VS. HEAD COEFFICIENT
CLEARANCE 0.024 IN.

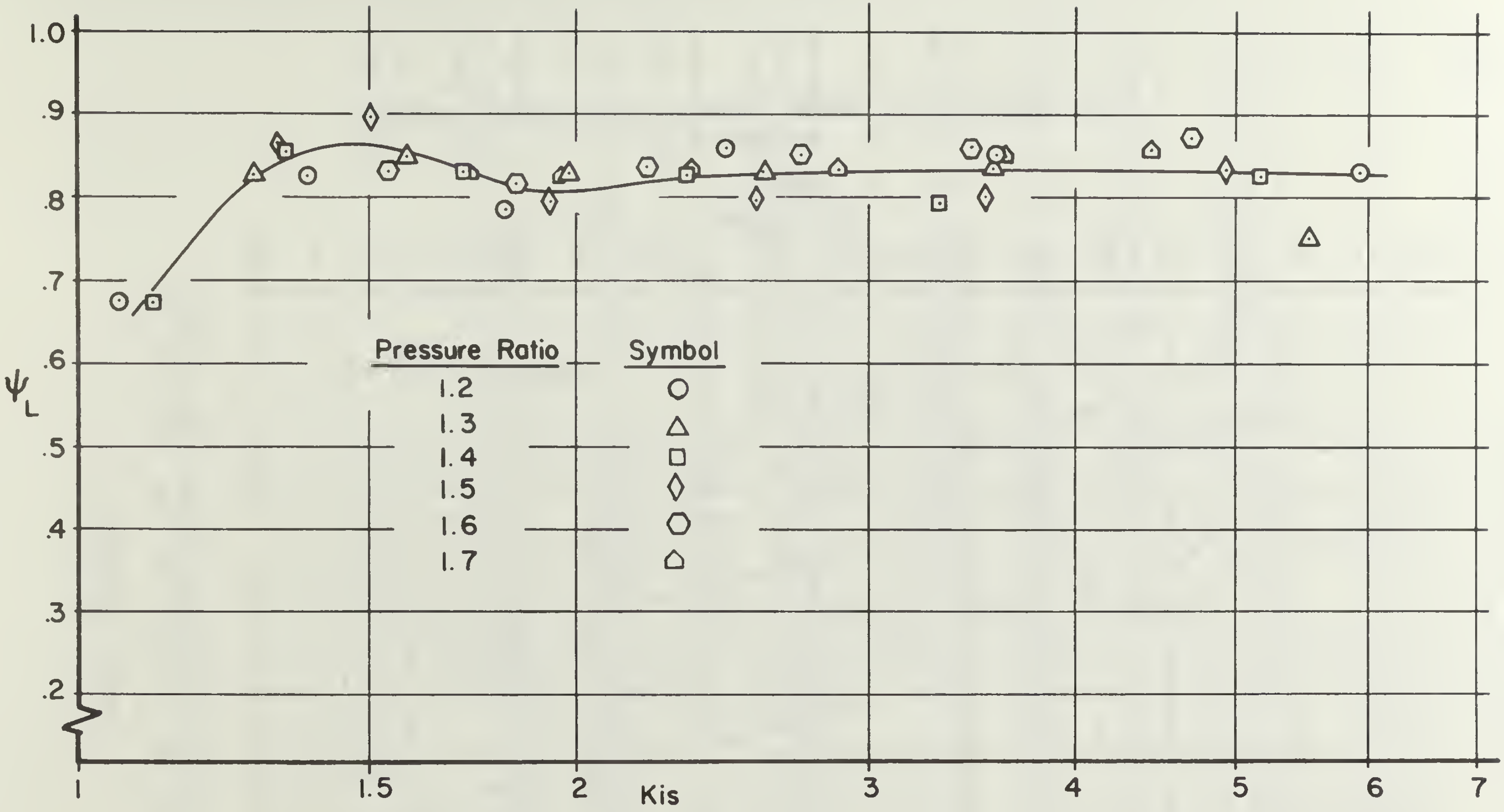

FIGURE 37
ROTOR VELOCITY COEFFICIENT (WITH BEARING LOSSES) VS. HEAD COEFFICIENT
CLEARANCE 0.015 IN.

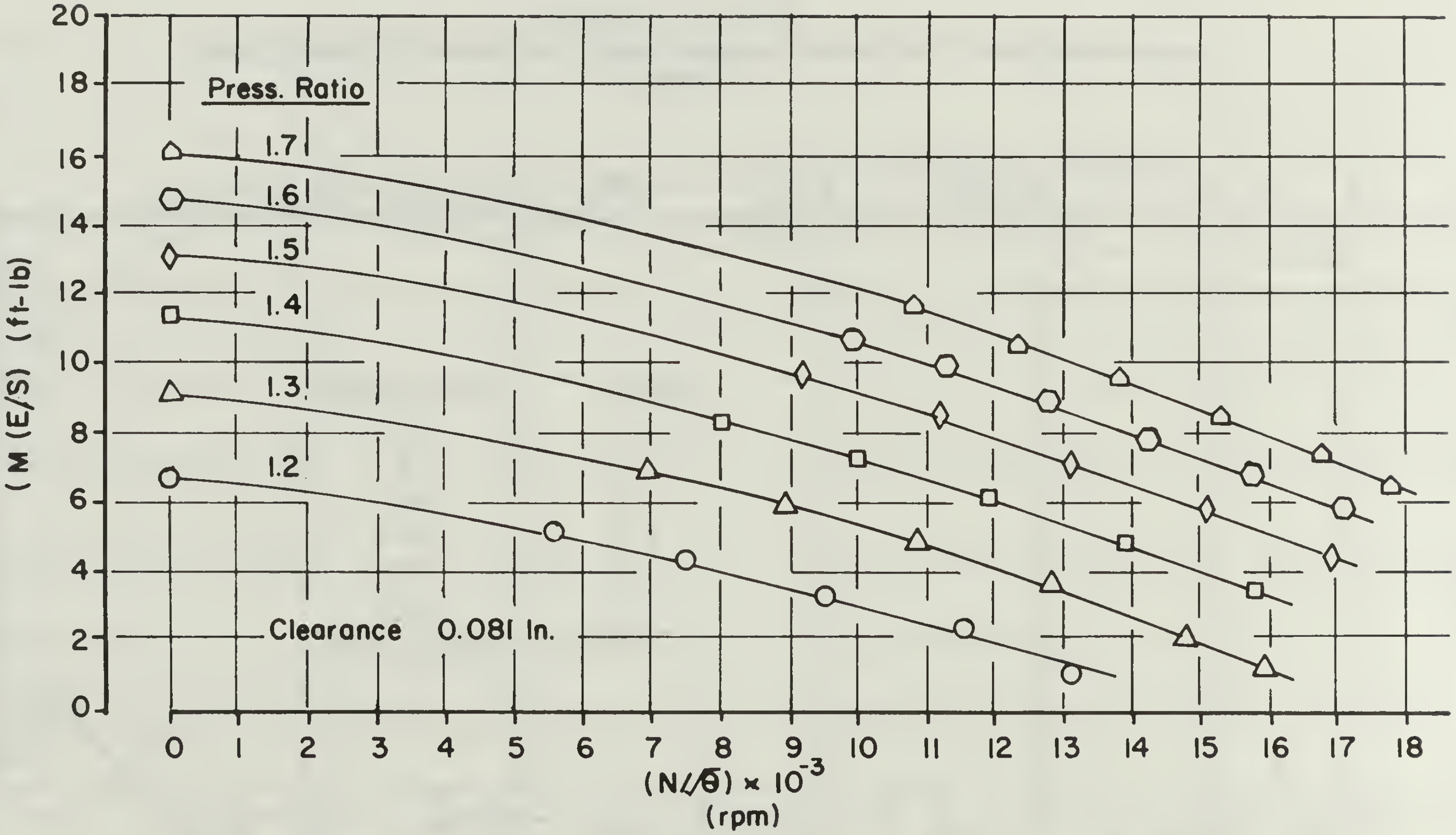

FIGURE 38
REFERRED MOMENT (WITH BEARING LOSSES) VS. REFERRED SPEED

REFERENCES

1. Vavra, M. H., Results of Turbine Air Testing Program, Phase II, *Report AGLR-VA No. 29*, for Aerojet General Corporation, January 1965.

2. Finn, W. A., "Performance Investigation of a Dual Discharge Radial Inflow Turbine." Master's thesis, Naval Postgraduate School, May 1966.

3. Riley, M. W., "The Effect of Axial Clearance on the Performance of a Dual Discharge Radial Turbine." Master's thesis, Naval Postgraduate School, December 1966.

4. Boshoven, R. L., "An Investigation of Compressible Flows with Large Whirl Components." Engineer's thesis, Naval Postgraduate School, June 1967.

5. Stearns, R. F., *et al*. *Flow Measurement with Orifice Meters*. New York: D. van Nostrand Company, 1951.

6. Vavra, M. H. *Aero-Thermodynamics and Flow in Turbomachines*. New York: John Wiley and Sons, 1960.

7. Vavra, M. H., Private communication, 1968.

8. Vavra, M. H., "Flow in Radial Turbines." Lecture notes for a short course on flow in turbines, von Karman Institute for Fluid Dynamics, March 1968.

9. Csanady, G. T. *Theory of Turbomachines*. New York: McGraw-Hill Book Company, 1964.

10. National Research Council. *International Critical Tables*, Vol. III. New York: McGraw-Hill Book Company, 1928.

11. Shenker, H. *Reference Tables for Thermocouples*. National Bureau of Standards, United States Department of Commerce, Circular 561. Washington: Government Printing Office, 1955.

12. Keenan, J. M. and J. Kaye. *Gas Tables*. New York: John Wiley and Sons, 1948.

APPENDIX A

PROGRAM SCROLL

Program SCROLL computes the losses in the scroll and guide vanes and the absolute rotor inlet flow angle from torque, mass flow rate, pressure, and temperature data obtained in the dummy rotor tests The program is essentially that used by Riley (3) and by Boshoven (4), with several changes as specified below. It can process any number of runs, with a maximum of ten sets of data per run. A listing of program SCROLL is given in Table A1. The input and output values which constitute the results of the eight sets of dummy rotor test data obtained are presented in Tables A2 through A9.

A1 Main Program

The value of the specific gravity of mercury, G_{hg}, at room temperature t_{rm}, was determined from

$$G_{hg} = 13.63905 - (1.36303 \times 10^{-3})\, t_{rm} \tag{A1}$$

for temperatures between 32°F and 113°F. The factor for converting inches Hg to lb/ft^2 is

$$C_{f1} = 70.438824 \left(G_{hg} / 13.54 \right) \tag{A2}$$

The value of the specific gravity of water at room temperature is

$$G_{H2O} = 0.9983763 + (1.060576 \times 10^{-4})\, t_{rm} - (1.593186 \times 10^{-6})\, t_{rm}^2 \tag{A3}$$

The specific gravity relations were obtained from the tabulated data of Reference 10.. These equations are slightly different from those used previously.

A2 Subroutine TEMP

The relations for the evaluation of the temperatures in this subroutine from the thermocouple readings in millivolts are different from those previously used because of the substitution of iron-constantan thermocouples for the chromel-alumel type. Thus, for iron-constantan thermocouples producing a millivolt output V, and using a cold junction reference temperature, t_{cj}, the temperature relations are

$$t = t_{cj} + 0.144 + 35.77\,V - 0.4518\,V^2 \qquad \text{(A4)}$$

for $t \leq 100°F$

$$t = t_{cj} + 1.252 + 34.86\,V - 0.1855\,V^2 \qquad \text{(A5)}$$

for $100°F < t \leq 200°F$

Equations (A4) and (A5) were obtained from data tabulated in Reference 11.

A3 Subroutine FLOW

The evaluation of the flow rate using the measured data from the particular flow orifices employed in the radial turbine test setup was carried out in accordance with a method developed originally by Vavra (1), after the techniques given by Stearns, et al. (5). The values thus determined by Vavra applied to a sharp-edged orifice of 2.800 inches diameter. Before this series of tests was begun, the flow orifice diameter was measured and found to be 2.7965 inches. Additionally, the conversion factors and the value of the specific gravity of mercury used herein are slightly different than those previously used, the latter being 13.54 vice 13.59. The equations given below are thus those of Vavra (1), with these modifications introduced. Computations were made for the vena contracta taps only, although flange tap data were available, because these data give a more accurate flow rate (1).

The relation for the flow rate is

$$\dot{W} = C \alpha Y_1 F_r \sqrt{\frac{P_{1VC} \, \Delta h_{1VC}}{T_4}} \qquad \text{(A6)}$$

where:

C - factor dependent on orifice diameter, type of pressure taps, and dimensional units

α - area multiplier to account for thermal expansion of orifice

Y_1 - factor which accounts for compressibility effects

F_r - Reynolds number correction factor

P_{1VC} - absolute pressure at upstream tap

Δh_{1VC} - pressure differential across orifice

T_4 - temperature ahead of orifice

For vena contracta taps, $C = 0.9057$.

For a stainless steel orifice:

$$\alpha = 1.0 + (1.85 \times 10^{-5})(T_4 - 532.) \qquad \text{(A7)}$$

$$Y_1 = 1.0 - 0.351 \frac{\Delta h_{1VC}}{P_{1VC}} \qquad \text{(A8)}$$

Also,

$$F_r = 1.0 + \frac{0.001275}{X} \qquad \text{(A9)}$$

where

$$X = 0.8131 \frac{\dot{W}}{Z} \qquad \text{(A10)}$$

$$Z = 1.9 + (2.4 \times 10^{-3})(T_4 - 559.69) \qquad \text{(A11)}$$

where Equation (A11) is valid for air between 50°F and 300°F.

TABLE A1
LISTING OF PROGRAM SCROLL

```
C   PROGRAM SCROLL
      DIMENSION DPVC(10),PUVC(10),P5P(10),PATM(10),HREF1(10),H1(10),
     1SR(10),TRM(10),V4(10),V5(10),WVCP(10),PRP(10),PHIP(10),ALPH(10),
     2VEL(10),TS(10),ACH(10),PS(10)
      COMMON GHG,GWR,CF1,TCJ,STARE,T4,T5,WVC,PR,P1,PHI,ALF1,PAT,V1,T1,
     *ACH1,B1
      READ(5,10) NRUNS
      DO 99 J=1,NRUNS
      READ(5,10) NPTS
      READ(5,11) (DPVC(K),PUVC(K),P5P(K),PATM(K),HREF1(K),H1(K),SR(K),
     *TRM(K),V4(K),V5(K),K=1,NPTS)
      READ(5,12) TCJ,STARE,B1
      CLNC=(B1-.894)/2.
      WRITE(6,20) CLNC
      WRITE(6,21) (K,DPVC(K),PUVC(K),P5P(K),PATM(K),HREF1(K),H1(K),SR(K)
     *,TRM(K),V4(K),V5(K),K=1,NPTS)
      WRITE(6,24) TCJ,STARE,B1
      DO 100 K=1,NPTS
      GHG=13.63905-1.363030E-3*TRM(K)
      GWR=.9983763+1.060576E-4*TRM(K)-1.593186E-6*TRM(K)**2
      CF1=70.438824*GHG/13.54
      DPV=DPVC(K)
      PUV=PUVC(K)
      P5=P5P(K)
      PAT=PATM(K)
      HRF1=HREF1(K)
      P1P=H1(K)
      S=SR(K)
      V4T=V4(K)
      V5T=V5(K)
      CALL TEMP (V4T,V5T)
      CALL FLOW (DPV,PUV)
      CALL PRESS (P5,HRF1,P1P)
      CALL ALFSI (S)
      WVCP(K)=WVC
      PRP(K)=PR
      PHIP(K)=PHI
      ALPH(K)=ALF1
      VEL(K)=V1
      TS(K)=T1
      ACH(K)=ACH1
      PS(K)=P1
  100 CONTINUE
      WRITE(6,22)
      WRITE(6,23) (K,PRP(K),WVCP(K),PHIP(K),ALPH(K),
     1VEL(K),TS(K),ACH(K),PS(K),K=1,NPTS)
   99 CONTINUE
   10 FORMAT(I4)
   11 FORMAT(10F7.3)
   12 FORMAT(3F7.3)
   20 FORMAT(1H1,/////,T5,'PROGRAM SCROLL',T74,'D.D. WILLIAMS',//,T21,
     *'SCROLL AND GUIDE VANE TESTS OF ICP RADIAL TURBINE',///,T17,'TABLE
     *',T53,'CLEARANCE = ',F5.3,1X,'IN.',///,T41,'INPUT DATA',//,T5,'PT
     *     DPVC      PUVC      P5P      PATM      HREF1      H1        SR        TRM
     *   V4        V5',/)
   21 FORMAT(I6,10F8.3)
   22 FORMAT(///,T40,'OUTPUT DATA',//,T10,'PT     PTO/P1    WVC       PHI
     *  ALPH(1)    V1         T1         MACH1       P1',/)
   23 FORMAT(5X,I6,2F8.3,F8.4,3F9.2,2F9.3)
   24 FORMAT(/19X5HTCJ -F6.2,9X7HSTARE -F5.2,9X4HB1 -F6.3)
      RETURN
      END
C




      SUBROUTINE TEMP (V4,V5)
      COMMON GHG,GWR,CF1,TCJ,STARE,T4,T5,WVC,PR,P1,PHI,ALP1,PAT,V1,T1,
     *ACH1,B1
      V=V4
      J=1
  100 T=TCJ+0.144+35.77*V-0.4518*V**2
      IF( T - 100.) 102,102,101
  101 T=TCJ+1.252+34.86*V-0.1855*V**2
  102 T=T+459.69
      IF(J-1)103,103,104
  103 J=2
      T4=T
      V=V5
      GO TO 100
  104 T5=T
      RETURN
      END
C
```

```
      SUBROUTINE FLOW (DPVC,PUVC)
      COMMON GHG,GWR,CF1,TCJ,STARE,T4,T5,WVC,PR,P1,PHI,ALP1,PAT,V1,T1,
     *ACH1,B1
      DVC=DPVC*GHG/13.54
      PVC=(PUVC+PAT)*GHG/13.54
      A=1.+1.85E-5*(T4-532.)
      Z=1.9+2.4E-3*(T4-560.)
      Y=1.-.351*DVC/PVC
      WVC=2.2854*A*Y*SQRT(PVC*DVC/T4)
      X=WVC*.8131/Z
      WVC=(1.+.001275/X)*WVC
      RETURN
      END
C
      SUBROUTINE PRESS(P5P,HPF1,H1)
      COMMON GHG,GWP,CF1,TCJ,STARE,T4,T5,WVC,PR,P1,PHI,ALP1,PAT,V1,T1,
     *ACH1,B1
      A=T5-459.69
      CP=.23943+3.4E-6*A+2.E-8*A**2
      P1=((PAT+HPF1)*GHG+H1*GWP)/13.54
      PS5=(PAT+P5P)*GHG/13.54
      TT=T5
  100 RHO=PS5*CF1/(TT*53.3448)
      VO=WVC/(RHO*3.14159*6.25/144.)
      TO=T5-(VO**2)/(2.*32.174*778.16*CP)
      DTT=TT-TO
      TT=TO
      IF(ABS(DTT)-.01)101,101,100
  101 PTO=PS5+RHO*(VO**2)/(2.*32.174*CF1)
      PR=PTO/P1
      RETURN
      END
C
```

```
      SUBROUTINE ALPSI (SR)
      COMMON GHG,GWR,CF1,TCJ,STAPE,T4,T5,WVC,PR,P1,PHI,ALP1,PAT,V1,T1,
     *ACH1,B1
      T=T5-459.69
      GAM=1.4018-2.E-5*T
      EXP=(GAM-1.)/GAM
      CP=.23943+3.4E-6*T+2.E-8*T**2
      G=2.*32.174*778.16*CP
      RM=(SR-STARE)*12.0
      VU1=RM*32.174/(WVC*4.75)
      B=T5*(1.-1./PR**EXP)
      A1=2.*3.14159*4.75*B1/144.
      PHI=1.
  100 V1=PHI*SQRT(G*B)
      T1=T5-(V1**2)/G
      RHO=P1*CF1/(T1*53.3448)
      VM1=WVC/(A1*RHO)
      V1A=SQRT(VM1**2+VU1**2)
      IF(ABS(V1-V1A)-.5)102,102,101
  101 PHI=PHI-.0001
      GO TO 100
  102 ALP1=57.29578*ATAN(VU1/VM1)
      ACH1=V1/SQRT(32.174*GAM*53.3448*T1)
      RETURN
      END
```

```
PROGRAM SCROLL                                                              D.D. WILLIAMS
                      SCROLL AND GUIDE VANE TESTS OF ICP RADIAL TURBINE

              TABLE A2                                       CLEARANCE = 0.081 IN.

                                               INPUT DATA
PT      CPVC      PUVC       P5P      PATM      HREF1     H1        SR       TRM        V4       V5

 1      1.134     2.640     1.520    30.040     0.0       2.089     1.820   83.000     1.597    1.495
 2      2.259     5.350     3.160    30.040     0.0       4.306     3.800   83.600     1.625    1.540
 3      3.399     8.310     4.990    30.040     0.0       6.799     6.010   84.000     1.643    1.560
 4      4.410    11.000     6.700    30.040     0.0       9.103     8.040   84.500     1.660    1.582
 5      5.443    14.000     8.640    30.040     0.0      11.781    10.330   85.000     1.655    1.590
 6      6.619    18.600    12.080    30.030     0.0      15.045    13.060   85.000     1.660    1.600
 7      7.768    21.290    13.550    30.030     0.0      18.561    15.940   85.200     1.665    1.605
 8      9.278    26.410    17.210    30.030     0.0      24.234    19.850   85.600     1.675    1.615
 9     10.795    31.850    21.110    30.030     0.0      30.913    24.000   86.000     1.680    1.630
10     11.582    37.830    23.250    30.030     0.0      34.725    26.300   86.000     1.685    1.635

              TCJ - 32.00            STARE - 0.0            B1 - 1.056


                                              OUTPUT DATA

        PT    PTO/P1     WVC       PHI       ALPH(1)    V1        T1        MACH1      P1

         1    1.047     0.590    0.8697      81.72    254.01    538.93     0.223    30.162
         2    1.097     0.855    0.8825      81.77    365.49    534.73     0.322    30.324
         3    1.152     1.081    0.8954      81.83    457.18    529.13     0.405    30.506
         4    1.203     1.263    0.8989      81.77    523.08    524.51     0.466    30.674
         5    1.260     1.445    0.9061      81.76    587.52    518.83     0.526    30.869
         6    1.363     1.666    0.8636      81.49    644.58    513.32     0.580    31.099
         7    1.400     1.843    0.9148      81.66    710.85    506.01     0.645    31.357
         8    1.499     2.101    0.9154      81.54    776.70    498.20     0.710    31.773
         9    1.600     2.364    0.9176      81.41    835.10    490.88     0.769    32.263
        10    1.654     2.567    0.8981      80.87    843.95    489.82     0.778    32.543
```

```
PROGRAM SCROLL                                                          D.D. WILLIAMS

                  SCROLL AND GUIDE VANE TESTS OF ICP RADIAL TURBINE

              TABLE  A3                                 CLEARANCE = 0.072 IN.

                                         INPUT DATA

PT     DPVC       PUVC      P5P      PATM      HREF1       H1        SR       TRM       V4       V5

 1     1.147      2.690     1.550    29.880     0.0       2.308     1.860    79.100    1.675    1.565
 2     2.278      5.460     3.210    29.880     0.0       4.708     3.880    80.000    1.702    1.620
 3     3.234      7.960     4.750    29.880     0.0       6.958     5.750    80.200    1.710    1.645
 4     4.232     10.660     6.460    29.880     0.0       9.406     7.750    81.300    1.755    1.690
 5     5.392     13.960     8.600    29.880     0.0      12.671    10.300    82.200    1.785    1.725
 6     6.653     17.750    11.180    29.880     0.0      16.517    13.160    83.000    1.800    1.750
 7     7.823     21.560    13.780    29.880     0.0      20.593    16.100    84.000    1.820    1.765
 8     9.392     26.950    17.560    29.880     0.0      26.829    20.330    84.700    1.830    1.785
 9    10.837     32.200    21.330    29.880     0.0      33.722    24.210    85.000    1.835    1.795
10    11.796     35.780    24.020    29.880     0.0      38.925    26.990    85.500    1.840    1.800

                TCJ  -  32.00          STARE  -  0.0            B1  -  1.038


                                         OUTPUT DATA

     PT    PTO/P1     WVC       PHI        ALPH(1)     V1         T1       MACH1      P1

      1    1.048     0.591    0.8789      81.66     259.13     541.12     0.227    30.031
      2    1.098     0.856    0.8929      81.72     372.74     537.03     0.328    30.204
      3    1.145     1.047    0.9038      81.76     451.70     532.47     0.399    30.369
      4    1.195     1.228    0.9043      81.69     518.70     528.60     0.460    30.546
      5    1.257     1.430    0.9134      81.68     592.06     523.01     0.528    30.784
      6    1.331     1.645    0.9116      81.57     658.04     517.00     0.590    31.064
      7    1.403     1.843    0.9174      81.53     718.33     510.61     0.649    31.361
      8    1.504     2.111    0.9252      81.47     791.94     502.04     0.721    31.817
      9    1.599     2.361    0.9225      81.30     843.57     495.35     0.773    32.323
     10    1.664     2.528    0.9249      81.25     878.58     490.51     0.809    32.704
```

```
PROGRAM SCROLL                                                                   D.D. WILLIAMS
                          SCROLL AND GUIDE VANE TESTS OF ICP RADIAL TURBINE

                TABLE A4                                        CLEARANCE = 0.061 IN.

                                              INPUT DATA
PT       DPVC      PUVC       P5P       PATM       HPEFI       H1         SR        TRM        V4        V5

 1       1.185     2.780      1.600     29.970     0.0        2.512      1.940     82.000     1.625     1.540
 2       2.393     5.760      3.390     29.970     0.0        5.337      4.100     82.000     1.630     1.560
 3       4.012    10.010      6.060     29.970     0.0        9.426      7.310     82.500     1.645     1.590
 4       4.610    11.700      7.130     29.970     0.0       11.001      8.510     83.100     1.635     1.595
 5       5.554    14.410      8.900     29.970     0.0       13.866     10.640     83.600     1.640     1.596
 6       6.720    17.990     11.310     29.970     0.0       17.546     13.350     83.400     1.640     1.605
 7       7.912    21.880     13.920     29.970     0.0       21.975     16.370     83.000     1.642     1.610
 8       9.405    26.960     17.590     29.970     0.0       28.241     20.320     83.000     1.650     1.620
 9      10.924    32.500     21.580     29.970     0.0       35.484     24.180     83.300     1.660     1.630
10      11.886    36.100     24.170     29.970     0.0       40.753     27.080     83.400     1.660     1.630

                 TCJ - 32.00            STARE - 0.0             R1 - 1.016


                                              OUTPUT DATA

         PT     PTO/P1     WVC       PHI        ALPH(1)     V1         T1          MACH1      P1

          1     1.049     0.603     0.8901     81.55     265.03     540.00     0.233     30.127
          2     1.102     0.883     0.8991     81.56     381.98     534.39     0.337     30.335
          3     1.181     1.193     0.9109     81.56     503.76     526.44     0.448     30.634
          4     1.213     1.301     0.9060     81.46     538.00     523.64     0.480     30.748
          5     1.263     1.465     0.9164     81.49     597.19     518.08     0.535     30.957
          6     1.331     1.666     0.9171     81.41     659.13     511.91     0.594     31.228
          7     1.402     1.871     0.9247     81.38     719.80     505.12     0.653     31.556
          8     1.499     2.126     0.9271     81.30     786.26     497.13     0.719     32.017
          9     1.599     2.391     0.9155     81.02     832.78     491.20     0.767     32.548
         10     1.660     2.560     0.9238     81.02     871.05     485.77     0.806     32.936
```

```
PROGRAM SCROLL                                                                D.D. WILLIAMS

                        SCROLL AND GUIDE VANE TESTS OF ICP RADIAL TURBINE

              TABLE A5                                      CLEARANCE = 0.050 IN.

                                             INPUT DATA

PT     DPVC      PLVC      P5P      PATM     HREF1       H1        SR       TRM        V4        V5

 1     1.158     2.720     1.560    29.920    0.0        2.547     1.880    78.000     1.493     1.435
 2     2.305     5.480     3.190    29.920    0.0        5.204     3.900    79.000     1.530     1.490
 3     3.285     8.110     4.840    29.920    0.0        7.926     5.860    79.200     1.540     1.515
 4     4.423    11.280     6.860    29.920    0.0       10.989     8.200    79.200     1.500     1.485
 5     5.333    13.820     8.540    29.920    0.0       13.858    10.040    79.600     1.530     1.510
 6     6.676    17.800    11.170    29.920    0.0       18.247    13.180    80.000     1.540     1.520
 7     7.788    21.460    13.610    29.920    0.0       22.750    16.020    80.000     1.550     1.530
 8     9.262    26.400    17.110    29.920    0.0       29.118    19.740    80.200     1.560     1.545
 9    10.712    31.350    20.690    29.920    0.0       35.069    23.520    80.600     1.575     1.558
10    11.753    35.500    23.700    29.920    0.0       42.194    26.780    80.600     1.595     1.575

                TCJ - 32.00             STARE - 0.0             R1 - 0.994


                                            OUTPUT DATA

     PT    PTO/P1     WVC       PHI       ALPH(1)     V1        T1        MACH1      P1

      1    1.047     0.598    0.8857      81.29     259.21    536.64     0.228    30.091
      2    1.096     0.866    0.9005      81.29     370.67    532.69     0.328    30.284
      3    1.145     1.063    0.9111      81.41     453.76    527.85     0.403    30.484
      4    1.204     1.275    0.9112      81.36     529.32    520.63     0.473    30.709
      5    1.251     1.433    0.9049      81.20     576.79    517.12     0.517    30.919
      6    1.325     1.662    0.9177      81.20     652.60    509.70     0.590    31.241
      7    1.390     1.854    0.9271      81.20     711.14    503.40     0.647    31.572
      8    1.481     2.106    0.9249      81.05     771.79    496.43     0.707    32.041
      9    1.574     2.351    0.9226      80.88     823.91    489.95     0.759    32.477
     10    1.641     2.539    0.9328      80.92     868.80    484.21     0.805    33.002
```

```
PROGRAM SCROLL                                                                  D.D. WILLIAMS
                     SCROLL AND GUIDE VANE TESTS OF ICP RADIAL TURBINE

            TABLE  A6                                  CLEARANCE = 0.041 IN.

                                            INPUT DATA
PT    DPVC     PLVC      P5P      PATM      HREF1      H1        SP       TRM       V4       V5

 1    1.159    2.700     1.560   30.010     0.0       2.696     1.880   80.000    1.610    1.530
 2    2.348    5.610     3.310   30.010     0.0       5.815     3.980   80.200    1.620    1.560
 3    3.549    8.770     5.260   30.010     0.0       9.279     6.310   80.900    1.625    1.580
 4    4.422   11.170     6.800   30.010     0.0      11.986     8.120   80.000    1.635    1.595
 5    5.682   14.810     9.180   30.010     0.0      16.047    10.870   80.000    1.635    1.598
 6    6.933   18.700    11.770   30.010     0.0      20.842    13.800   80.100    1.645    1.605
 7    8.094   22.450    14.390   30.010     0.0      25.428    16.750   81.000    1.675    1.640
 8    9.715   27.990    18.280   30.010     0.0      33.019    21.020   81.900    1.695    1.660
 9   11.254   33.650    22.400   30.010     0.0      41.769    25.290   82.000    1.702    1.675
10   12.258   37.450    25.200   30.010     0.0      47.581    28.050   82.600    1.720    1.690

                  TCJ - 32.00            STARE - 0.0           R1 - 0.976


                                           OUTPUT DATA
       PT    PTO/P1     WVC      PHI       ALPH(1)    V1        T1        MACH1      P1

        1    1.047     0.596    0.8902     81.14    259.91    539.88     0.228    30.186
        2    1.098     0.874    0.8998     81.15    374.98    534.83     0.331    30.415
        3    1.155     1.110    0.9097     81.17    468.02    528.99     0.415    30.668
        4    1.199     1.269    0.9147     81.17    526.84    524.63     0.469    30.870
        5    1.265     1.489    0.9185     81.12    600.87    517.78     0.539    31.169
        6    1.335     1.704    0.9227     81.06    666.68    511.08     0.602    31.522
        7    1.405     1.900    0.9283     81.04    725.68    505.44     0.658    31.856
        8    1.503     2.177    0.9331     80.94    795.34    497.31     0.728    32.412
        9    1.601     2.445    0.9342     80.82    852.15    490.03     0.785    33.055
       10    1.666     2.620    0.9311     80.69    882.28    486.20     0.816    33.481
```

```
PROGRAM SCROLL                                                              D.D. WILLIAMS

                    SCROLL AND GUIDE VANE TESTS OF ICP RADIAL TURBINE

                TABLE A7                                    CLEARANCE = 0.030 IN.

                                        INPUT DATA

PT     DPVC      PUVC       P5P      PATM      HREF1      H1        SR       TRM        V4        V5

 1     0.840     2.000     1.150    30.000     0.0       2.096     1.360    75.200     1.399     1.395
 2     2.352     5.670     3.350    30.000     0.0       6.133     4.000    76.000     1.420     1.410
 3     3.228     7.900     4.750    30.000     0.0       8.606     5.670    76.300     1.435     1.425
 4     4.291    10.900     6.630    30.000     0.0      12.080     7.900    78.000     1.440     1.430
 5     5.555    14.450     8.920    30.000     0.0      16.384    10.630    78.400     1.485     1.480
 6     7.038    18.950    11.980    30.000     0.0      22.028    13.940    78.800     1.505     1.500
 7     8.202    22.830    14.600    30.000     0.0      27.082    16.940    78.800     1.520     1.515
 8     9.895    28.550    18.650    30.000     0.0      35.422    21.450    79.000     1.555     1.545
 9    11.406    34.000    22.550    30.000     0.0      45.122    25.657    79.300     1.570     1.563
10    12.473    37.600    25.400    30.000     0.0      50.191    28.350    79.800     1.595     1.590

                   TCJ - 32.00             STARE - 0.0             R1 - 0.954


                                       OUTPUT DATA

    PT    PTO/P1    WVC       PHI       ALPH(1)    V1        T1        MACH1       P1

     1    1.034    0.508    0.8848      80.97    221.00    536.79      0.195     30.147
     2    1.099    0.881    0.8996      80.95    374.05    529.72      0.332     30.442
     3    1.139    1.056    0.9063      80.96    442.45    525.59      0.394     30.623
     4    1.193    1.255    0.9174      81.01    518.62    519.67      0.464     30.873
     5    1.256    1.475    0.9254      80.96    593.78    514.43      0.534     31.189
     6    1.339    1.728    0.9193      80.78    664.69    507.69      0.602     31.603
     7    1.407    1.929    0.9280      80.78    723.72    501.38      0.659     31.975
     8    1.507    2.216    0.9366      80.73    797.67    493.05      0.733     32.589
     9    1.594    2.477    0.9432      80.65    853.65    485.97      0.790     33.302
    10    1.663    2.654    0.9342      80.46    880.95    482.96      0.818     33.673
```

```
PROGRAM SCROLL                                                                          D.D. WILLIAMS

                          SCROLL AND GUIDE VANE TESTS OF ICP RADIAL TURBINE

            TABLE A8                                           CLEARANCE = 0.024 IN.

                                              INPUT DATA

PT     DPVC      PUVC      P5P      PATM      HREF1       H1        SR       TRM        V4        V5

 1    1.237     2.920     1.700    29.960     0.0       3.193     2.020    72.900     1.520     1.435
 2    2.295     5.500     3.250    29.960     0.0       6.135     3.890    73.900     1.535     1.465
 3    3.391     8.340     5.000    29.960     0.0       9.529     5.990    74.500     1.540     1.495
 4    4.514    11.400     6.930    29.960     0.0      13.098     8.270    75.100     1.543     1.505
 5    5.747    14.930     9.230    29.960     0.0      17.457    10.960    75.800     1.560     1.523
 6    6.904    18.540    11.660    29.960     0.0      21.845    13.680    76.200     1.580     1.545
 7    8.201    22.750    14.570    29.970     0.0      27.475    17.000    77.000     1.590     1.555
 8    9.913    28.600    18.200    29.970     0.0      35.859    21.440    77.900     1.600     1.565
 9   11.395    34.050    22.700    29.970     0.0      44.934    25.670    78.800     1.610     1.580
10   12.397    37.900    25.420    29.970     0.0      51.838    28.210    79.000     1.625     1.598

                  TCJ - 32.00             STARE - 0.0             B1 - 0.942


                                              OUTPUT DATA

         PT    PTO/P1     WVC       PHI       ALPH(1)     V1         T1         MACH1       P1

          1    1.050     0.619    0.8922      80.87     269.11     536.20      0.237     30.195
          2    1.096     0.866    0.9036      80.87     370.45     531.84      0.328     30.408
          3    1.146     1.083    0.9134      80.87     455.73     527.01      0.405     30.656
          4    1.200     1.288    0.9181      80.83     529.07     521.34      0.473     30.917
          5    1.263     1.502    0.9242      80.79     601.13     515.18      0.540     31.236
          6    1.329     1.701    0.9260      80.74     662.68     509.46      0.599     31.558
          7    1.405     1.923    0.9349      80.74     728.65     502.16      0.663     31.980
          8    1.492     2.215    0.9469      80.60     797.81     493.72      0.732     32.595
          9    1.600     2.474    0.9415      80.55     855.57     486.28      0.791     33.260
         10    1.658     2.650    0.9333      80.33     877.98     483.67      0.814     33.767
```

```
PROGRAM SCROLL                                                                     D.D. WILLIAMS

                     SCROLL AND GUIDE VANE TESTS OF ICP RADIAL TURBINE

                 TABLE A9                                  CLEARANCE = 0.015 IN.

                                          INPUT DATA
PT     DPVC      PUVC      P5P      PATM      HREF1      H1       SR       TRM        V4        V5

 1     1.309     3.070     1.780   30.120     0.0      3.548     2.120    75.000    1.545     1.460
 2     2.428     5.820     3.420   30.120     0.0      6.792     4.120    76.000    1.562     1.485
 3     3.503     8.590     5.130   30.120     0.0     10.197     6.170    76.900    1.580     1.510
 4     4.611    11.630     7.090   30.120     0.0     13.879     8.440    77.200    1.590     1.535
 5     5.776    14.960     9.250   30.120     0.0     18.168    10.970    78.100    1.605     1.550
 6     7.046    18.900    11.910   30.060     0.0     23.169    13.980    79.000    1.600     1.550
 7     8.328    23.050    14.710   30.060     0.0     28.797    17.240    79.200    1.615     1.565
 8     9.992    28.890    18.840   30.060     0.0     38.109    21.700    80.100    1.615     1.565
 9    11.853    35.650    23.810   30.060     0.0     50.719    26.790    80.100    1.620     1.570
10    12.683    38.820    26.150   30.060     0.0     56.909    29.050    80.600    1.635     1.580

                  TCJ - 32.00               STARE - 0.0               R1 - 0.924


                                          OUTPUT DATA

          PT    PTO/P1     WVC       PHI        ALPH(1)    V1        T1         MACH1      P1

           1    1.052     0.639     0.8942      80.60    273.97    536.85     0.241     30.374
           2    1.099     0.894     0.9090      80.68    379.91    531.94     0.336     30.610
           3    1.147     1.104     0.9177      80.67    460.69    527.15     0.409     30.858
           4    1.202     1.305     0.9201      80.64    533.13    522.01     0.476     31.128
           5    1.260     1.507     0.9262      80.61    600.20    516.20     0.539     31.441
           6    1.332     1.724     0.9305      80.58    668.51    508.98     0.604     31.747
           7    1.404     1.942     0.9397      80.56    732.03    502.09     0.666     32.160
           8    1.503     2.230     0.9447      80.49    802.56    493.08     0.737     32.843
           9    1.612     2.553     0.9462      80.36    865.81    484.47     0.802     33.771
          10    1.660     2.698     0.9440      80.26    888.48    481.50     0.826     34.225
```

APPENDIX B

PROGRAM RADIAL

Program RADIAL computes the referred flow rate, head coefficient, degree of reaction, relative and absolute rotor inlet flow angles, velocity and loss coefficients for the scroll and guide vanes, referred moment, absolute discharge flow angle, velocity and loss coefficients for the rotor, and efficiencies from the torque, speed, mass flow rate, and the pressure and temperature data obtained during the active rotor tests. The calculation technique generally follows that given in the theory of Section 4.3. It can process any number of clearances (sets) and any number of pressure ratios (runs) per clearance with a maximum of ten different speed settings (points) per run. A listing of program RADIAL is given in Table B1.

In program RADIAL, use was made of temporary memory disc storage of the input data in order to avoid the awkward procedure of subscripting the input variables. This procedure permits the processing and printing of the input data on a point-by-point basis and the presentation of the results in a compact, tabular form. Appropriate comments appear in the main program at the points where this procedure was used. The additional control cards required to implement this technique and to obtain necessary additional memory core storage space are shown in Table B2. As the table indicates, these cards are inserted just ahead of the data cards in the assembled deck.

The torque calibration data used for all runs are given in Table B3. The input and output values resulting from the five sets of test data are presented in Tables B4 through B13.

B1 Subroutines TEMP and FLOW

These subroutines perform the same functions as in program SCROLL, namely those of obtaining temperatures from the thermocouple readings and calculating mass flow rate, respectively. Subroutine TEMP has been expanded to include calculation of the temperatures of the bearing lubricating oil at the inlet and at the discharge of each bearing. However for reasons discussed in Section 4, these values were not used in this experiment.

B2 Subroutine PRESS

Subroutine PRESS establishes the total-to-static pressure ratios across the scroll and guide vanes (P_{to}/p_1) and across the turbine (P_{to}/p_2) and the ratio p_1/p_2. An iteration process is necessary in order to determine an average value of the total pressure at the turbine inlet, P_{to}. Three relations are used to accomplish this, these being the gas law,

$$\rho_o = C_{f1} \frac{P_o}{R_g T_o} \tag{B1}$$

the continuity equation,

$$V_o = \frac{\dot{W}}{\rho_o A_5} \tag{B2}$$

and the energy equation,

$$T_o = T_{to} - \frac{V_o^2}{2 g J c_p} \tag{B3}$$

where A_5 is the area of the five-inch inlet pipe and C_p is the specific heat of air at the temperature T_{t0}. Using T_{t0} as a first approximation of ρ_0, an initial value of V_0 is found, and from this, by Equation (B3), a new value of T_0. The iteration continues until a difference of 0.01

degrees or less exists between any two successive values of T_0. Since velocities are low, the total pressure P_{t0} is then obtained from

$$P_{t_0} = p_0 + \frac{\rho_0 V_0^2}{2 g C_{f_1}} \tag{B4}$$

B3 Subroutine EDC

This subroutine computes the mean values of γ and C_P based on the arithmetic mean of total turbine inlet and static isentropic discharge temperatures. From Reference 3, the variations of γ and C_p with temperature are

$$\gamma = 1.4018 - (2 \times 10^{-5})\, t \tag{B5}$$

$$C_p = 0.23943 + (3.4 \times 10^{-6})\, t + (2 \times 10^{-8})\, t^2 \tag{B6}$$

These relations were originally obtained from data tabulated in Reference 12 and are valid from approximately 40°F to 170°F.

The values of γ_{avg} and $C_{P(avg)}$ correspond to the average temperature through the turbine based on an isentropic expansion. This average temperature, t, is given by

$$t = (T_{t_0} - 459.69) - \frac{\Delta T_{is}}{2} \tag{B7}$$

where

$$\Delta T_{is} = T_{t_0} \left[1 - (P_2 / P_{t_0})^{\frac{\gamma - 1}{\gamma}} \right] \tag{B8}$$

Using an iteration process, the first approximation of ΔT_{is} is based on a value of γ corresponding to T_{t0}. The value of t resulting from Equation (B6) is compared with the previous value of t in each iteration until the difference between any two successive values of t is less than

1.0°. Using the final value of t, values of γ_{avg}, $C_{P(avg)}$, and ΔT_{is} are computed from Equations (B5), (B6), and (B8), respectively. The reference parameter θ, given by

$$\theta = (\gamma_{avg}/1.4)(T_5/518.7) \tag{B9}$$

is also computed in this subroutine.

The subscript indicating the average values of γ and C_p will be dropped in subsequent discussions. The average values of these quantities are assumed in the remainder of the program unless otherwise stated.

B4 Subroutines TORQ and DYNA

These subroutines compute the net torque produced by the turbine by evaluating the bearing friction moment and the torque measured by the dynamometer.

In subroutine TORQ, the bearing friction moment is evaluated from turbine rpm by Equations (27), (28), and (29). The net moment is calculated by Equation (30), where the dynamometer torque output is found in subroutine DYNA, called from subroutine TORQ.

Subroutine DYNA determines the torque from the dynamometer calibration data obtained for each run. These data are tabulated in Table B3 for all runs.

The values of the torque calibration data constitute a one-dimensional array with five elements, representing the torque scale reading for loads of zero to 400 inch-pounds, respectively, taken at 100 inch-pound intervals. Thus, TCD(1) represents the torque scale readout value for the no load condition. Using a DO loop with index I, the torque indicator reading for the test point being processed, TQ, is compared with the values of TCD(I) to determine the interval (I, I+1) within which TQ lies. Since the calibration curve data are very nearly linear, the torque is computed assuming a straight line approximation between TCD(I) and TCD(I-1), by the equation

$$T = 100(I-1) + 100 \left[\frac{TQ - TCD(I)}{TCD(I+1) - TCD(I)} \right] \qquad \text{(B10)}$$

This procedure was adapted from that used by Riley (3).

B5 Subroutine TURB

The turbine performance parameters described in Section 4 are calculated by subroutine TURB in a manner which follows the theory previously given. No iterations are involved, and the equations used are self-explanatory. Therefore, the steps will not be discussed here. The velocity coefficient, ϕ , and the absolute rotor inlet flow angle, α_1, are provided from subroutine PHIAL, for which TURB is the calling subroutine.

B6 Subroutine PHIAL

This subroutine calculates the values of ϕ , α_1, V_1, and ζ_N, from the results of program SCROLL. The values of γ and C_p used are based on the total inlet temperature, rather than the average temperature as computed in subroutine EDC, because the values of ϕ and α_1 obtained in program SCROLL were computed in this manner.

The values of ϕ and α_1 are obtained from Equations (13) and (14), for which the entering arguments are CLNC, the axial clearance, and ACH1, or M_1, the Mach number at the rotor inlet. Since V_1 and T_1 are not known at this point in the computations, they must be obtained by iteration. An initial value of V_1 is obtained from Equation (4) by assuming $\phi = 1.0$, and initial values of T_1 and M_1 are obtained from Equations (35) and (36), respectively. Using this value of M_1, called ACHIA, and CLNC, a value of

ϕ, called PHIA, is obtained from Equation (13). The assumed value of ϕ is reduced in increments of 0.001 until succeeding values of ϕ and ϕ_A differ by no more than 0.001. Thus, values of V_1, M_1, and ϕ are established, and α_1 is then computed from Equation (14). The loss coefficient for the scroll and guide vanes, ζ_N, is then obtained from Equation (12).

B7 Subroutine REFER

This subroutine computes the referred speed, referred flow rate, and referred moment in accordance with Equations (60), (61), and (62), respectively.

B8 Method of Assembly of Input Data

In order to facilitate future use of program RADIAL, the order of assembly of the input data cards is given. The actual formats for the numerical entries may be obtained directly from the program listing. All items of data are given in the order in which they must appear on the data cards. For convenience, the symbols are redefined.

Card No.	FORTRAN	Description
1	NSETS	Number of sets of data (clearances to be processed
2	CLNC	Clearance for set
3	NRUNS	Number of runs (pressure ratios) in data set
4	TCD	Torque calibration data for run (5 values).
5	NPTS	Number of data points (speeds) in run
6	RPM	Measured turbine speed (rpm)
	TQ	Torque indicator reading (counts)
	PUVC	Measured pressure upstream of flow measuring orifice, from vena contracta taps (in. Hg gage)

Card No.	FORTRAN	Description
	P5P	Measured static pressure at turbine inlet (in. Hg gage)
	H1	Average static pressure ahead of rotor (in H_2O gage)
	DPVC	Measured pressure differential across flow orifice, from vena contracta taps (in. Hg)
	PATM	Barometric pressure (in. Hg)
	HREF1	Measured reference pressure applied to water manometer board (in. Hg gage)
	V4	Thermocouple reading ahead of orifice (mv.)
	V5	Thermocouple reading at turbine inlet (mv.)
7	V20	Thermocouple reading at lube oil inlet (mv.)
	V21	Thermocouple reading at lube oil discharge from right bearing (mv.)
	V22	Thermocouple reading at lub oil discharge from left bearing (mv.)
	TRM	Control room temperature (°F)
	TCJ	Cold junction temperature (°F)

Cards 6 and 7 comprise the input data for one test point and are repeated for a total of NPTS test points for each run. Each new run begins with card 4, and each new set begins with card 2.

TABLE B1
LISTING OF PROGRAM RADIAL

```
C
C  PROGRAM RADIAL.  PERFORMANCE EVALUATION OF ICP RADIAL TURBINE.
C
      DIMENSION RPM(10),TQ(10),PUVC(10),P5P(10),H1(10),PATM(10),HREF1(10
     *),V4(10),V5(10),V20(10),V21(10),V22(10),TRM(10),TCJ(10),TCD(50),
     *DPVC(10)
      COMMON T4,T5,T20,T21,T22,WVC,P1,PTO,PR1,PR2,PSR,DTIS,DHIS,CP,GAM,E
     *XP,TNET,ROSP,T,ETA,ETAL,ACH1,PHI,V1,ALPH1,ZETAN,BETA1,PSI,PSIL,
     *ZETR,ZETRL,TR,TNETR,ALF2,ALF2L,RPMR,WVCR,BFM,HEAD,DR
      READ(5,1) NSETS
    1 FORMAT(I4)
      DO 11 N=1,NSETS
      READ(5,3) CLNC
    3 FORMAT(F5.3)
C  WRITE HEADING FOR INPUT DATA.
      WRITE(6,100)
  100 FORMAT(1H1,///,T43,'PERFORMANCE EVALUATION OF ICP RADIAL TURBINE',
     *//)
      WRITE(6,101) CLNC
  101 FORMAT(T20,'TABLE',T60,'INPUT DATA',T89,'CLEARANCE = ',F5.3,1X,'IN
     *.',//,T4,'RUN/PT    RPM   TORQUE  PUVC     P5P      H1      DPVC
     * PATM    HREF1     V4      V5     V20     V21     V22    TRM    TC
     *J',/,T20,'COUNTS  IN.HG   IN.HG   IN.H20   IN.HG   IN.HG   IN.HG
     *   MV      MV      MV      MV      MV    DEG.F  DEG.F',/)
      WRITE(6,102)
  102 FORMAT(T2,'-------------------------------------------------------
     *------------------------------------------------------------------
     *-----',//)
C  REWIND TEMPORARY DATA SET TO HOLD VALUES FOR RUN UNTIL PROCESSED.
      REWIND 8
      READ(5,1) NRUNS
      DO 12 J=1,NRUNS
      READ(5,4) (TCD(I),I=1,5)
    4 FORMAT(5F7.1)
C  WRITE TORQUE CALIBRATION DATA ON TEMPORARY DATA SET.
      WRITE(8)(TCD(I),I=1,5)
      READ(5,1) NPTS
      WRITE(8) NPTS
      DO 13 K=1,NPTS
C  READ INPUT DATA.
      READ(5,5) RPM(K),TQ(K),PUVC(K),P5P(K),H1(K),DPVC(K),PATM(K),HREF1(
     *K),V4(K),V5(K)
      READ(5,6) V20(K),V21(K),V22(K),TRM(K),TCJ(K)
    5 FORMAT(2F7.0,3F7.2,F7.3,F6.2,F7.2,2F7.3)
    6 FORMAT(3F7.3,F6.1,F7.2)
```

```
C   WRITE INPUT DATA.
       WRITE(6,7) J,K,RPM(K),TQ(K),PUVC(K),P5P(K),H1(K),DPVC(K),PATM(K),
      *HREF1(K),V4(K),V5(K),V20(K),V21(K),V22(K),TRM(K),TCJ(K)
     7 FORMAT(2X,2I3,1X,F7.0,2X,F6.0,3F8.2,F9.3,2F8.2,5F8.3,2F7.1)
       IF(K.EQ.NPTS) GO TO 8
       GO TO 13
     8 WRITE(6,103)
   103 FORMAT(/)
    13 CONTINUE
C   WRITE DATA FOR ONE RUN ON TEMPORARY DATA SET.
       WRITE(8)(RPM(I),TQ(I),PUVC(I),P5P(I),H1(I),DPVC(I),PATM(I),HREF1(I
      *),V4(I),V5(I),V20(I),V21(I),V22(I),TRM(I),TCJ(I),I=1,NPTS)
    12 CONTINUE
C   WRITE HEADING FOR PRINTOUT OF RESULTS.
       WRITE(6,200)
   200 FORMAT(1H1,///,T44,'PERFORMANCE EVALUATION OF ICP RADIAL TURBINE',
      *//)
       WRITE(6,201) CLNC
   201 FORMAT(T22,'TABLE',T61,'OUTPUT DATA',T91,'CLEARANCE = ',F5.3,1X,
      *'IN.',//)
       WRITE(6,202)
   202 FORMAT(T39,'REDUCED TO STANDARD AIR IN ACCORDANCE WITH NASA METHOD
      *.',/,T39,'TOTAL INLET PRESS. = 14.7 PSIA, TOTAL INLET TEMPERATURE'
      *,/,T39,'= 518.7 DEG.R., GAMMA = 1.4, CP = 0.24 BTU/LBM-DEG.F.',//)
       WRITE(6,203)
   203 FORMAT(/,T76,'NO BEARING LOSSES',T106,'MAXIMUM BEARING LOSSES',/,
      *T69,'------------------------------  ---------------------------
      *---',/,T10,'PRESS  REF.   REF.  HEAD   DEG  ANGLE  ANGLE  VEL  LOS
      *S     REF   ANGLE  VEL  LOSS  EFFIC-   REF   ANGLE  VEL  LOSS  EFF
      *IC-',/,T2,'RUN/PT  RATIO SPEED   FLOW  COEFF REACT ALPH1  BETA1 CO
      *EFF COEFF    MOM   ALF20 COEFF COEFF IENCY    MOM   ALF20 COEFF CO
      *EFF IENCY',/,T17,'RPM  LB/SEC',T43,'DEG    DEG   GV     GV     FT.
      *LB   DEG         ROTOR             FT.LB   DEG          ROTOR',/)
       WRITE(6,204)
   204 FORMAT(T2,'-------------------------------------------------------------
      *--------------------------------------------------------------
      *-----------')
       REWIND 8
C   PROCESS DATA POINTS.
       DO 21 J=1,NRUNS
C   READ TORQUE CALIBRATION DATA FROM TEMPORARY DATA SET.
       READ(8)(TCD(I),I=1,5)
       READ(8) NPTS
C   READ DATA FOR ONE RUN FROM TEMPORARY DATA SET.
       READ(8)(RPM(I),TQ(I),PUVC(I),P5P(I),H1(I),DPVC(I),PATM(I),HREF1(I)
     *,V4(I),V5(I),V20(I),V21(I),V22(I),TRM(I),TCJ(I),I=1,NPTS)
      WRITE(6,205)
  205 FORMAT(/)
      DO 22 K=1,NPTS
      GHG=13.63905-1.363030E-3*TRM(K)
      GWR=.9983763+1.060576E-4*TRM(K)-1.593186E-6*TRM(K)**2
      CF1=70.438824*GHG/13.54
      CALL TEMP (V4(K),V5(K),V20(K),V21(K),V22(K),TCJ(K))
      CALL FLOW (GHG,DPVC(K),PUVC(K),PATM(K))
      CALL PRESS (PATM(K),HREF1(K),GHG,GWR,H1(K),P5P(K),CF1)
      CALL EDC (THETA)
      CALL TORQ (RPM(K),TCD,TQ(K))
      CALL TURB (RPM(K),CLNC)
      CALL REFER (RPM(K),THETA,GHG)
C  WRITE OUTPUT DATA.
      WRITE(6,9) J,K,PR2,RPMR,WVCR,HEAD,DR,ALPH1,BETA1,PHI,ZETAN,TR,ALF2
     *,PSI,ZETR,ETA,TNETR,ALF2L,PSIL,ZETRL,ETAL
    9 FORMAT(2I3,F8.3,F7.0,F7.3,2F6.3,F6.2,F7.2,2F6.3,F8.2,F7.2,2F6.3,
     *F6.2,F8.2,F7.2,2F6.3,F6.2)
   22 CONTINUE
   21 CONTINUE
   11 CONTINUE
      RETURN
      END




      SUBROUTINE TEMP (V4,V5,V20,V21,V22,TCJ)
C  CALCULATES TEMPERATURES FROM THERMOCOUPLE READINGS.
C  THERMOCOUPLE EQUATIONS VALID FOR IRON-CONSTANTAN ONLY.
      COMMON T4,T5,T20,T21,T22,WVC,P1,PTO,PR1,PR2,PSR,DTIS,DHIS,CP,GAM,E
     *XP,TNET,ROSP,T,ETA,ETAL,ACH1,PHI,V1,ALPH1,ZETAN,BETA1,PSI,PSIL,
     *ZETR,ZETRL,TR,TNETR,ALF2,ALF2L,RPMR,WVCR,BFM,HEAD,DR
      DO 122 J=1,5
      GO TO (110,111,112,113,114),J
  110 V=V4
      GO TO 123
  111 V=V5
      GO TO 123
  112 V=V20
```

```
      GO TO 123
  113 V=V21
      GO TO 123
  114 V=V22
  123 T=TCJ+0.144+35.77*V-0.4518*V**2
      IF(T.LE.100.) GO TO 115
      T=TCJ+1.252+34.86*V-0.1855*V**2
  115 IF(J.GT.2) GO TO 116
      T=T+459.69
  116 GO TO (117,118,119,120,121),J
  117 T4=T
      GO TO 122
  118 T5=T
      GO TO 122
  119 T20=T
      GO TO 122
  120 T21=T
      GO TO 122
  121 T22=T
  122 CONTINUE
      RETURN
      END
```

```
      SUBROUTINE FLOW (GHG,DPVC,PUVC,PATM)
C   CALCULATES FLOW RATE FROM ORIFICE MEASUREMENTS.
      COMMON T4,T5,T20,T21,T22,WVC,P1,PTO,PR1,PR2,PSR,DTIS,DHIS,CP,GAM,E
     *XP,TNET,RCSP,T,ETA,ETAL,ACH1,PHI,V1,ALPH1,ZETAN,BETA1,PSI,PSIL,
     *ZETR,ZETRL,TR,TNETR,ALF2,ALF2L,RPMR,WVCR,BFM,HEAD,DR
      DVC=DPVC*GHG/13.54
      PVC=(PUVC+PATM)*GHG/13.54
      A=1.+1.85E-5*(T4-532.)
      Z=1.9+2.4E-3*(T4-560.)
      Y=1.-.351*DVC/PVC
      WVC=2.2854*A*Y*SQRT(PVC*DVC/T4)
      X=WVC*.8131/Z
      WVC=(1.+.001275/X)*WVC
      RETURN
      END
      SUBROUTINE PRESS (PATM,HREF1,GHG,GWR,H1,P5P,CF1)
C   CALCULATES INLET TOTAL PRESSURE AND PRESSURE RATIOS WITHIN TURBINE.
      COMMON T4,T5,T20,T21,T22,WVC,P1,PTO,PR1,PR2,PSR,DTIS,DHIS,CP,GAM,E
     *XP,TNET,ROSP,T,ETA,ETAL,ACH1,PHI,V1,ALPH1,ZETAN,BETA1,PSI,PSIL,
     *ZETR,ZETRL,TR,TNETR,ALF2,ALF2L,RPMR,WVCR,BFM,HEAD,DR
      A=T5-459.69
      CP5=.23943+3.4E-6*A+2.E-8*A**2
      P1=((PATM+HREF1)*GHG+(H1*GWR))/13.54
      PS5=(PATM+P5P)*GHG/13.54
      TT=T5
  100 RHO=PS5*CF1/(TT*53.3448)
      VO=WVC/(RHO*3.14159*6.25/144.)
      TO=T5-(VO**2)/(2.*32.174*778.16*CP5)
      DTT=TT-TO
      TT=TO
      IF(ABS(DTT)-.01) 101,101,100
  101 PTO=PS5+RHO*(VO**2)/(2.*32.174*CF1)
      PR1=PTO/P1
      PR2=PTO/(PATM*GHG/13.54)
      PSR=P1/(PATM*GHG/13.54)
      RETURN
      END
```

```
      SUBROUTINE EDC (THETA)
C   CALCULATES AVERAGE TEMP. FOR DETERMINATION OF CP,GAMMA,AND SQ. ROOT
C     OF TEMP. RATIO (THETA), AND ISENTROPIC ENTHALPY DROP (DHIS).
      COMMON T4,T5,T20,T21,T22,WVC,P1,PTO,PR1,PR2,PSR,DTIS,DHIS,CP,GAM,E
     *XP,TNET,ROSP,T,ETA,ETAL,ACH1,PHI,V1,ALPH1,ZETAN,BETA1,PSI,ZETAR,AL
     *F20,RPMR,WVCR,TNETR,BFM,HEAD,DR
      A=T5-459.69
```

```
  105 GA=1.4018-2.E-5*A
      EX=(GA-1.)/GA
      DT=T5*(1.-1./PR2**EX)
      AA=T5-459.69-DT/2.
      AAA=ABS(AA-A)
      IF(AAA-1.) 107,107,106
  106 A=AA
      GO TO 105
  107 GAM=GA
      EXP=EX
      DTIS=DT
      CP=.23943+3.4E-6*AA+2.E-8*AA**2
      DHIS=CP*DTIS
      IF(GAM*T5) 2050,2051,2051
 2050 WRITE(6,2052) K,GAM,T5
 2052 FORMAT(//,6X,I4,2F8.3)
 2051 CONTINUE
      THETA=(GAM/1.4)*(T5/518.7)
      RETURN
      END


      SUBROUTINE TORQ (RPM,TCD,TQ)
C   CALCULATES NET TORQUE (MEASURED PLUS THAT DUE TO BEARING FRICTION).
      DIMENSION TCD(5)
      COMMON T4,T5,T20,T21,T22,WVC,P1,PTO,PR1,PR2,PSR,DTIS,DHIS,CP,GAM,E
     *XP,TNET,ROSP,T,ETA,ETAL,ACH1,PHI,V1,ALPH1,ZETAN,BETA1,PSI,PSIL,
     *ZETR,ZETRL,TR,TNETR,ALF2,ALF2L,RPMR,WVCR,BFM,HEAD,DR
      ROSP=3.14159*RPM/30.
C   COMPUTE BEARING FRICTION MOMENT FROM COAST-DOWN DATA OF VAVRA, FOR
C       MAXIMUM LOSS CONDITION.
      IF(RPM.LE.10500.) GO TO 99
      HPF=-.6+(.17143)*(RPM/1000.)-(4.898E-3)*(RPM/1000.-10.5)**2
      GO TO 100
   99 HPF=-.6+(.17143)*(RPM/1000.)
  100 BFM=(HPF*550.)/ROSP
      CALL DYNA (TQ,TCD,T)
      TNET=T+BFM
      RETURN
      END




      SUBROUTINE DYNA (TQ,TCD,T)
C  CALCULATES DYNAMOMETER TORQUE FROM TORQUE READOUT AND TORQUE CAPSULE
C     CALIBRATION DATA.
      DIMENSION TCD(5)
      DO 100 I=1,5
      IF(TCD(I)-TQ) 100,100,101
  100 CONTINUE
  101 AI=100.*(I-1)
      T=AI+100.*((TQ-TCD(I))/(TCD(I+1)-TCD(I)))
      T=T/12.
      RETURN
      END




      SUBROUTINE TURB (RPM,CLNC)
C  CALCULATES HEAD COEFFICIENT, LOSS COEFFICIENTS, EFFICIENCIES, AND FLOW
C     ANGLES.
      COMMON T4,T5,T2C,T21,T22,WVC,P1,PTO,PR1,PR2,PSR,DTIS,DHIS,CP,GAM,E
     *XP,TNET,ROSP,T,ETA,ETAL,ACH1,PHI,V1,ALPH1,ZETAN,BETA1,PSI,PSIL,
     *ZETR,ZETRL,TR,TNETR,ALF2,ALF2L,RPMR,WVCR,BFM,HEAD,DR
      DTW=(TNET*ROSP)/(CP*WVC*778.16)
      ETAL=DTW/DTIS
      DTWNL=(T*ROSP)/(CP*WVC*778.16)
      ETA=DTWNL/DTIS
      CC=SQRT(2.*32.174*778.16*CP*DTIS)
      D1=9.40
      U1=3.14159*RPM*D1/720.
      CC=CC/U1
      HEAD=CC**2
      DR=1.-(T5/DTIS)*(1.-(1./PR1)**EXP)
      CALL PHIAL (CLNC)
C   THE LETTER L AT END OF VARIABLE NAME INDICATES DIVISION BY U1.
      V1U=V1/U1
      X=ALPH1/57.29578
      VU1U=V1U*SIN(X)
      WU1U=VU1U-1.
      VM1U=V1U*COS(X)
C   W1U12=(W1/U1)**2
      W1U12=VM1U**2+WU1U**2
      Y=WU1U/VM1U
      BET=ATAN(Y)
      BETA1=BET*57.29578
      R1=4.7
      R20=2.94
      VU2U=(R1/R20)*(VU1U-(ETA/2.)*HEAD)
      VU2UL=(R1/R20)*(VU1U-(ETAL/2.)*HEAD)
C   BET20 = -69.85 DEGREES.
      BET20=(-69.85)/57.29578
      W20U=(VU2U-R20/R1)/SIN(BET20)
      W20UL=(VU2UL-R20/R1)/SIN(BET20)
C   W20TU=W2OTH/U1
      W20TU=SQRT(DR*HEAD+(VM1U**2)+((R20/R1)**2)-1.)
      PSI=W20U/W20TU
      PSIL=W20UL/W20TU
      ZETR=1.-PSI**2
      ZETRL=1.-PSIL**2
      VM2U=W20U*COS(BET20)
      VM2UL=W20UL*COS(BET20)
      ALF2=57.29578*ATAN(VU2U/VM2U)
      ALF2L=57.29578*ATAN(VU2UL/VM2UL)
      ETA=100.*ETA
      ETAL=100.*ETAL
      RETURN
      END
      SUBROUTINE PHIAL (CLNC)
C  CALCULATES VALUES OF PHI, ALPH1, V1, ZETAN, FROM RESULTS OF PROGRAM
C     SCROLL.
      COMMON T4,T5,T20,T21,T22,WVC,P1,PTO,PR1,PR2,PSR,DTIS,CHIS,CP,GAM,E
     *XP,TNET,ROSP,T,ETA,ETAL,ACH1,PHI,V1,ALPH1,ZETAN,BETA1,PSI,PSIL,
     *ZETR,ZETRL,TR,TNETR,ALF2,ALF2L,RPMR,WVCR,BFM,HEAD,DR
      A=T5-459.69
      GAMMA=1.4018-2.E-5*A
      EXP=(GAMMA-1.)/GAMMA
      CP5=.23943+3.4E-6*A+2.E-8*A**2
      G=2.*32.174*778.16*CP5
      B=T5*(1.-1./PR1**EXP)
      PHI=1.
  100 V1=PHI*SQRT(G*B)
      T1=T5-(V1**2)/G
      ACH1A=V1/SQRT(32.174*GAMMA*53.3448*T1)
      PHIA=(.92473)*(1.01433-1.24601*CLNC+24.06839*CLNC**2-180.36258*CLN
     *C**3)*(.93149+.18292*ACH1A-.09202*ACH1A**2)
      IF(ABS(PHI-PHIA)-.0001) 102,102,101
  101 PHI=PHI-.0001
      GO TO 100
  102 ACH1=ACH1A
      PHI=PHIA
      ALPH1=(81.762)*(.98267+.26958*CLNC-.65080*CLNC**2)*(.99624+.02223*
     *ACH1-.02940*ACH1**2)
      ZETAN=1.-PHI**2
      RETURN
      END


      SUBROUTINE REFER (RPM,THETA,GHG)
C  COMPUTES SPEED, NET MOMENT, FLOW RATE, REDUCED TO STANDARD AIR IN
C     ACCORDANCE WITH NASA METHOD.
      COMMON T4,T5,T20,T21,T22,WVC,P1,PTO,PR1,PR2,PSR,DTIS,DHIS,CP,GAM,E
     *XP,TNET,ROSP,T,ETA,ETAL,ACH1,PHI,V1,ALPH1,ZETAN,BETA1,PSI,PSIL,
     *ZETR,ZETRL,TR,TNETR,ALF2,ALF2L,RPMR,WVCR,BFM,HEAD,DR
C  REFERRED SPEED.  (THETA OBTAINED IN SUBROUTINE EDC.)
      RPMR=RPM/SQRT(THETA)
      DEL=(PTO*(GHG/13.54))/29.92
      X=(GAM+1.)/(2.*(GAM-1.))
      EPS=(.810/GAM)*((GAM+1.)/2.)**X
C   REFERRED FLOW RATE.
      WVCR=WVC*(SQRT(THETA))*EPS/DEL
C   REFERRED MOMENT.
      TR=T*EPS/DEL
      TNETR=TNET*EPS/DEL
      RETURN
      END
      END
/*
//G0.FT06F001    DD SYSOUT=A,SPACE=(CYL,(15,1))
//G0.FT08F001   DD UNIT=SYSDA,SPACE=(TRK,(2,1)),                        *
//               DCB=(RECFM=V,LRECL=500,BLKSIZE=504)
//G0.SYSIN DD*
```

```
1     7        16                 COLUMN                              72
```

TABLE B2
ADDITIONAL CONTROL CARDS REQUIRED FOR PROGRAM RADIAL

TABLE B3

TORQUE CALIBRATION DATA

SET	CLEARANCE (IN)	RUNS	APPLIED TORQUE (IN-LB)				
			0	100	200	300	400
1	0.081	1-4	5.	261.	518.	768.	1013.
		5-6, NOSPD 1	2.	255.	510.	762.	1009.
2	0.061	1-3	0.	255.	511.	760.	1007.
		4-6, NOSPD 2	3.	259.	514.	762.	1007.
3	0.041	1-3	0.	257.	511.	760.	1007.
		4-6, NOSPD 3	0.	257.	510.	759.	1004.
4	0.024	1-3	0.	256.	510.	760.	1006.
		4-6, NOSPD 4	1.	259.	513.	762.	1007.
5	0.015	1-4	0.	255.	511.	760.	1008.
		5-6, NOSPD 5	-2.	255.	510.	759.	1004.

PERFORMANCE EVALUATION OF ICP RADIAL TURBINE

TABLE B4 INPUT DATA CLEARANCE = 0.081 IN.

RUN/PT		RPM	TORQUE COUNTS	PUVC IN.HG	P5P IN.HG	H1 IN.H2O	DPVC IN.HG	PATM IN.HG	HREF1 IN.HG	V4 MV	V5 MV	V20 MV	V21 MV	V22 MV	TEM DEG F	TCJ DEG F
1	1	5650.	185.	9.06	5.85	23.25	3.246	30.07	0.0	1.340	1.245	0.0	0.0	0.0	77.8	32.0
1	2	7620.	149.	8.76	5.90	27.05	2.801	30.07	0.0	1.365	1.280	0.0	0.0	0.0	78.8	32.0
1	3	9670.	107.	8.27	5.90	35.51	2.413	30.07	0.0	1.380	1.300	0.0	0.0	0.0	79.2	32.0
1	4	11720.	65.	7.77	5.91	45.76	1.883	30.07	0.0	1.380	1.305	0.0	0.0	0.0	80.0	32.0
1	5	13330.	25.	7.30	5.96	55.79	1.366	30.07	0.0	1.380	1.320	0.0	0.0	0.0	80.5	32.0
2	1	7040.	272.	13.36	8.82	34.78	4.617	30.07	0.0	1.380	1.325	0.0	0.0	0.0	85.0	32.0
2	2	9090.	228.	12.97	8.83	40.31	4.208	30.07	0.0	1.390	1.335	0.0	0.0	0.0	85.0	32.0
2	3	11030.	181.	12.50	8.85	49.78	3.689	30.07	0.0	1.385	1.340	0.0	0.0	0.0	85.5	32.0
2	4	13050.	131.	11.98	8.90	62.08	3.113	30.07	0.0	1.390	1.340	0.0	0.0	0.0	85.0	32.0
2	5	15050.	70.	11.21	8.87	76.39	2.388	30.07	0.0	1.405	1.360	0.0	0.0	0.0	86.2	32.0
2	6	16220.	35.	10.81	8.91	85.26	1.932	30.07	0.0	1.405	1.360	0.0	0.0	0.0	86.2	32.0
3	1	8140.	356.	17.52	11.76	4.84	5.806	30.06	3.02	1.375	1.330	0.0	0.0	0.0	87.0	32.0
3	2	10140.	307.	17.10	11.75	10.35	5.391	30.06	3.02	1.375	1.325	0.0	0.0	0.0	87.4	32.0
3	3	12120.	251.	16.60	11.78	21.39	4.834	30.06	3.02	1.380	1.335	0.0	0.0	0.0	87.5	32.0
3	4	14120.	192.	16.00	11.80	9.33	4.219	30.06	5.03	1.390	1.320	0.0	0.0	0.0	87.8	32.0
3	5	16040.	135.	15.35	11.81	23.27	3.560	30.06	5.05	1.400	1.335	0.0	0.0	0.0	87.8	32.0
4	1	9320.	438.	21.62	14.67	11.33	6.981	30.06	3.40	1.310	1.255	0.0	0.0	0.0	84.1	32.0
4	2	11330.	380.	21.20	14.71	18.93	6.518	30.06	3.40	1.315	1.260	0.0	0.0	0.0	85.0	32.0
4	3	13310.	320.	20.64	14.74	8.02	5.964	30.06	5.10	1.325	1.265	0.0	0.0	0.0	85.0	32.0
4	4	15300.	255.	20.01	14.78	24.05	5.346	30.06	5.10	1.340	1.285	0.0	0.0	0.0	85.0	32.0
4	5	17200.	194.	19.43	14.81	39.14	4.675	30.06	5.10	1.340	1.290	0.0	0.0	0.0	85.0	32.0
5	1	10130.	509.	25.65	17.60	14.16	8.081	30.07	4.02	1.665	1.470	0.0	0.0	0.0	84.0	32.0
5	2	11480.	467.	25.37	17.60	19.03	7.782	30.07	4.03	1.585	1.390	0.0	0.0	0.0	85.3	32.0
5	3	12980.	417.	25.04	17.65	12.66	7.381	30.07	5.22	1.575	1.375	0.0	0.0	0.0	86.0	32.0
5	4	14450.	369.	24.61	17.66	8.02	6.919	30.07	6.42	1.565	1.360	0.0	0.0	0.0	86.0	32.0
5	5	16000.	313.	24.04	17.70	8.21	6.424	30.07	7.41	1.575	1.365	0.0	0.0	0.0	86.1	32.0
5	6	17350.	275.	23.76	17.83	17.66	6.079	30.07	7.40	1.560	1.340	0.0	0.0	0.0	86.9	32.0
6	1	10960.	590.	30.00	20.55	7.53	9.120	30.07	5.40	1.525	1.300	0.0	0.0	0.0	87.0	32.0
6	2	12500.	535.	29.34	20.57	14.58	8.766	30.07	5.38	1.525	1.290	0.0	0.0	0.0	87.0	32.0
6	3	14020.	482.	28.91	20.58	11.75	8.329	30.07	6.37	1.535	1.295	0.0	0.0	0.0	87.0	32.0
6	4	15550.	428.	28.40	20.61	12.32	7.853	30.07	7.31	1.540	1.285	0.0	0.0	0.0	87.1	32.0
6	5	17030.	369.	28.93	20.69	16.48	7.331	30.07	8.12	1.560	1.310	0.0	0.0	0.0	87.3	32.0
6	6	18070.	326.	28.53	20.66	12.88	6.923	30.07	9.11	1.560	1.320	0.0	0.0	0.0	87.3	32.0

PERFORMANCE EVALUATION OF ICP RADIAL TURBINE

TABLE B5 OUTPUT DATA CLEARANCE = 0.081 IN.

REDUCED TO STANDARD AIR IN ACCORDANCE WITH NASA METHOD.
TOTAL INLET PRESS. = 14.7 PSIA, TOTAL INLET TEMPERATURE
= 518.7 DEG.R., GAMMA = 1.4, CP = 0.24 BTU/LBM-DEG.F.

										NO BEARING LOSSES					MAXIMUM BEARING LOSSES				
RUN/PT	PRESS RATIO	REF. SPEED RPM	REF. FLOW LB/SEC	HEAD COEFF	DEG REACT	ANGLE ALPH1 DEG	ANGLE BETA1 DEG	VEL COEFF GV	LOSS COEFF GV	REF MOM FT.LB	ANGLE ALF20 DEG	VEL COEFF	LOSS COEFF ROTOR	EFFIC-IENCY	REF MOM FT.LB	ANGLE ALF2? DEG	VEL COEFF	LOSS COEFF ROTOR	EFFIC-IENCY
1 1	1.200	5559.	0.911	6.076	0.299	81.82	72.31	0.891	0.206	4.87	-30.22	0.751	0.437	63.43	5.15	-44.35	0.92	0.153	67.13
1 2	1.201	7488.	0.846	3.362	0.345	81.82	58.53	0.890	0.208	3.90	32.48	0.705	0.502	73.34	4.30	-18.17	0.989	0.121	81.02
1 3	1.200	9497.	0.783	2.085	0.451	81.81	-24.54	0.886	0.215	2.77	69.21	0.573	0.672	71.58	3.25	28.05	0.943	0.111	82.89
1 4	1.200	11509.	0.692	1.416	0.578	81.80	-73.37	0.881	0.224	1.64	79.65	0.473	0.776	58.35	2.16	53.59	0.951	0.106	76.90
1 5	1.200	13083.	0.588	1.100	0.696	81.77	-81.74	0.876	0.233	0.57	87.80	0.157	0.975	26.73	1.10	73.12	0.740	0.430	52.10
2 1	1.301	6908.	1.048	5.616	0.303	81.80	71.55	0.899	0.192	6.49	-12.70	0.675	0.544	63.93	6.84	-34.40	0.828	0.315	47.35
2 2	1.300	8917.	0.999	3.368	0.350	81.81	58.93	0.897	0.195	5.57	27.42	0.720	0.482	74.32	5.99	-11.91	0.929	0.138	79.98
2 3	1.300	10818.	0.935	2.287	0.429	81.81	4.51	0.894	0.200	4.40	56.66	0.682	0.535	76.21	4.87	20.35	0.935	0.125	84.27
2 4	1.301	12800.	0.857	1.637	0.529	81.82	-63.77	0.890	0.207	3.16	70.27	0.635	0.597	70.40	3.65	45.91	0.932	0.131	81.44
2 5	1.299	14752.	0.750	1.225	0.647	81.81	-78.97	0.884	0.218	1.64	81.46	0.443	0.804	48.58	2.15	68.06	0.798	0.364	63.46
2 6	1.299	15899.	0.674	1.056	0.717	81.80	-82.52	0.880	0.225	0.77	86.29	0.256	0.934	27.31	1.27	76.79	0.665	0.558	45.09
3 1	1.401	7986.	1.136	5.329	0.306	81.77	70.94	0.904	0.183	8.02	-17.20	0.723	0.478	66.47	8.39	-34.33	0.855	0.269	69.40
3 2	1.400	9950.	1.094	3.426	0.342	81.78	60.43	0.903	0.185	6.87	34.22	0.689	0.525	73.76	7.29	0.33	0.859	0.262	78.28
3 3	1.400	11889.	1.035	2.400	0.411	81.79	21.09	0.900	0.190	5.71	53.40	0.704	0.505	77.46	6.16	24.35	0.902	0.187	83.61
3 4	1.399	13857.	0.964	1.765	0.506	81.81	-55.25	0.896	0.197	4.35	65.97	0.668	0.553	73.82	4.81	45.67	0.886	0.215	81.73
3 5	1.399	15734.	0.884	1.367	0.593	81.82	-74.52	0.892	0.204	3.03	74.38	0.626	0.608	63.80	3.50	60.75	0.875	0.234	73.64
4 1	1.499	9165.	1.206	4.818	0.313	81.72	69.46	0.908	0.176	9.31	-17.78	0.773	0.402	70.01	9.68	-32.59	0.891	0.206	72.82
4 2	1.500	11140.	1.164	3.264	0.352	81.74	58.14	0.906	0.179	8.02	28.76	0.732	0.465	75.93	8.43	0.74	0.875	0.235	79.84
4 3	1.500	13085.	1.111	2.366	0.413	81.76	19.47	0.904	0.183	6.69	54.20	0.705	0.503	77.94	7.12	31.82	0.866	0.250	82.96
4 4	1.500	15032.	1.049	1.794	0.493	81.79	-50.68	0.901	0.189	5.41	62.92	0.720	0.482	76.58	5.84	46.15	0.895	0.200	82.75
4 5	1.500	16896.	0.980	1.419	0.566	81.81	-71.70	0.897	0.195	4.09	70.95	0.713	0.492	69.76	4.53	59.28	0.909	0.174	77.12
5 1	1.598	9894.	1.253	4.744	0.317	81.68	69.12	0.911	0.171	10.37	-18.03	0.776	0.398	70.60	10.74	-31.31	0.879	0.227	73.11
5 2	1.598	11241.	1.230	3.673	0.339	81.69	63.04	0.910	0.172	9.51	10.37	0.758	0.425	75.03	9.90	-11.56	0.875	0.235	73.10
5 3	1.599	12716.	1.196	2.874	0.379	81.71	48.90	0.908	0.175	8.47	36.80	0.730	0.467	77.67	8.88	13.32	0.856	0.267	81.36
5 4	1.598	14162.	1.157	2.316	0.430	81.74	11.46	0.907	0.178	7.49	48.61	0.735	0.460	79.06	7.89	28.54	0.868	0.247	83.37
5 5	1.599	15679.	1.111	1.890	0.487	81.76	-42.91	0.904	0.182	6.33	60.50	0.706	0.501	76.97	6.74	45.73	0.846	0.284	81.93
5 6	1.603	17015.	1.078	1.612	0.522	81.78	-62.29	0.903	0.185	5.53	66.68	0.726	0.473	74.95	5.94	55.39	0.877	0.230	80.42
6 1	1.698	10762.	1.297	4.490	0.324	81.63	68.01	0.913	0.167	11.27	-15.61	0.782	0.388	72.05	11.63	-28.29	0.875	0.234	74.35
6 2	1.698	12278.	1.266	3.449	0.350	81.65	60.55	0.912	0.168	10.18	16.98	0.751	0.436	76.06	10.56	-3.51	0.854	0.270	78.87
6 3	1.698	13769.	1.233	2.742	0.389	81.68	44.20	0.911	0.171	9.24	32.88	0.772	0.404	79.58	9.63	12.65	0.882	0.222	82.88
6 4	1.698	15277.	1.194	2.228	0.438	81.71	2.52	0.909	0.174	8.19	45.64	0.778	0.394	80.78	8.58	28.28	0.894	0.201	84.57
6 5	1.700	16717.	1.162	1.864	0.490	81.74	-44.73	0.907	0.178	7.04	59.02	0.729	0.468	77.88	7.42	46.48	0.848	0.282	82.10
6 6	1.698	17732.	1.130	1.654	0.526	81.76	-60.98	0.905	0.181	6.21	64.85	0.714	0.490	75.12	6.59	54.79	0.837	0.299	79.71

PERFORMANCE EVALUATION OF ICP RADIAL TURBINE

TABLE B6

INPUT DATA

CLEARANCE = 0.061 IN.

RUN/PT	RPM	TORQUE COUNTS	PUVC IN.HG	P5P IN.HG	H1 IN.H2O	DPVC IN.HG	PATM IN.HG	HREF1 IN.HG	V4 MV	V5 MV	V20 MV	V21 MV	V22 MV	TRM DEG.F	TCJ DEG.F
1 1	5710.	179.	9.09	5.84	9.88	3.241	30.03	1.01	1.780	1.665	1.180	1.260	1.345	80.5	32.0
1 2	7200.	151.	8.80	5.84	12.64	2.986	30.03	1.00	1.805	1.695	1.170	1.280	1.340	81.0	32.0
1 3	8670.	125.	8.52	5.86	12.09	2.680	30.03	1.37	1.800	1.685	1.165	1.325	1.380	82.5	32.0
1 4	10200.	97.	8.21	5.90	8.92	2.320	30.03	2.12	1.800	1.685	1.180	1.375	1.450	83.5	32.0
1 5	11810.	63.	7.81	5.91	9.12	1.896	30.03	2.75	1.795	1.675	1.195	1.440	1.680	84.0	32.0
1 6	13660.	17.	7.20	5.95	10.10	1.254	30.03	3.53	1.805	1.675	1.205	1.505	1.915	84.0	32.0
2 1	7080.	266.	13.34	8.78	16.65	4.573	30.03	1.35	1.845	1.750	1.195	1.265	1.345	84.0	32.0
2 2	9050.	223.	12.99	8.80	3.68	4.176	30.03	2.69	1.855	1.760	1.210	1.310	1.400	84.0	32.0
2 3	11060.	177.	12.51	8.81	12.79	3.729	30.03	2.69	1.855	1.775	1.230	1.395	1.595	84.5	32.0
2 4	13050.	128.	11.93	8.84	13.00	3.125	30.03	3.59	1.865	1.785	1.250	1.505	1.895	84.5	32.0
2 5	15100.	70.	11.28	8.85	9.11	2.453	30.03	4.93	1.865	1.780	1.270	1.605	2.040	84.5	32.0
2 6	16740.	18.	10.60	8.91	12.80	1.706	30.03	5.70	1.855	1.770	1.290	1.690	2.095	85.0	32.0
3 1	8270.	348.	17.52	11.72	8.89	5.825	30.03	2.80	1.870	1.795	1.295	1.320	1.425	85.0	32.0
3 2	10230.	299.	17.13	11.72	8.12	5.399	30.03	3.30	1.835	1.775	1.275	1.315	1.445	85.0	32.0
3 3	12220.	243.	16.63	11.73	19.19	4.873	30.03	3.31	1.830	1.755	1.275	1.365	1.775	85.0	32.0
3 4	14220.	187.	16.04	11.79	9.26	4.261	30.03	5.10	1.820	1.750	1.295	1.495	1.925	84.5	32.0
3 5	16260.	131.	15.37	11.83	8.35	3.578	30.03	6.25	1.810	1.740	1.295	1.605	1.980	84.0	32.0
3 6	17940.	65.	14.60	11.88	12.41	2.744	30.03	7.24	1.805	1.725	1.305	1.705	2.190	84.0	32.0
4 1	9150.	425.	21.60	14.66	11.57	6.945	30.14	3.42	1.674	1.615	1.130	1.172	1.283	68.2	32.0
4 2	11040.	374.	21.23	14.69	18.05	6.554	30.14	3.42	1.715	1.662	1.163	1.273	1.506	69.0	32.0
4 3	12980.	317.	20.72	14.70	4.15	6.034	30.14	5.30	1.731	1.684	1.196	1.385	1.935	69.8	32.0
4 4	15060.	247.	20.05	14.72	11.61	5.355	30.14	6.01	1.750	1.703	1.255	1.588	2.029	70.1	32.0
4 5	17040.	186.	19.40	14.76	12.92	4.679	30.14	7.15	1.762	1.709	1.316	1.857	2.204	71.0	32.0
5 1	10100.	512.	25.70	17.61	12.54	8.042	30.14	4.29	1.774	1.729	1.318	1.304	1.512	71.2	32.0
5 2	11500.	467.	25.35	17.61	17.78	7.737	30.14	4.29	1.782	1.739	1.302	1.270	1.603	72.0	32.0
5 3	13000.	418.	25.00	17.64	11.10	7.337	30.14	5.41	1.786	1.743	1.304	1.345	1.792	72.0	32.0
5 4	14540.	370.	24.51	17.65	6.30	6.873	30.14	6.60	1.774	1.745	1.326	1.459	1.987	72.0	32.0
5 5	16070.	312.	24.00	17.69	7.67	6.332	30.14	7.65	1.765	1.737	1.345	1.594	2.020	72.5	32.0
5 6	17500.	262.	23.52	17.70	6.04	5.811	30.14	8.67	1.772	1.736	1.385	1.685	2.143	73.0	32.0
6 1	11000.	589.	29.61	20.52	10.45	9.063	30.10	5.32	1.828	1.779	1.275	1.159	1.472	76.9	32.0
6 2	12480.	542.	29.27	20.55	11.27	8.735	30.10	5.72	1.842	1.775	1.297	1.276	1.724	78.0	32.0
6 3	13990.	489.	28.91	20.59	14.79	8.341	30.10	6.24	1.831	1.753	1.320	1.391	1.883	78.0	32.0
6 4	15460.	437.	28.43	20.62	8.78	7.854	30.10	7.60	1.810	1.738	1.350	1.527	1.981	78.5	32.0
6 5	16970.	371.	27.90	20.63	5.83	7.278	30.10	8.99	1.801	1.722	1.361	1.699	2.058	78.2	32.0
6 6	17950.	337.	27.57	20.66	15.42	6.933	30.10	9.00	1.784	1.718	1.376	1.707	2.140	78.2	32.0

PERFORMANCE EVALUATION OF ICP RADIAL TURBINE

TABLE B7 OUTPUT DATA CLEARANCE = 0.061 IN.

REDUCED TO STANDARD AIR IN ACCORDANCE WITH NASA METHOD.
TOTAL INLET PRESS. = 14.7 PSIA, TOTAL INLET TEMPERATURE
= 518.7 DEG.R., GAMMA = 1.4, CP = 0.24 BTU/LBM-DEG.F.

											NO BEARING LOSSES					MAXIMUM BEARING LOSSES				
RUN/PT		PRESS RATIO	REF. SPEED RPM	REF. FLOW LB/SEC	HEAD COEFF	DEG REACT	ANGLE ALPH1 DEG	ANGLE BETA1 DEG	VEL COEFF GV	LOSS COEFF GV	REF MOM FT.LB	ANGLE ALF20 DEG	VEL COEFF	LOSS COEFF ROTOR	EFFIC-IENCY	REF MOM FT.LB	ANGLE ALF20 DEG	VEL COEFF	LOSS COEFF ROTOR	EFFIC-IENCY
1	1	1.200	5544.	0.911	6.108	0.303	81.53	71.93	0.902	0.187	4.87	-27.34	0.716	0.488	63.25	5.16	-43.27	0.886	0.215	[illegible]
1	2	1.199	6984.	0.874	3.841	0.337	81.53	63.34	0.901	0.189	4.12	31.14	0.638	0.593	70.33	4.5[illegible]	-18.65	0.889	0.209	76.9[illegible]
1	3	1.199	8413.	0.827	2.649	0.393	81.53	37.25	0.899	0.192	3.41	58.21	0.617	0.620	74.15	3.86	7.02	0.943	0.117	83.86
1	4	1.200	9897.	0.769	1.921	0.478	81.52	-40.46	0.896	0.197	2.65	68.51	0.603	0.636	72.73	3.14	25.94	0.988	0.023	86.22
1	5	1.200	11463.	0.694	1.429	0.586	81.51	-72.52	0.892	0.205	1.73	77.27	0.519	0.730	61.03	2.26	46.93	0.978	0.043	79.48
1	6	1.200	13259.	0.563	1.070	0.724	81.48	-82.27	0.885	0.217	0.49	87.15	0.192	0.963	24.42	1.03	70.57	0.780	0.377	51.55
2	1	1.300	6856.	1.044	5.687	0.306	81.51	71.28	0.910	0.173	6.50	-11.79	0.658	0.567	64.00	6.85	-34.25	0.810	0.344	67.44
2	2	1.300	8761.	0.997	3.483	0.350	81.52	60.15	0.908	0.175	5.60	29.28	0.685	0.531	73.77	6.02	-11.15	0.890	0.208	79.35
2	3	1.299	10702.	0.941	2.331	0.427	81.52	12.84	0.905	0.180	4.45	59.28	0.643	0.586	75.99	4.92	24.22	0.893	0.202	84.05
2	4	1.299	12623.	0.859	1.676	0.529	81.53	-60.49	0.901	0.188	3.23	69.93	0.616	0.621	71.09	3.72	44.77	0.914	0.182	82.03
2	5	1.299	14608.	0.760	1.248	0.646	81.52	-77.96	0.895	0.199	1.78	80.44	0.462	0.786	51.33	2.28	66.12	0.804	0.354	65.89
2	6	1.299	16200.	0.633	1.017	0.756	81.50	-83.36	0.889	0.211	0.48	87.17	0.195	0.962	18.25	0.98	77.89	0.605	0.634	37.51
3	1	1.400	7997.	1.139	5.306	0.313	81.47	70.40	0.915	0.163	8.00	-11.60	0.681	0.537	66.30	8.37	-31.47	0.812	0.341	69.37
3	2	1.399	9898.	1.096	3.458	0.352	81.49	60.09	0.913	0.166	6.83	39.56	0.634	0.598	72.92	7.25	5.35	0.799	0.362	77.43
3	3	1.399	11831.	1.040	2.418	0.424	81.50	21.69	0.911	0.171	5.67	56.61	0.645	0.585	76.37	6.12	28.93	0.834	0.304	82.49
3	4	1.399	13769.	0.970	1.788	0.512	81.52	-52.32	0.907	0.177	4.37	67.42	0.623	0.611	73.21	4.83	48.08	0.833	0.306	81.04
3	5	1.400	15749.	0.887	1.368	0.601	81.53	-73.90	0.903	0.185	3.06	74.07	0.618	0.618	64.29	3.53	60.30	0.859	0.262	74.06
3	6	1.400	17385.	0.774	1.123	0.704	81.52	-81.14	0.896	0.196	1.53	82.04	0.424	0.820	40.58	1.99	73.24	0.693	0.520	52.76
4	1	1.498	8897.	1.201	5.100	0.316	81.43	69.85	0.919	0.156	9.05	-0.07	0.646	0.583	66.56	9.42	-22.26	0.759	0.423	69.27
4	2	1.498	10719.	1.165	3.515	0.349	81.44	61.01	0.918	0.158	7.92	44.25	0.604	0.635	72.24	8.32	16.27	0.741	0.451	75.95
4	3	1.498	12594.	1.117	2.544	0.408	81.47	33.55	0.915	0.162	6.65	62.85	0.574	0.671	74.47	7.08	43.99	0.727	0.471	79.25
4	4	1.497	14603.	1.050	1.891	0.494	81.50	-41.89	0.912	0.169	5.26	69.70	0.571	0.674	72.66	5.69	56.09	0.736	0.458	78.66
4	5	1.497	16520.	0.980	1.478	0.576	81.52	-69.87	0.908	0.176	3.94	74.55	0.568	0.677	65.98	4.37	64.43	0.749	0.439	73.2[illegible]
5	1	1.597	9785.	1.255	4.844	0.326	81.39	68.90	0.921	0.151	10.31	-12.56	0.715	0.489	69.42	10.67	-27.92	0.815	0.337	71.88
5	2	1.597	11138.	1.229	3.736	0.349	81.40	62.91	0.921	0.152	9.37	21.43	0.677	0.542	73.37	9.76	-2.91	0.780	0.377	76.41
5	3	1.597	12590.	1.196	2.926	0.385	81.42	50.01	0.919	0.155	8.35	46.49	0.647	0.582	75.90	8.75	24.36	0.769	0.408	79.54
5	4	1.597	14080.	1.156	2.338	0.433	81.45	15.69	0.918	0.158	7.35	56.74	0.652	0.575	77.32	7.75	39.29	0.782	0.388	81.60
5	5	1.597	15566.	1.108	1.914	0.498	81.47	-40.47	0.915	0.163	6.14	65.43	0.614	0.623	74.45	6.54	52.64	0.748	0.441	79.38
5	6	1.597	16951.	1.061	1.613	0.548	81.49	-63.39	0.912	0.168	5.09	71.12	0.598	0.642	70.39	5.59	61.47	0.741	0.452	75.96
6	1	1.697	10641.	1.295	4.585	0.331	81.34	67.86	0.924	0.147	11.20	-10.79	0.727	0.471	71.01	11.56	-25.20	0.818	0.332	73.29
6	2	1.697	12074.	1.269	3.562	0.355	81.36	51.25	0.923	0.148	10.26	18.08	0.712	0.494	75.31	10.64	-2.79	0.811	0.342	78.06
6	3	1.698	13544.	1.238	2.833	0.394	81.38	47.03	0.922	0.151	9.27	38.04	0.705	0.503	78.15	9.65	17.98	0.811	0.342	81.38
6	4	1.698	14974.	1.200	2.318	0.439	81.41	13.46	0.920	0.154	8.25	49.77	0.706	0.501	79.30	8.63	33.12	0.817	0.332	82.99
6	5	1.697	16445.	1.154	1.921	0.496	81.45	-38.62	0.917	0.158	6.95	61.85	0.657	0.568	76.38	7.33	49.95	0.771	0.405	80.58
6	6	1.698	17396.	1.125	1.717	0.530	81.46	-56.71	0.916	0.161	6.28	64.84	0.666	0.557	74.82	6.66	54.50	0.783	0.387	79.32

PERFORMANCE EVALUATION OF ICP RADIAL TURBINE

TABLE B8

INPUT DATA

CLEARANCE = 0.041 IN.

RUN/PT		RPM	TORQUE COUNTS	PUVC IN.HG	P5P IN.HG	H1 IN.H2O	DPVC IN.HG	PATM IN.HG	HREF1 IN.HG	V4 MV	V5 MV	V20 MV	V21 MV	V22 MV	TRM DEG.F	TCJ DEG.F
1	1	5770.	171.	9.94	5.80	5.18	3.259	30.10	1.33	1.727	1.668	1.194	1.269	1.433	75.0	32.0
1	2	7260.	144.	8.82	5.83	8.19	2.997	30.10	1.35	1.748	1.694	1.213	1.330	1.454	74.4	32.0
1	3	8670.	120.	8.57	5.87	12.67	2.732	30.10	1.35	1.822	1.761	1.238	1.396	1.483	75.8	32.0
1	4	10180.	90.	8.26	5.87	14.63	2.362	30.10	1.66	1.845	1.780	1.262	1.459	1.599	76.0	32.0
1	5	11810.	63.	7.83	5.91	11.91	1.954	30.10	2.49	1.869	1.797	1.285	1.500	1.796	76.8	32.0
1	6	13760.	12.	7.19	5.94	11.79	1.250	30.10	2.51	1.885	1.801	1.298	1.589	2.002	77.0	32.0
2	1	7160.	261.	13.34	8.77	15.59	4.600	30.10	1.43	1.927	1.858	1.317	1.369	1.469	79.0	32.0
2	2	8550.	231.	13.10	8.80	19.14	4.337	30.10	1.43	1.926	1.859	1.319	1.404	1.500	79.6	32.0
2	3	10010.	198.	12.76	8.80	6.78	4.020	30.10	2.75	1.929	1.881	1.337	1.453	1.601	81.0	32.0
2	4	11530.	163.	12.42	8.91	9.35	3.636	30.10	3.11	1.935	1.883	1.357	1.525	1.834	81.7	32.0
2	5	12970.	127.	12.02	8.92	3.77	3.220	30.10	4.21	1.937	1.887	1.376	1.604	1.950	82.6	32.0
2	6	14620.	88.	11.53	8.87	14.26	2.714	30.10	4.24	1.923	1.879	1.380	1.667	2.120	83.6	32.0
2	7	16100.	40.	10.94	8.91	11.24	2.071	30.10	5.36	1.906	1.858	1.381	1.736	2.236	83.5	32.0
3	1	8340.	350.	17.54	11.72	11.69	5.835	30.10	2.60	1.895	1.855	1.355	1.380	1.495	83.4	32.0
3	2	10010.	311.	17.23	11.75	16.99	5.501	30.10	2.61	1.886	1.846	1.339	1.381	1.543	83.4	32.0
3	3	11750.	261.	16.82	11.76	26.12	5.090	30.10	2.61	1.899	1.860	1.334	1.421	1.736	83.4	32.0
3	4	13940.	197.	16.16	11.80	10.52	4.419	30.10	4.89	1.914	1.872	1.350	1.544	1.970	83.5	32.0
3	5	16140.	137.	15.47	11.82	11.01	3.694	30.10	5.96	1.925	1.876	1.371	1.690	2.095	83.5	32.0
3	6	17970.	68.	14.65	11.87	6.19	2.821	30.10	5.99	1.927	1.877	1.385	1.804	2.229	83.5	32.0
4	1	9250.	433.	21.63	14.65	12.80	7.005	30.02	3.41	1.827	1.757	1.258	1.301	1.428	74.6	32.0
4	2	10980.	386.	21.29	14.66	13.34	6.627	30.02	3.80	1.834	1.772	1.275	1.356	1.562	74.6	32.0
4	3	12450.	344.	21.00	14.66	15.55	6.237	30.02	4.27	1.857	1.795	1.314	1.447	1.870	75.0	32.0
4	4	13990.	292.	20.50	14.72	11.96	5.780	30.02	5.32	1.861	1.799	1.356	1.541	2.013	75.0	32.0
4	5	15520.	243.	19.99	14.75	24.90	5.252	30.02	5.32	1.866	1.816	1.385	1.619	2.048	75.0	32.0
4	6	17080.	197.	19.43	14.75	13.21	4.712	30.02	7.09	1.875	1.826	1.411	1.753	2.133	75.0	32.0
4	7	17830.	169.	19.19	14.80	18.93	4.393	30.02	7.09	1.879	1.824	1.429	1.823	2.220	75.0	32.0
5	1	10230.	510.	25.67	17.60	7.49	8.079	30.02	4.70	2.003	1.929	1.370	1.334	1.508	75.0	32.0
5	2	11500.	475.	25.42	17.63	11.97	7.793	30.02	4.70	2.012	1.936	1.373	1.355	1.624	75.0	32.0
5	3	12980.	430.	25.04	17.66	8.33	7.434	30.02	5.49	2.015	1.943	1.385	1.425	1.834	75.0	32.0
5	4	14540.	380.	24.61	17.65	13.56	6.984	30.02	6.00	2.019	1.936	1.412	1.542	1.919	75.0	32.0
5	5	15960.	328.	24.13	17.68	9.49	6.485	30.02	7.29	2.023	1.946	1.436	1.640	2.054	75.0	32.0
5	6	17480.	272.	23.62	17.69	15.26	5.917	30.02	7.90	2.023	1.947	1.471	1.782	2.182	75.0	32.0
6	1	11120.	595.	29.70	20.52	8.14	9.097	30.02	5.50	2.037	1.920	1.421	1.322	1.617	75.0	32.0
6	2	12530.	548.	29.34	20.54	12.55	8.755	30.02	5.65	2.030	1.920	1.416	1.358	1.744	75.0	32.0
6	3	14040.	498.	28.98	20.56	9.60	8.383	30.02	6.56	2.026	1.919	1.417	1.462	1.869	75.0	32.0
6	4	15570.	439.	28.50	20.60	10.46	7.911	30.02	7.48	2.029	1.929	1.427	1.554	1.961	75.0	32.0
6	5	17000.	381.	27.94	20.61	7.38	7.358	30.02	8.80	2.024	1.931	1.442	1.654	2.044	75.0	32.0
6	6	18110.	340.	27.50	20.63	8.94	6.897	30.02	9.56	2.022	1.933	1.449	1.748	2.141	75.0	32.0

PERFORMANCE EVALUATION OF ICP RADIAL TURBINE

TABLE B9 OUTPUT DATA CLEARANCE = 0.041 IN.

REDUCED TO STANDARD AIR IN ACCORDANCE WITH NASA METHOD.
TOTAL INLET PRESS. = 14.7 PSIA, TOTAL INLET TEMPERATURE
= 518.7 DEG.R., GAMMA = 1.4, CP = 0.24 BTU/LBM-DEG.F.

										NO BEARING LOSSES					MAXIMUM BEARING LOSSES				
RUN/PT	PRESS RATIO	REF. SPEED RPM	REF. FLOW LB/SEC	HEAD COEFF	DEG REACT	ANGLE ALPH1 DEG	ANGLE BETA1 DEG	VEL COFF GV	LOSS COEFF GV	REF MOM FT.LB	ANGLE ALF20 DEG	VEL COEFF	LOSS COEFF ROTOR	EFFIC-IENCY	REF MOM FT.LB	ANGLE ALF20 DEG	VEL COEFF	LOSS COEFF ROTOR	EFFIC-IENCY
1 1	1.198	5602.	0.925	5.939	0.301	81.19	71.08	0.906	0.179	4.57	24.82	0.508	0.742	59.53	4.87	-19.07	0.691	0.537	63.36
1 2	1.198	7043.	0.876	3.765	0.341	81.20	61.87	0.905	0.181	3.84	62.57	0.459	0.790	66.18	4.22	15.66	0.710	0.496	72.85
1 3	1.199	8393.	0.835	2.661	0.396	81.19	36.87	0.903	0.185	3.18	74.37	0.418	0.825	68.35	3.63	41.06	0.732	0.464	77.90
1 4	1.199	9849.	0.776	1.927	0.474	81.19	-36.82	0.900	0.190	2.37	81.27	0.346	0.891	64.35	2.86	58.76	0.730	0.467	77.67
1 5	1.199	11420.	0.704	1.438	0.577	81.18	-70.88	0.896	0.197	1.63	82.15	0.378	0.857	56.52	2.15	60.63	0.837	0.299	74.61
1 6	1.199	13304.	0.563	1.059	0.579	81.18	-77.35	0.896	0.197	0.24	-84.64	-2.023	-3.091	12.38	0.79	89.43	0.154	0.976	39.68
2 1	1.299	6910.	1.046	5.582	0.306	81.18	70.45	0.914	0.165	6.36	6.45	0.590	0.652	63.10	6.71	-25.29	0.743	0.448	66.62
2 2	1.299	8252.	1.015	3.921	0.336	81.18	63.63	0.913	0.167	5.73	37.34	0.597	0.643	69.87	6.14	-4.57	0.788	0.379	74.84
2 3	1.299	9654.	0.977	2.860	0.383	81.19	46.56	0.911	0.170	4.90	60.67	0.558	0.689	72.80	5.35	25.95	0.783	0.387	79.47
2 4	1.302	11120.	0.926	2.174	0.441	81.19	-3.67	0.909	0.174	4.01	72.33	0.506	0.744	71.81	4.49	49.14	0.765	0.415	80.35
2 5	1.302	12507.	0.871	1.717	0.518	81.19	-55.80	0.906	0.179	3.11	77.25	0.467	0.782	66.67	3.61	59.77	0.751	0.437	77.24
2 6	1.299	14101.	0.800	1.341	0.610	81.19	-74.33	0.901	0.188	2.14	80.03	0.461	0.788	56.60	2.64	65.70	0.785	0.384	69.90
2 7	1.299	15539.	0.697	1.106	0.706	81.18	-81.02	0.896	0.197	0.93	86.28	0.237	0.944	31.10	1.43	76.94	0.611	0.627	47.87
3 1	1.399	8050.	1.140	5.227	0.314	81.14	69.57	0.919	0.156	8.03	-11.87	0.687	0.527	67.05	8.40	-31.56	0.819	0.329	70.16
3 2	1.399	9664.	1.105	3.629	0.348	81.15	61.19	0.918	0.158	7.10	28.23	0.664	0.559	73.31	7.51	-5.27	0.823	0.323	77.62
3 3	1.399	11339.	1.062	2.634	0.406	81.17	36.79	0.916	0.162	5.91	59.22	0.588	0.655	74.58	6.36	32.76	0.768	0.410	80.23
3 4	1.399	13448.	0.987	1.874	0.501	81.18	-43.75	0.912	0.169	4.53	68.24	0.588	0.655	72.93	4.99	49.42	0.790	0.377	80.41
3 5	1.399	15568.	0.901	1.397	0.593	81.19	-72.12	0.907	0.177	3.13	75.38	0.576	0.668	64.00	3.60	62.59	0.812	0.340	73.53
3 6	1.399	17333.	0.785	1.127	0.566	81.19	-75.36	0.909	0.175	1.52	-89.32	-0.112	0.987	39.62	1.98	86.60	0.469	0.780	51.61
4 1	1.499	8955.	1.208	5.048	0.321	81.10	68.96	0.923	0.148	9.36	-16.16	0.716	0.487	68.69	9.74	-31.83	0.829	0.313	71.42
4 2	1.499	10624.	1.175	3.584	0.352	81.11	60.77	0.922	0.150	8.32	22.96	0.690	0.524	74.52	8.73	-4.91	0.823	0.323	78.17
4 3	1.499	12038.	1.140	2.789	0.396	81.13	44.30	0.920	0.153	7.39	43.46	0.679	0.539	77.36	7.81	16.74	0.824	0.320	81.81
4 4	1.500	13526.	1.094	2.213	0.449	81.15	0.64	0.918	0.157	6.23	61.80	0.618	0.618	76.15	6.66	43.20	0.775	0.400	81.46
4 5	1.500	14997.	1.042	1.801	0.513	81.17	-49.31	0.915	0.162	5.23	65.90	0.635	0.597	74.49	5.67	50.49	0.800	0.360	80.69
4 6	1.499	16500.	0.985	1.486	0.574	81.18	-68.52	0.912	0.168	4.23	70.02	0.655	0.570	70.10	4.66	57.57	0.835	0.303	77.28
4 7	1.500	17225.	0.950	1.365	0.600	81.19	-72.89	0.911	0.171	3.61	74.57	0.608	0.630	64.71	4.04	64.65	0.798	0.363	72.40
5 1	1.600	9851.	1.258	4.792	0.328	81.05	68.03	0.926	0.143	10.30	-8.95	0.697	0.515	69.47	10.67	-25.64	0.797	0.366	71.96
5 2	1.600	11072.	1.234	3.796	0.347	81.06	62.70	0.925	0.144	9.65	10.04	0.717	0.486	74.51	10.04	-12.00	0.828	0.314	77.52
5 3	1.600	12494.	1.204	2.983	0.378	81.08	51.29	0.924	0.146	8.71	36.50	0.703	0.506	77.78	9.11	12.76	0.825	0.319	81.37
5 4	1.599	13999.	1.166	2.373	0.430	81.11	19.73	0.922	0.150	7.67	49.50	0.704	0.504	79.39	8.08	29.61	0.833	0.307	83.61
5 5	1.599	15356.	1.122	1.972	0.486	81.13	-30.74	0.920	0.154	6.59	59.27	0.678	0.540	77.66	7.00	43.83	0.811	0.342	82.47
5 6	1.599	16818.	1.071	1.643	0.543	81.16	-60.48	0.917	0.159	5.42	67.02	0.653	0.573	73.41	5.83	55.62	0.793	0.371	78.88
6 1	1.699	10711.	1.296	4.534	0.332	81.00	66.99	0.928	0.139	11.40	-16.81	0.765	0.415	72.50	11.76	-29.20	0.855	0.269	74.80
6 2	1.699	12069.	1.271	3.571	0.356	81.02	60.54	0.927	0.140	10.46	9.51	0.744	0.446	76.49	10.83	-9.78	0.843	0.289	79.24
6 3	1.699	13524.	1.242	2.844	0.391	81.04	47.04	0.926	0.143	9.54	28.91	0.755	0.431	80.01	9.93	8.46	0.860	0.260	83.22
6 4	1.699	14993.	1.205	2.315	0.439	81.08	13.81	0.924	0.146	8.38	47.09	0.724	0.475	80.28	8.77	29.87	0.834	0.304	83.97
6 5	1.699	16369.	1.160	1.941	0.493	81.11	-34.23	0.922	0.150	7.25	56.60	0.706	0.501	78.71	7.63	42.94	0.819	0.329	82.86
6 6	1.698	17437.	1.122	1.711	0.534	81.13	-56.17	0.920	0.154	6.44	60.00	0.719	0.493	77.07	6.82	48.03	0.835	0.303	81.59

PERFORMANCE EVALUATION OF ICP RADIAL TURBINE

TABLE B10 INPUT DATA CLEARANCE = 0.024 IN.

RUN/PT		RPM	TORQUE COUNTS	PUVC IN.HG	P5P IN.HG	H1 IN.H2O	DPVC IN.HG	PATM IN.HG	HREF1 IN.HG	V4 MV	V5 MV	V20 MV	V21 MV	V22 MV	TRM DEG.F	TCJ DEG.F
1	1	5770.	175.	9.10	5.84	23.48	3.306	30.11	0.0	1.809	1.739	1.234	1.287	1.462	80.0	32.0
1	2	7010.	152.	8.90	5.86	25.71	3.071	30.11	0.0	1.837	1.766	1.249	1.332	1.496	80.9	32.0
1	3	8510.	126.	8.62	5.86	25.32	2.797	30.11	0.0	1.838	1.768	1.262	1.393	1.492	81.0	32.0
1	4	10040.	94.	8.24	5.88	37.44	2.413	30.11	0.0	1.824	1.758	1.278	1.443	1.593	81.0	32.0
1	5	11600.	65.	7.90	5.90	45.66	2.008	30.11	0.0	1.836	1.763	1.301	1.510	1.783	81.0	32.0
1	6	13730.	14.	7.16	5.93	59.93	1.239	30.11	0.0	1.812	1.739	1.310	1.571	1.980	80.9	32.0
2	1	7170.	265.	13.38	8.76	35.06	4.641	30.11	0.0	1.862	1.796	1.300	1.345	1.419	79.9	32.0
2	2	8500.	236.	13.12	8.79	38.55	4.377	30.11	0.0	1.869	1.801	1.304	1.379	1.442	80.0	32.0
2	3	10000.	202.	12.81	8.81	44.76	4.056	30.11	0.0	1.861	1.796	1.309	1.408	1.527	80.0	32.0
2	4	11450.	166.	12.45	8.82	52.56	3.691	30.11	0.0	1.876	1.806	1.339	1.482	1.772	80.0	32.0
2	5	13000.	128.	12.01	8.82	62.11	3.238	30.11	0.0	1.889	1.821	1.377	1.574	1.971	80.1	32.0
2	6	14630.	94.	11.54	8.87	72.67	2.726	30.11	0.0	1.908	1.833	1.399	1.650	2.056	80.5	32.0
2	7	16520.	28.	10.67	8.90	89.40	1.805	30.11	0.0	1.937	1.848	1.411	1.764	2.180	80.5	32.0
3	1	8370.	353.	17.59	11.70	46.95	5.899	30.11	0.0	1.970	1.888	1.399	1.426	1.517	80.8	32.0
3	2	9950.	314.	17.67	11.73	52.75	5.483	30.11	0.0	1.986	1.909	1.388	1.431	1.555	80.5	32.0
3	3	11520.	272.	17.28	11.74	14.48	5.155	30.11	3.30	1.996	1.934	1.403	1.452	1.754	80.3	32.0
3	4	12510.	244.	17.05	11.76	21.12	4.887	30.11	3.32	2.001	1.946	1.415	1.500	1.894	80.2	32.0
3	5	13990.	202.	16.53	11.78	31.20	4.438	30.11	3.32	2.013	1.956	1.440	1.595	1.974	80.2	32.0
3	6	15530.	160.	16.02	11.81	42.55	3.929	30.11	3.32	2.008	1.960	1.455	1.680	2.096	80.0	32.0
3	7	17040.	110.	15.38	11.84	19.71	3.297	30.11	6.00	2.012	1.959	1.475	1.794	2.235	79.9	32.0
3	8	18250.	62.	14.68	11.90	33.07	2.649	30.11	6.00	2.015	1.952	1.488	1.884	2.306	79.8	32.0
4	1	9310.	437.	21.82	14.70	13.06	7.047	30.10	3.40	1.745	1.651	1.191	1.262	1.366	80.7	32.0
4	2	10810.	398.	21.43	14.72	11.38	6.763	30.10	3.89	1.872	1.777	1.252	1.346	1.554	80.8	32.0
4	3	12310.	354.	21.12	14.71	6.86	6.393	30.10	4.84	1.903	1.812	1.286	1.434	1.788	79.5	32.0
4	4	13840.	307.	20.67	14.71	11.65	5.941	30.10	5.28	1.936	1.851	1.354	1.559	1.987	79.8	32.0
4	5	15310.	258.	20.20	14.75	9.59	5.431	30.10	6.30	1.957	1.865	1.639	1.387	1.915	80.0	32.0
4	6	16800.	212.	19.62	14.80	11.59	4.875	30.10	7.03	1.959	1.873	1.427	1.752	2.218	79.0	32.0
4	7	18380.	155.	19.02	14.82	10.43	4.202	30.10	8.21	1.963	1.874	1.446	1.857	2.297	79.0	32.0
5	1	10350.	525.	25.80	17.65	8.70	8.170	30.10	4.60	1.982	1.887	1.386	1.367	1.528	79.1	32.0
5	2	12070.	470.	25.48	17.69	7.82	7.777	30.10	5.16	1.977	1.886	1.392	1.392	1.690	79.5	32.0
5	3	13500.	424.	25.10	17.69	9.65	7.393	30.10	5.80	1.978	1.890	1.397	1.487	1.818	79.0	32.0
5	4	15030.	368.	24.60	17.71	6.71	6.872	30.10	6.95	1.975	1.888	1.420	1.590	1.986	79.0	32.0
5	5	16510.	314.	24.10	17.73	6.58	6.327	30.10	7.92	1.971	1.891	1.450	1.699	2.152	78.5	32.0
5	6	18090.	260.	23.51	17.76	7.56	5.716	30.10	8.89	1.970	1.899	1.477	1.818	2.240	78.1	32.0
6	1	11220.	605.	29.80	20.54	10.44	9.214	30.04	5.30	1.968	1.902	1.437	1.370	1.655	76.0	32.0
6	2	12530.	559.	29.50	20.56	9.76	8.884	30.04	5.80	1.971	1.902	1.426	1.396	1.707	76.9	32.0
6	3	14000.	509.	29.10	20.59	19.16	8.490	30.04	5.80	1.966	1.896	1.424	1.456	1.819	76.3	32.0
6	4	15550.	448.	28.60	20.61	12.20	7.976	30.04	7.42	1.966	1.890	1.435	1.569	1.978	76.3	32.0
6	5	17000.	389.	28.02	20.64	6.59	7.391	30.04	8.89	1.970	1.887	1.446	1.657	2.053	77.0	32.0
6	6	18030.	349.	27.62	20.65	10.80	6.986	30.04	9.40	1.960	1.883	1.471	1.739	2.149	77.1	32.0

PERFORMANCE EVALUATION OF ICP RADIAL TURBINE

TABLE B11 OUTPUT DATA CLEARANCE = 0.024 IN.

REDUCED TO STANDARD AIR IN ACCORDANCE WITH NASA METHOD.
TOTAL INLET PRESS. = 14.7 PSIA, TOTAL INLET TEMPERATURE
= 518.7 DEG.R., GAMMA = 1.4, CP = 0.24 BTU/LBM-DEG.F.

										NO BEARING LOSSES					MAXIMUM BEARING LOSSES				
RUN/PT	PRESS RATIO	REF. SPEED RPM	REF. FLOW LB/SEC	HEAD COEFF	DEG REACT	ANGLE ALPH1 DEG	ANGLE BETA1 DEG	VEL COEFF GV	LOSS COEFF GV	REF MOM FT.LB	ANGLE ALF20 DEG	VEL COEFF	LOSS COEFF ROTOR	EFFICIENCY	REF MOM FT.LB	ANGLE ALF20 DEG	VEL COEFF	LOSS COEFF ROTOR	EFFICIENCY
1 1	1.199	5589.	0.920	5.997	0.302	80.88	70.62	0.910	0.171	4.71	2.27	0.578	0.665	61.15	5.00	-30.67	0.750	0.437	64.97
1 2	1.200	6785.	0.886	4.075	0.329	80.88	63.81	0.910	0.173	4.08	51.91	0.510	0.740	66.73	4.46	0.08	0.749	0.439	72.85
1 3	1.199	8236.	0.845	2.760	0.325	80.88	48.91	0.910	0.173	3.38	78.82	0.407	0.834	70.39	3.82	52.88	0.784	0.386	79.56
1 4	1.199	9720.	0.784	1.982	0.476	80.87	-31.63	0.904	0.182	2.50	78.50	0.398	0.841	66.42	2.99	51.59	0.763	0.418	79.33
1 5	1.199	11229.	0.715	1.485	0.577	80.86	-68.99	0.900	0.189	1.72	81.36	0.382	0.854	57.64	2.23	58.65	0.814	0.337	75.10
1 6	1.199	13300.	0.560	1.058	0.749	80.82	-82.38	0.891	0.205	0.33	88.51	0.102	0.990	16.60	0.87	74.07	0.671	0.550	44.07
2 1	1.298	6933.	1.051	5.540	0.307	80.86	69.78	0.918	0.157	6.51	-5.21	0.636	0.595	64.60	6.86	-30.98	0.789	0.378	68.10
2 2	1.299	8218.	1.020	3.949	0.336	80.86	63.17	0.917	0.159	5.88	26.62	0.640	0.591	71.17	6.28	-12.98	0.827	0.316	76.08
2 3	1.299	9670.	0.980	2.853	0.388	80.87	45.31	0.915	0.162	5.02	54.37	0.602	0.637	74.40	5.47	16.25	0.822	0.324	81.04
2 4	1.299	11068.	0.934	2.176	0.453	80.88	-6.18	0.913	0.167	4.12	67.67	0.555	0.693	73.37	4.60	40.03	0.803	0.356	81.86
2 5	1.298	12561.	0.874	1.686	0.533	80.88	-57.81	0.909	0.173	3.17	73.90	0.530	0.719	68.54	3.66	53.20	0.808	0.347	79.24
2 6	1.299	14131.	0.800	1.335	0.617	80.88	-74.11	0.905	0.181	2.31	75.57	0.578	0.666	61.30	2.81	56.97	0.897	0.196	74.61
2 7	1.298	15949.	0.650	1.047	0.750	80.85	-82.41	0.897	0.195	0.65	85.83	0.259	0.933	24.13	1.15	75.53	0.645	0.585	42.60
3 1	1.398	8071.	1.145	5.192	0.314	80.82	68.90	0.923	0.147	8.14	-15.30	0.707	0.501	67.95	8.51	-33.33	0.838	0.298	71.06
3 2	1.399	9588.	1.108	3.682	0.351	80.83	60.86	0.922	0.150	7.21	20.95	0.682	0.535	73.83	7.62	-11.01	0.837	0.299	78.08
3 3	1.398	11093.	1.073	2.749	0.392	80.85	42.69	0.921	0.153	6.21	53.29	0.628	0.606	76.06	6.66	23.70	0.807	0.349	81.50
3 4	1.399	12038.	1.045	2.336	0.436	80.86	13.91	0.919	0.156	5.65	57.20	0.642	0.587	77.03	6.10	30.46	0.829	0.312	83.24
3 5	1.398	13458.	0.993	1.868	0.498	80.87	-41.41	0.916	0.161	4.67	65.90	0.626	0.609	74.88	5.13	45.63	0.829	0.313	82.33
3 6	1.399	14937.	0.933	1.517	0.567	80.88	-66.50	0.913	0.167	3.69	70.73	0.631	0.602	69.86	4.15	54.63	0.852	0.273	78.70
3 7	1.399	16390.	0.853	1.260	0.648	80.88	-76.63	0.908	0.175	2.52	76.38	0.568	0.677	57.34	2.98	64.31	0.811	0.343	67.87
3 8	1.399	17558.	0.761	1.100	0.726	80.87	-81.22	0.903	0.184	1.40	81.76	0.427	0.818	38.11	1.86	72.77	0.690	0.523	50.56
4 1	1.500	9042.	1.211	4.954	0.321	80.78	68.12	0.927	0.140	9.37	-12.73	0.707	0.500	69.19	9.74	-29.70	0.820	0.327	71.95
4 2	1.500	10458.	1.184	3.704	0.347	80.79	61.37	0.926	0.142	8.50	20.39	0.687	0.528	74.28	8.91	-6.96	0.818	0.332	77.80
4 3	1.499	11897.	1.151	2.858	0.390	80.81	46.48	0.925	0.145	7.53	44.69	0.663	0.560	77.06	7.95	18.30	0.806	0.350	81.39
4 4	1.498	13360.	1.109	2.264	0.445	80.83	7.31	0.923	0.149	6.49	57.73	0.646	0.582	77.51	6.92	37.21	0.799	0.361	82.68
4 5	1.499	14772.	1.058	1.853	0.503	80.85	-42.36	0.920	0.154	5.51	63.47	0.656	0.569	76.22	5.95	46.82	0.819	0.330	82.24
4 6	1.500	16206.	1.000	1.541	0.560	80.86	-64.75	0.917	0.159	4.51	68.54	0.665	0.558	72.26	4.94	55.27	0.840	0.294	79.19
4 7	1.499	17730.	0.927	1.287	0.631	80.88	-75.26	0.913	0.166	3.27	74.54	0.619	0.616	61.83	3.69	64.74	0.811	0.343	69.90
5 1	1.600	9979.	1.263	4.671	0.327	80.73	67.07	0.930	0.135	10.53	-15.90	0.749	0.439	71.66	10.90	-29.88	0.852	0.276	74.18
5 2	1.600	11638.	1.231	3.437	0.355	80.75	58.66	0.929	0.137	9.47	18.27	0.730	0.467	76.97	9.86	-4.93	0.846	0.285	80.18
5 3	1.600	13015.	1.200	2.746	0.400	80.77	42.47	0.928	0.140	8.51	36.23	0.723	0.477	79.51	8.92	13.23	0.845	0.287	83.29
5 4	1.600	14491.	1.155	2.215	0.454	80.80	1.65	0.925	0.144	7.35	52.21	0.696	0.516	79.38	7.75	33.69	0.823	0.322	83.79
5 5	1.599	15917.	1.107	1.835	0.508	80.83	-43.75	0.923	0.148	6.22	61.79	0.676	0.543	77.07	6.63	47.81	0.810	0.343	82.10
5 6	1.599	17436.	1.051	1.529	0.565	80.85	-65.26	0.920	0.153	5.10	67.47	0.681	0.536	72.88	5.50	56.59	0.825	0.320	78.61
6 1	1.699	10813.	1.306	4.450	0.330	80.68	66.11	0.932	0.131	11.53	-16.00	0.773	0.403	73.46	11.89	-28.51	0.864	0.254	75.77
6 2	1.699	12076.	1.282	3.569	0.353	80.70	60.05	0.932	0.132	10.61	10.07	0.746	0.444	76.96	10.99	-9.18	0.845	0.287	79.68
6 3	1.699	13495.	1.251	2.859	0.388	80.72	47.29	0.931	0.134	9.69	28.56	0.757	0.427	80.45	10.07	8.24	0.862	0.257	83.63
6 4	1.699	14991.	1.211	2.316	0.442	80.76	13.70	0.928	0.138	8.50	44.53	0.734	0.461	80.97	8.88	26.88	0.843	0.290	84.63
6 5	1.699	16391.	1.163	1.937	0.493	80.79	-32.73	0.926	0.142	7.34	55.05	0.720	0.482	79.59	7.72	40.99	0.832	0.308	83.73
6 6	1.699	17386.	1.130	1.721	0.533	80.81	-53.92	0.924	0.145	6.56	59.48	0.720	0.482	77.65	6.93	47.38	0.835	0.303	82.13

PERFORMANCE EVALUATION OF ICP RADIAL TURBINE

TABLE B12

INPUT DATA

CLEARANCE = 0.015 IN.

RUN/PT	RPM	TORQUE COUNTS	PUVC IN.HG	P5P IN.HG	H1 IN.H2O	DPVC IN.HG	PATM IN.HG	HREF1 IN.HG	V4 MV	V5 MV	V20 MV	V21 MV	V22 MV	TRM DEG.F	TCJ DEG.F
1 1	5790.	178.	9.10	5.83	23.53	3.295	30.16	0.0	1.841	1.759	1.163	1.250	1.422	79.0	32.0
1 2	7480.	147.	8.82	5.86	27.09	2.970	30.16	0.0	1.851	1.767	1.180	1.311	1.417	79.1	32.0
1 3	9030.	118.	8.50	5.89	33.01	2.659	30.16	0.0	1.848	1.772	1.199	1.378	1.457	79.2	32.0
1 4	10490.	84.	8.16	5.90	39.93	2.283	30.16	0.0	1.857	1.783	1.227	1.444	1.611	79.8	32.0
1 5	12050.	54.	7.73	5.91	47.79	1.869	30.16	0.0	1.869	1.788	1.243	1.496	1.820	79.8	32.0
1 6	13700.	11.	7.15	5.94	60.55	1.201	30.16	0.0	1.865	1.775	1.247	1.534	1.957	79.7	32.0
2 1	7190.	266.	13.43	8.79	35.28	4.671	30.16	0.0	1.896	1.836	1.264	1.326	1.390	78.2	32.0
2 2	8960.	227.	13.07	8.80	40.36	4.285	30.16	0.0	1.900	1.841	1.268	1.369	1.455	78.0	32.0
2 3	10500.	190.	12.69	8.81	47.34	3.940	30.16	0.0	1.908	1.840	1.283	1.423	1.571	77.9	32.0
2 4	12000.	153.	12.32	8.82	56.00	3.533	30.16	0.0	1.909	1.839	1.295	1.471	1.790	78.0	32.0
2 5	13440.	119.	11.91	8.83	12.60	3.103	30.16	3.81	1.911	1.840	1.310	1.544	1.948	78.0	32.0
2 6	14960.	77.	11.36	8.86	24.19	2.523	30.16	3.81	1.913	1.838	1.319	1.620	2.083	78.1	32.0
2 7	16720.	15.	10.54	8.91	21.96	1.612	30.16	3.81	1.914	1.835	1.333	1.733	2.210	78.1	32.0
3 1	8370.	356.	17.64	11.72	7.79	5.929	30.16	2.90	1.928	1.862	1.335	1.391	1.446	78.5	32.0
3 2	10460.	300.	17.17	11.73	15.54	5.444	30.16	2.90	1.929	1.864	1.319	1.397	1.551	78.6	32.0
3 3	12490.	243.	16.66	11.76	27.28	4.931	30.16	2.90	1.923	1.868	1.320	1.459	1.819	79.0	32.0
3 4	14600.	182.	16.03	11.80	22.21	4.230	30.16	4.32	1.908	1.861	1.329	1.552	2.017	79.0	32.0
3 5	16460.	128.	15.31	11.82	22.69	3.517	30.16	5.34	1.889	1.838	1.355	1.673	2.168	79.0	32.0
3 6	18050.	60.	14.49	11.89	20.46	2.637	30.16	6.92	1.864	1.817	1.358	1.762	2.272	78.5	32.0
4 1	9410.	442.	21.85	14.70	17.76	7.131	30.13	3.02	1.871	1.836	1.330	1.343	1.482	78.1	32.0
4 2	11090.	392.	21.54	14.74	12.93	6.765	30.13	3.83	1.864	1.838	1.321	1.322	1.619	78.0	32.0
4 3	13010.	336.	21.05	14.77	11.72	6.290	30.13	4.81	1.851	1.820	1.315	1.371	1.838	78.0	32.0
4 4	15000.	272.	20.40	14.79	14.93	5.589	30.13	5.70	1.838	1.798	1.331	1.529	1.984	78.0	32.0
4 5	17000.	209.	19.61	14.83	15.07	4.817	30.13	6.97	1.837	1.796	1.347	1.632	2.044	77.5	32.0
4 6	18100.	165.	19.11	14.87	10.86	4.277	30.13	8.08	1.836	1.793	1.360	1.702	2.174	77.2	32.0
5 1	10320.	534.	26.04	17.72	13.79	8.310	30.21	4.20	1.938	1.834	1.238	1.277	1.463	69.1	32.0
5 2	12040.	477.	25.63	17.75	10.23	7.902	30.21	5.00	1.972	1.873	1.285	1.354	1.652	71.0	32.0
5 3	13520.	428.	25.28	17.77	8.48	7.506	30.21	5.88	1.986	1.886	1.327	1.460	1.893	72.2	32.0
5 4	15060.	372.	24.77	17.80	10.91	6.957	30.21	6.63	1.980	1.891	1.357	1.570	2.011	73.5	32.0
5 5	16500.	317.	24.20	17.82	11.91	6.398	30.21	7.53	1.989	1.896	1.372	1.641	2.049	73.5	32.0
5 6	17980.	266.	23.70	17.83	9.45	5.839	30.21	8.75	1.986	1.905	1.400	1.779	2.256	73.1	32.0
6 1	11290.	611.	30.08	20.69	7.64	9.376	30.21	5.49	2.145	2.048	1.347	1.345	1.532	70.8	32.0
6 2	12500.	571.	29.80	20.72	8.91	9.094	30.21	5.87	2.144	2.054	1.355	1.357	1.101	70.0	32.0
6 3	14020.	516.	29.35	20.72	8.86	8.665	30.21	6.56	2.145	2.057	1.362	1.430	1.784	70.0	32.0
6 4	15530.	455.	28.90	20.74	9.19	8.133	30.21	7.62	2.145	2.056	1.373	1.550	1.933	69.5	32.0
6 5	16980.	396.	28.29	20.78	8.28	7.565	30.21	8.80	2.136	2.052	1.393	1.643	2.010	69.0	32.0
6 6	18150.	351.	27.80	20.81	11.95	7.105	30.21	9.35	2.134	2.050	1.414	1.733	2.134	69.5	32.0

PERFORMANCE EVALUATION OF ICP RADIAL TURBINE

TABLE B13 OUTPUT DATA CLEARANCE = 0.015 IN.

REDUCED TO STANDARD AIR IN ACCORDANCE WITH NASA METHOD.
TOTAL INLET PRESS. = 14.7 PSIA, TOTAL INLET TEMPERATURE
= 518.7 DEG.R., GAMMA = 1.4, CP = 0.24 BTU/LBM-DEG.F.

										NO BEARING LOSSES					MAXIMUM BEARING LOSSES				
RUN/PT	PRESS RATIO	REF. SPEED RPM	REF. FLOW LB/SEC	HEAD COEFF	DEG REACT	ANGLE ALPH1 DEG	ANGLE BETA1 DEG	VEL COEFF GV	LOSS COEFF GV	REF MOM FT.LB	ANGLE ALF20 DEG	VEL COEFF	LOSS COEFF ROTOR	EFFIC-IENCY	REF MOM FT.LB	ANGLE ALF20 DEG	VEL COEFF	LOSS COEFF ROTOR	EFFIC-IENCY
1 1	1.199	5605.	0.918	5.945	0.303	80.70	70.24	0.915	0.163	4.83	-14.71	0.651	0.576	63.22	5.12	-37.91	0.824	0.322	67.09
1 2	1.199	7240.	0.870	3.571	0.347	80.70	59.08	0.913	0.166	3.99	45.22	0.584	0.659	71.01	4.39	-6.75	0.844	0.288	78.08
1 3	1.200	8739.	0.822	2.457	0.420	80.70	22.60	0.911	0.170	3.21	66.59	0.535	0.713	72.76	3.66	22.80	0.857	0.265	83.11
1 4	1.199	10148.	0.762	1.819	0.506	80.69	-47.22	0.908	0.176	2.29	79.00	0.401	0.839	65.27	2.79	52.65	0.782	0.388	79.42
1 5	1.199	11655.	0.688	1.377	0.602	80.68	-72.34	0.904	0.184	1.48	82.64	0.360	0.871	53.79	2.01	61.64	0.823	0.323	72.83
1 6	1.199	13257.	0.551	1.064	0.756	80.64	-82.31	0.895	0.198	0.32	88.28	0.112	0.987	16.67	0.86	73.06	0.674	0.546	44.46
2 1	1.299	6944.	1.054	5.531	0.308	80.68	69.48	0.923	0.149	6.47	3.90	0.598	0.642	64.06	6.92	-26.39	0.750	0.438	67.55
2 2	1.299	8652.	1.008	3.560	0.351	80.69	59.28	0.921	0.152	5.67	34.45	0.640	0.591	73.19	6.09	-6.69	0.837	0.300	78.60
2 3	1.298	10140.	0.965	2.590	0.410	80.69	33.36	0.919	0.156	4.75	58.91	0.594	0.647	75.13	5.21	23.62	0.823	0.323	82.38
2 4	1.298	11588.	0.913	1.981	0.482	80.70	-29.39	0.916	0.161	3.83	68.74	0.565	0.681	73.26	4.32	42.44	0.822	0.325	82.51
2 5	1.298	12979.	0.855	1.578	0.551	80.70	-62.78	0.913	0.167	2.99	73.91	0.559	0.688	68.38	3.48	53.41	0.849	0.278	79.75
2 6	1.298	14447.	0.770	1.273	0.644	80.69	-76.00	0.908	0.175	1.94	78.71	0.499	0.751	54.96	2.44	62.82	0.826	0.317	69.15
2 7	1.298	16149.	0.614	1.020	0.626	80.70	-78.49	0.909	0.174	0.40	-86.35	-0.722	0.478	15.78	0.90	88.96	0.161	0.974	35.55
3 1	1.398	8077.	1.147	5.184	0.315	80.64	68.60	0.928	0.139	8.15	-13.03	0.693	0.520	67.96	8.52	-32.05	0.823	0.322	71.07
3 2	1.398	10093.	1.098	3.317	0.365	80.66	56.24	0.926	0.142	6.82	40.53	0.630	0.603	74.35	7.25	6.85	0.793	0.372	78.99
3 3	1.398	12051.	1.043	2.327	0.438	80.68	13.65	0.923	0.148	5.64	57.46	0.637	0.594	77.22	6.10	30.90	0.823	0.323	83.44
3 4	1.398	14089.	0.965	1.703	0.526	80.69	-54.13	0.919	0.155	4.23	69.14	0.615	0.622	73.19	4.70	51.46	0.826	0.318	81.23
3 5	1.398	15895.	0.878	1.337	0.613	80.70	-73.14	0.915	0.163	2.98	74.20	0.615	0.621	64.07	3.45	60.59	0.856	0.267	74.24
3 6	1.398	17442.	0.758	1.112	0.725	80.69	-80.87	0.908	0.176	1.41	81.86	0.413	0.829	38.40	1.87	72.80	0.674	0.546	50.86
4 1	1.500	9087.	1.219	4.902	0.319	80.59	67.75	0.932	0.132	9.51	-14.00	0.723	0.478	70.16	9.89	-30.36	0.836	0.301	72.92
4 2	1.500	10709.	1.187	3.534	0.350	80.61	59.56	0.931	0.134	8.40	29.73	0.668	0.554	74.94	8.81	1.43	0.800	0.359	78.57
4 3	1.500	12570.	1.142	2.565	0.411	80.64	34.18	0.929	0.138	7.16	52.72	0.649	0.579	77.87	7.59	29.65	0.795	0.367	82.52
4 4	1.500	14503.	1.074	1.926	0.487	80.66	-31.95	0.925	0.144	5.74	64.24	0.638	0.593	76.64	6.18	47.97	0.798	0.363	82.44
4 5	1.500	16437.	0.995	1.499	0.572	80.69	-66.28	0.921	0.152	4.53	65.29	0.723	0.477	73.99	4.96	50.58	0.898	0.193	81.03
4 6	1.500	17503.	0.936	1.323	0.623	80.69	-73.77	0.918	0.157	3.58	71.08	0.676	0.543	66.13	4.00	59.49	0.862	0.257	74.02
5 1	1.600	9967.	1.271	4.685	0.324	80.54	66.91	0.935	0.126	10.72	-18.49	0.766	0.413	72.38	11.09	-31.39	0.866	0.250	74.87
5 2	1.600	11614.	1.237	3.452	0.355	80.56	58.60	0.934	0.128	9.62	14.18	0.745	0.444	77.70	10.01	-8.04	0.859	0.262	80.86
5 3	1.600	13036.	1.205	2.739	0.398	80.59	42.68	0.932	0.131	8.61	36.21	0.728	0.471	80.13	9.01	13.47	0.848	0.280	83.87
5 4	1.600	14519.	1.159	2.209	0.451	80.62	3.53	0.930	0.135	7.45	51.48	0.708	0.499	80.30	7.86	32.95	0.835	0.303	84.67
5 5	1.600	15905.	1.110	1.840	0.505	80.64	-41.44	0.928	0.139	6.32	61.13	0.684	0.532	77.90	6.72	47.01	0.818	0.332	82.88
5 6	1.600	17327.	1.060	1.549	0.563	80.67	-63.63	0.925	0.145	5.26	66.08	0.691	0.522	74.09	5.66	54.71	0.832	0.308	79.71
6 1	1.700	10829.	1.312	4.443	0.327	80.49	65.89	0.937	0.122	11.62	-14.16	0.767	0.411	73.73	11.98	-27.16	0.858	0.265	76.02
6 2	1.701	11988.	1.291	3.628	0.351	80.51	60.41	0.936	0.123	10.82	6.80	0.752	0.434	77.23	11.20	-11.57	0.849	0.279	79.89
6 3	1.700	13444.	1.259	2.882	0.385	80.54	48.05	0.935	0.125	9.74	32.89	0.730	0.467	79.98	10.12	12.79	0.834	0.304	83.10
6 4	1.700	14893.	1.219	2.348	0.439	80.57	17.93	0.933	0.129	8.63	44.81	0.726	0.473	81.11	9.01	27.35	0.833	0.306	84.69
6 5	1.700	16285.	1.173	1.964	0.492	80.61	-28.55	0.931	0.133	7.48	54.62	0.712	0.493	79.83	7.86	40.58	0.822	0.325	83.88
6 6	1.700	17408.	1.135	1.719	0.531	80.63	-52.42	0.929	0.137	6.60	60.53	0.712	0.493	77.86	6.98	48.98	0.826	0.318	82.27

APPENDIX C

PROGRAM NOSPD

Program NOSPD calculates the referred moments and referred flow rates for the stopped-rotor tests and is in essence a much simplified version of program RADIAL. The computational techniques used are the same in both programs and will not be repeated. Program NOSPD is listed in Table C1, and the input and output date are given in Table C2. Table B3 lists the torque calibration data used for each run. The items of input data defined in the preceding section apply to this program, except as noted below.

Card No.	FORTRAN	Description
1	NRUNS	Number of runs (clearances) to be processed
2	CLNC	
3	TCD	
4	NPTS	
5	V4, V5, TCJ, PATM, P5P, DPVC, TQ, TRM	

TABLE C1

LISTING OF PROGRAM NOSPD

```
C   PROGRAM NOSPD.
C   CALCULATES REFERRED MOMENTS AND REFERRED FLOW RATES FOR
C      STOPPED-ROTOR TESTS.
C
      DIMENSION V4(10),V5(10),TCJ(10),PATM(10),P5P(10),DPVC(10),PUVC(10)
     *,TQ(10),TRM(10),TCD(50)
C     WRITE HEADING FOR OUTPUT.
      WRITE(6,1)
    1 FORMAT(1H1,///,T38,'PERFORMANCE EVALUATION OF ICP RADIAL TURBINE',
     *///,T56,'TABLE',//,T47,'RESULTS OF ZERO-SPEED TESTS',//,T40,'INPUT
     * DATA',T97,'OUTPUT DATA',//,T99,'REF.',T109,'REF.',/,T15,'V4',T23,
     *'V5',T31,'TCJ    PATM     P5P     DPVC     PUVC   TORQUE   TRM',T90
     *,'PRESS.  MOMENT  FLOW RATE',/,T5,'PT',T15,'MV        MV     DEG.F.
     * IN.HG   IN.HG     IN.HG    IN.HG   COUNTS  DEG.F        RATIO   FT.LB
     *     LBM/SEC',/)
      WRITE(6,103)
  103 FORMAT(T2,'--------------------------------------------------------
     *----------------------------------------------------------')
C   READ INPUT DATA.
      READ(5,2) NRUNS
    2 FORMAT(I4)
      DO 3 N=1,NRUNS
      READ(5,4) CLNC
    4 FORMAT(F5.3)
      READ(5,5) (TCD(I),I=1,5)
    5 FORMAT(5F7.1)
C   WRITE HEADING FOR RUN.
      WRITE(6,6) CLNC
    6 FORMAT(//,T40,'RUN',T61,'CLEARANCE = ',F5.3,/)
      READ(5,2) NPTS
      DO 7 K=1,NPTS
      READ(5,8) V4(K),V5(K),TCJ(K),PATM(K),P5P(K),DPVC(K),PUVC(K),TQ(K),
     *TRM(K)
    8 FORMAT(9F8.4)
C   PROCESS DATA POINT.
      GHG=13.63905-1.363030E-3*TRM(K)
      CF1=70.438824*GHG/13.54
      CALL TEMP (V4(K),V5(K),TCJ(K),T4,T5)
      CALL FLOW (DPVC(K),PUVC(K),PATM(K),GHG,T4,WVC)
      CALL PRESS(T5,PATM(K),P5P(K),GHG,CF1,WVC,PR2,PTO)
      CALL EDC (T5,PR2,GAM,EXP,CP,THETA)
      CALL TORQ (TCD,TQ(K),TNET)
      CALL REFER (PTO,GHG,GAM,THETA,TNET,WVC,WVCR,TNETR)
C   WRITE INPUT DATA AND RESULTS FOR THE DATA POINT.
      WRITE(6,10) K,V4(K),V5(K),TCJ(K),PATM(K),P5P(K),DPVC(K),PUVC(K),TQ
     *(K),TRM(K),PR2,TNETR,WVCR
  10 FORMAT(2X,I4,4X,2F8.3,3F8.2,F9.3,F8.2,F7.0,F7.1,6X,F7.3,F8.2,F10.3
     *)
   7 CONTINUE
     IF(N.EQ.NRUNS) GO TO 100
     GO TO 3
 100 WRITE(6,101)
 101 FORMAT(1H1)
   3 CONTINUE
     RETURN
     END




     SUBROUTINE TEMP (V4,V5,TCJ,T4,T5)
     V=V4
     J=1
 100 T=TCJ+0.144+35.77*V-0.4518*V**2
     IF(T-100.)102,102,101
 101 T=TCJ+1.252+34.86*V-0.1855*V**2
 102 T=T+459.69
     IF(J-1) 103,103,104
 103 J=2
     T4=T
     V=V5
     GO TO 100
 104 T5=T
     RETURN
     END
```

```
      SUBROUTINE FLOW(DPVC,PUVC,PATM,GHG,T4,WVC)
      DVC=DPVC*GHG/13.54
      PVC=(PUVC+PATM)*GHG/13.54
      A=1.+1.85E-5*(T4-532.)
      Z=1.9+2.4E-3*(T4-560.)
      Y=1.-.351*DVC/PVC
      WVC=2.2854*A*Y*SQRT(PVC*DVC/T4)
      X=WVC*.8131/Z
      WVC=(1.+.001275/X)*WVC
      RETURN
      END
```

```
      SUBROUTINE PRESS (T5,PATM,P5P,GHG,CF1,WVC,PR2,PTO)
      A=T5-459.69
      CP=.23943+3.4E-6*A+2.E-8*A**2
      PS5=(PATM+P5P)*GHG/13.54
      TT=T5
  100 RHO=PS5*CF1/(TT*53.3448)
      VO=WVC/(RHO*3.14159*6.25/144.)
      TO=T5-(VO**2)/(2.*32.174*778.16*CP)
      DTT=TT-TO
      TT=TO
      IF(ABS(DTT)-.01)101,101,100
  101 PTO=PS5+RHO*(VO**2)/(2.*32.174*CF1)
      PR2=PTO/(PATM*GHG/13.54)
      RETURN
      END
      SUBROUTINE EDC (T5,PR2,GAM,EXP,CP,THETA)
      A=T5-459.69
  105 GA=1.4018-2.E-5*A
      EX=(GA-1.)/GA
      DT=T5*(1.-1./PR2**EX)
      AA=T5-459.69-DT/2.
      AAA=ABS(AA-A)
      IF(AAA-1.) 107,107,106
  106 A=AA
      GO TO 105
  107 GAM=GA
      EXP=EX
      CP=.23943+3.4E-6*AA+2.E-8*AA**2
      IF(GAM*T5)2050,2050,2051
 2050 WRITE(6,2052) K,GAM,T5
 2052 FORMAT(//,6X,I4,2F8.3)
 2051 CONTINUE
      THETA=(GAM/1.4)*(T5/518.7)
      RETURN
      END
```

```
      SUBROUTINE TORQ (TCD,TQ,TNET)
      DIMENSION TCD(5)
      BFM=0.0
      DO 100 I=1,5
      IF(TCD(I)-TQ) 100,100,101
  100 CONTINUE
  101 IF(I.LT.5) GO TO 102
      T=100.*(I-2)+100.*((TQ-TCD(I-1))/(TCD(I)-TCD(I-1)))
      GO TO 103
  102 AI=100.*(I-1)
      T=AI+100.*((TQ-TCD(I))/(TCD(I+1)-TCD(I)))
  103 T=T/12.
      TNET=T+BFM
      RETURN
      END
```

```
SUBROUTINE REFER (PTO,GHG,GAM,THETA,TNET,WVC,WVCR,TNETR)
DEL=(PTO*(.4891585*GHG/13.54))/14.7
X=(GAM+1.)/(2.*(GAM-1.))
EPS=(.810/GAM)*((GAM+1.)/2.)**X
WVCR=WVC*(SQRT(THETA))*EPS/DEL
TNETR=TNET*EPS/DEL
RETURN
END
```

PERFORMANCE EVALUATICN OF ICP RADIAL TURBINE

TABLE C2

RESULTS OF ZERO-SPEED TESTS

	INPUT DATA									OUTPUT DATA		
PT	V4 MV	V5 MV	TCJ DEG.F.	PATM IN.HG	P5P IN.HG	DPVC IN.HG	PUVC IN.HG	TORQUE COUNTS	TRM DEG.F	PRESS. RATIO	REF. MOMENT FT.LB	REF. FLOW RATE LBM/SEC
				RUN 1			CLEARANCE = 0.081					
1	1.640	1.395	32.00	30.07	2.90	2.066	4.93	125.	87.8	1.100	3.72	0.757
2	1.640	1.400	32.00	30.07	5.87	3.926	9.75	249.	87.9	1.201	6.79	1.004
3	1.635	1.400	32.00	30.07	8.76	5.452	14.20	367.	87.5	1.300	9.20	1.142
4	1.635	1.395	32.00	30.07	11.70	6.891	18.54	488.	87.5	1.400	11.40	1.240
5	1.620	1.380	32.00	30.07	14.64	8.184	22.83	605.	87.1	1.500	13.15	1.309
6	1.620	1.375	32.00	30.07	17.56	9.364	26.94	718.	87.1	1.599	14.73	1.358
7	1.620	1.375	32.00	30.07	20.51	10.502	31.00	829.	87.0	1.699	16.07	1.397
				RUN 2			CLEARANCE = 0.061					
1	1.719	1.626	32.00	30.10	2.91	2.043	4.94	126.	76.0	1.100	3.62	0.756
2	1.762	1.679	32.00	30.10	5.82	3.348	9.63	250.	75.2	1.199	6.70	0.936
3	1.816	1.738	32.00	30.10	8.81	5.429	14.23	374.	75.0	1.302	9.18	1.143
4	1.823	1.759	32.00	30.10	11.74	6.830	18.64	492.	75.0	1.401	11.35	1.240
5	1.834	1.774	32.00	30.10	14.70	8.083	22.85	608.	75.0	1.502	13.14	1.306
6	1.847	1.784	32.00	30.10	17.60	9.265	26.91	724.	75.0	1.600	14.79	1.357
7	1.851	1.783	32.00	30.10	20.53	10.371	30.95	835.	75.0	1.699	16.14	1.394
				RUN 3			CLEARANCE = 0.041					
1	1.984	1.885	32.00	30.02	2.90	2.076	5.00	127.	73.6	1.100	3.69	0.763
2	2.000	1.910	32.00	30.02	5.81	3.873	9.69	247.	73.5	1.200	6.68	1.003
3	2.026	1.942	32.00	30.02	8.73	5.410	14.14	369.	73.9	1.300	9.20	1.143
4	2.047	1.970	32.00	30.02	11.67	6.809	18.50	487.	74.0	1.400	11.37	1.240
5	2.064	1.987	32.00	30.02	14.61	8.031	22.79	602.	73.8	1.500	13.12	1.305
6	2.076	2.010	32.00	30.02	17.52	9.237	26.82	718.	73.8	1.599	14.77	1.357
7	2.076	2.013	32.00	30.02	20.47	10.032	30.84	827.	73.5	1.699	16.09	1.376
				RUN 4			CLEARANCE = 0.024					
1	1.973	1.853	32.00	30.04	2.90	2.063	4.96	129.	77.2	1.100	3.70	0.760
2	1.985	1.884	32.00	30.04	5.91	3.876	9.66	253.	77.8	1.203	6.77	1.000
3	1.996	1.899	32.00	30.04	8.72	5.448	14.19	372.	77.9	1.299	9.21	1.147
4	2.000	1.910	32.00	30.04	11.63	6.844	18.50	489.	77.3	1.398	11.35	1.243
5	2.005	1.920	32.00	30.04	14.61	8.141	22.82	606.	77.5	1.500	13.14	1.313
6	2.004	1.920	32.00	30.04	17.53	9.315	26.90	720.	77.0	1.599	14.75	1.362
7	2.005	1.921	32.00	30.04	20.43	10.415	30.96	829.	76.6	1.697	16.08	1.400
				RUN 5			CLEARANCE = 0.015					
1	2.005	1.879	32.00	30.21	2.92	2.110	5.00	127.	72.0	1.100	3.75	0.766
2	2.013	1.923	32.00	30.21	5.84	3.916	9.75	251.	72.5	1.200	6.90	1.005
3	2.010	1.931	32.00	30.21	8.80	5.458	14.20	371.	72.5	1.300	9.19	1.143
4	2.005	1.932	32.00	30.21	11.73	6.863	18.63	492.	72.5	1.399	11.41	1.241
5	1.975	1.908	32.00	30.21	14.70	8.148	22.95	607.	72.2	1.500	13.14	1.310
6	1.953	1.889	32.00	30.21	17.68	9.344	27.06	727.	72.1	1.601	14.85	1.359
7	1.944	1.885	32.00	30.21	20.61	10.419	31.09	836.	72.0	1.699	16.15	1.395

INITIAL DISTRIBUTION LIST

		No. Copies
1.	Defense Documentation Center Cameron Station Alexandria, Virginia 22314	20
2.	Library Naval Postgraduate School Monterey, California 93940	2
3.	Commander, Naval Air Systems Command Navy Department Washington, D. C. 20360	1
4.	Mr. I. Silver Propulsion Administrator (Code 330) Research and Technology Naval Air Systems Command Navy Department Washington, D. C. 20360	1
5.	Dr. F. I. Tanczos Technical Director (Code 033) Research and Technology Naval Air Systems Command Navy Department Washington, D. C. 20360	1
6.	Commander, Naval Ship Systems Command Navy Department Washington, D. C. 20360	1
7.	Office of Naval Research (Power Branch) Attn: Mr. J. K. Patton, Jr. Navy Department Washington, D. C. 20360	1
8.	Superintendent Naval Academy Annapolis, Maryland 21402	1
9.	Chairman Department of Engineering Naval Academy Annapolis, Maryland 21402	1
10.	Chairman, Department of Aeronautics Naval Postgraduate School Monterey, California 93940	2

No. Copies

11. Professor R. D. Zucker 3
Department of Aeronautics
Naval Postgraduate School
Monterey, California 93940

12. Professor M. H. Vavra 2
Department of Aeronautics
Naval Postgraduate School
Monterey, California 93940

13. LT David D. Williams, USN 3
1637 77th Avenue, N. E.
Bellevue, Washington, 98004

14. Dr. Allen E. Fuhs 1
Chief Scientist (Code APX)
AeroPropulsion Laboratory (AFSC)
Wright Patterson Air Force Base, Ohio 45433

15. Dr. D. M. Dix 1
Chief Engineer
Northern Research and Engineering Corp.
219 Vassar St.,
Cambridge, Mass. 02139

DOCUMENT CONTROL DATA - R & D

(Security classification of title, body of abstract and indexing annotation must be entered when the overall report is classified)

1. ORIGINATING ACTIVITY (Corporate author) Naval Postgraduate School Monterey, California 93940	2a. REPORT SECURITY CLASSIFICATION Unclassified 2b. GROUP None

3. REPORT TITLE

Determination of Performance Parameters of a Dual Discharge Radial Turbine

4. DESCRIPTIVE NOTES (Type of report and, inclusive dates)

None

5. AUTHOR(S) (First name, middle initial, last name)

David Daniel Williams

6. REPORT DATE December 1968	7a. TOTAL NO. OF PAGES 158	7b. NO. OF REFS 12
8a. CONTRACT OR GRANT NO. b. PROJECT NO. N/A c. d.	9a. ORIGINATOR'S REPORT NUMBER(S) N/A 9b. OTHER REPORT NO(S) (Any other numbers that may be assigned this report)	

10. DISTRIBUTION STATEMENT

Distribution of this document is unlimited.

11. SUPPLEMENTARY NOTES None	12. SPONSORING MILITARY ACTIVITY Naval Postgraduate School Monterey, California 93940

13. ABSTRACT

This study was conducted to establish the performance parameters of a radial inflow, dual discharge turbine and to determine the effect of variations in axial clearance on these parameters. The representative stream surface is taken at the outer discharge radius instead of at a computed mass-average discharge radius, as was done previously. This technique results in considerably simplified computations and in better correlation of the rotor loss parameters.

Tests were conducted at axial clearances from 0.015 to 0.081 inches and at total-to-static pressure ratios from 1.2 to 1.7 for each clearance. The test installation is located at the Turbo-Propulsion Laboratory of the Naval Postgraduate School, Monterey, California.

14 KEY WORDS	LINK A		LINK B		LINK C	
	ROLE	WT	ROLE	WT	ROLE	WT
RADIAL TURBINE						
AXIAL CLEARANCE						
PERFORMANCE PARAMETERS						

Gaylord
SHELF BINDER
Syracuse, N. Y.
Stockton, Calif.

DUDLEY KNOX LIBRARY
NAVAL POSTGRADUATE SCHOOL
MONTEREY CA 93943-5101

DUDLEY KNOX LIBRARY
3 2768 00305694 6